

BAS  
Instrumentation Notes

Note 1

February 1980

Topological Concepts As Applied to Electromagnetic  
Isolation and Mechanical Cable Survivability

Neal P. Baum  
CERF  
University of New Mexico

ABSTRACT

This report discusses the use of topological concepts as applied to the grounding and shielding of long signal cables and the applicability of such systems to data acquisition on large-scale high-explosive tests. Two experiments are described. The first was a signal isolation experiment performed as a part of HAVE HOST Event SIM CAL III. The second was a Close-In Data-Acquisition System (CIDAS) experiment performed in conjunction with the HAVE HOST Vertical Shelter Test (VST). These experiments demonstrated that the grounding and shielding systems used were far superior to the single-point grounding system currently in use. Cable-hardening methods are described in Appendix A, which is primarily a summary and discussion of a report on methods used in past underground tests.

## CONTENTS

<u>Section</u>		<u>Page</u>
I	INTRODUCTION	4
II	BACKGROUND: ELECTRICAL SIGNAL ISOLATION	5
III	TEST PROCEDURES AND RESULTS	12
	SIMCAL III Test	12
	Close-in Data-Acquisition Experiments	23
IV	CONCLUSIONS AND RECOMMENDATIONS	61
	APPENDIX A: MECHANICAL CABLE-HARDENING ON UNDERGROUND TESTS	63
	APPENDIX B: CIDAS VAN ENVIRONMENT MEASUREMENTS	68
	APPENDIX C: VST NEAR-FIELD ENVIRONMENT PREDICTIONS AND EXPLOSIVES DOCUMENTATION	81
	SYMBOLS	84

## ILLUSTRATIONS

<u>Figure</u>		<u>Page</u>
1	Cylindrical shield	6
2	Tree network	8
3	Single-point grounding	9
4	Distributed (continuous) grounding of external conductor	11
5	Grounding and shielding topology	14
6	SIMCAL III motion data	17
7	SIMCAL III acceleration data	21
8	Dummy bridge data	24
9	Partial tree map showing one channel of VST grounding and shielding experiment topology	26
10	Comparative stress measurements, gage 1	28
11	Comparative vertical shear measurements, gage 1	31
12	Comparative tangential shear measurements, gage 1	34
13	Comparative stress measurements, gage 2	37
14	Comparative vertical shear measurements, gage 2	41
15	Comparative tangential shear measurements, gage 2	44
16	Comparative rebar strain measurements, gage 2	48
17	CIDAS test-bed layout, HAVE HOST VST-1	54
18	Photograph of van E-8 and test bed	55
19	Environmental measurements, CIDAS experiment, HAVE HOST VST-1	56
20	Incident pressure at roof center	58
21	Reflected pressure at van rear	59
22	Vertical acceleration under van	60

## TABLES

<u>Table</u>		<u>Page</u>
1	Comparison of cylindrical shields	6
2	Stress-gage results	23
3	Measurements for CIDAS van environment experiment	53
A-1	Summary of results for cable load coefficient	66

## SECTION I

### INTRODUCTION

The success of any testing program is dependent, to a large degree, on the quality of the instrumentation used. The United States Air Force is interested in developing better instrumentation and associated equipment in order to overcome known shortcomings and to improve the credibility of field-test data. In response to this need, the University of New Mexico Engineering Research Institute (NMERI) has examined the problems of electrical signal isolation and mechanical cable survivability.

NMERI performed two signal-isolation experiments, the first in conjunction with HAVE HOST Event SIMCAL III and the second in conjunction with the HAVE HOST Vertical Shelter Test (VST). Both experiments are described in this report, and conclusions and recommendations are presented. The subject of mechanical cable survivability has recently been addressed by another author; a summary and discussion of his report is presented in Appendix A.

## SECTION II

### BACKGROUND: ELECTRICAL SIGNAL ISOLATION

A shield, in an electrical sense, is a conductor placed in the proximity of current carriers in order to block unwanted electromagnetic interference with the carriers. One should consider certain properties of the shield when deciding which shielding technique to use. The first property is the "skin depth" of the shield. This term recognizes that high frequencies tend to travel on the surface of conductors and do not penetrate deeply into them. The depth of penetration ( $\delta$ ) may be defined by the following relationship:

$$\delta = \sqrt{\frac{1}{\pi f \mu \sigma}} \quad (1)$$

where  $f$  is frequency,  $\mu$  is permeability, and  $\sigma$  is conductivity.

A second property of interest is the resistance per unit length ( $R'$ ) of the shield. If the shield is cylindrical (Fig. 1), with thickness  $\Delta$ , then

$$R' = \frac{1}{2\pi r_0 \Delta \sigma} \quad (2)$$

where  $r_0$  is the internal radius of the cylindrical shield. This property is important in that the electric field in the vicinity of the conductors is directly proportional to the current induced along the shield. Thus, one may grade shields by skin depth frequency (set  $\delta = \Delta$ ) and the  $R'$ . Table 1 compares the properties of typical shields made of various metals.

With reference to the table, one can see that a ferromagnetic material such as iron would make an appropriate shield for normal blast and shock (high-explosive) measurements. On the other hand, if the shield currents are expected to be large (e.g., in an underground test), then one would choose a good conductor such as aluminum or copper for the shield.

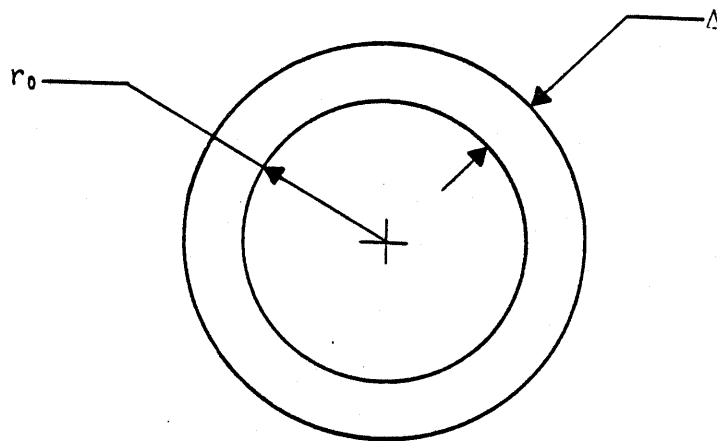


Figure 1. Cylindrical shield.

TABLE 1. COMPARISON OF CYLINDRICAL SHIELDS

Material	$\sigma$ (S/m)	$\mu$	$R'$ ( $\Omega$ /m)	f for $\Delta = \delta$ (KHz)
Aluminum	$3.5 \times 10^{-7}$	$\mu_0$	$4.5 \times 10^{-5}$	7.30
Copper	$5.8 \times 10^{-7}$	$\mu_0$	$2.8 \times 10^{-5}$	4.40
Iron	$10^{-7}$	$200\mu_0$	$1.6 \times 10^{-4}$	0.13

Notes:  $r_0 = 100$  mm.

$\Delta = 1$  mm.

$\mu_0 = 4\pi \times 10^{-7}$  H/m.

The next thing to consider is the shielding configuration, or topology. The following passage is quoted from Reference 1:

A set  $S$ , together with a collection of subsets called open sets, is called a topological space if and only if the collection of open sets satisfies the following Axioms:

- Axiom 1 Every open set is a set of points
- Axiom 2 The empty set is an open set
- Axiom 3 For each point  $p$ , there exists an open set containing  $p$
- Axiom 4 The union of any collection of open sets is an open set
- Axiom 5 The intersection of any finite collection of open sets is an open set.

The collection of open sets is called the topology of the topological space.

Thus, in this context, one of the topologies is that set of points contained inside the exterior shield. Another limitation is placed on the shield, namely, that it is simply closed. In other words, it is homeomorphic\* with a unit sphere. Thus, the shield behaves as a screen room around the conductors, transducers, and recording equipment. No holes should be allowed in the shield.

When the shield is homeomorphic with a unit sphere, any closed loops in the system are eliminated. Thus, one is led to the concept of a tree network, which is made up of tubes corresponding to the shields. These tubes contain all the conductors such as instrumentation cables, power lines, and telephone lines. Figure 2 is an example of a tree network. From the outside this tree network is made to behave as a single conductor. Thus, one can see that to be most effective, the shield should be closed and one should be able to describe it with a tree diagram.

The next point to consider is the grounding of the tree network. The Air Force typically uses a single-point ground at the instrumentation van (Fig. 3a). If one assumes that noise in the system is generated by a local

---

1. Hall, D. W., and Spencer, G. L., *Elementary Topology*, John Wiley & Sons, Inc., New York, 1964.

\* There exists a one-to-one continuous mapping.

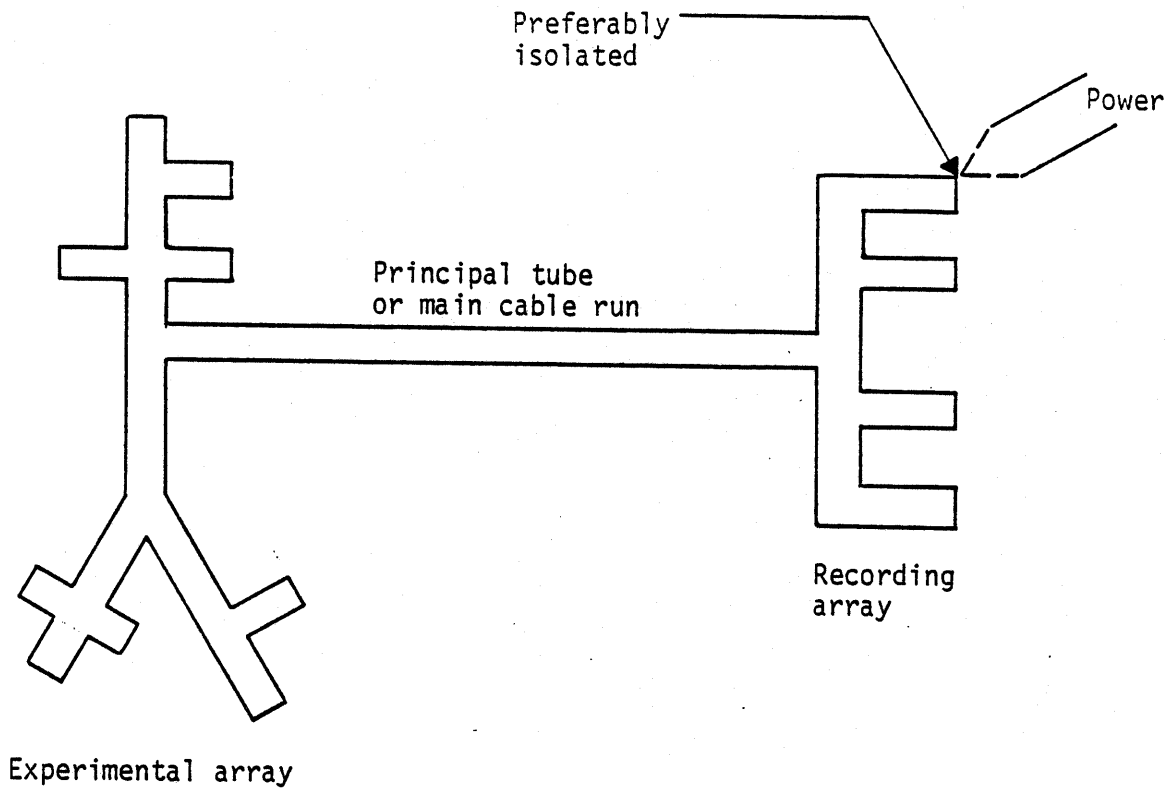
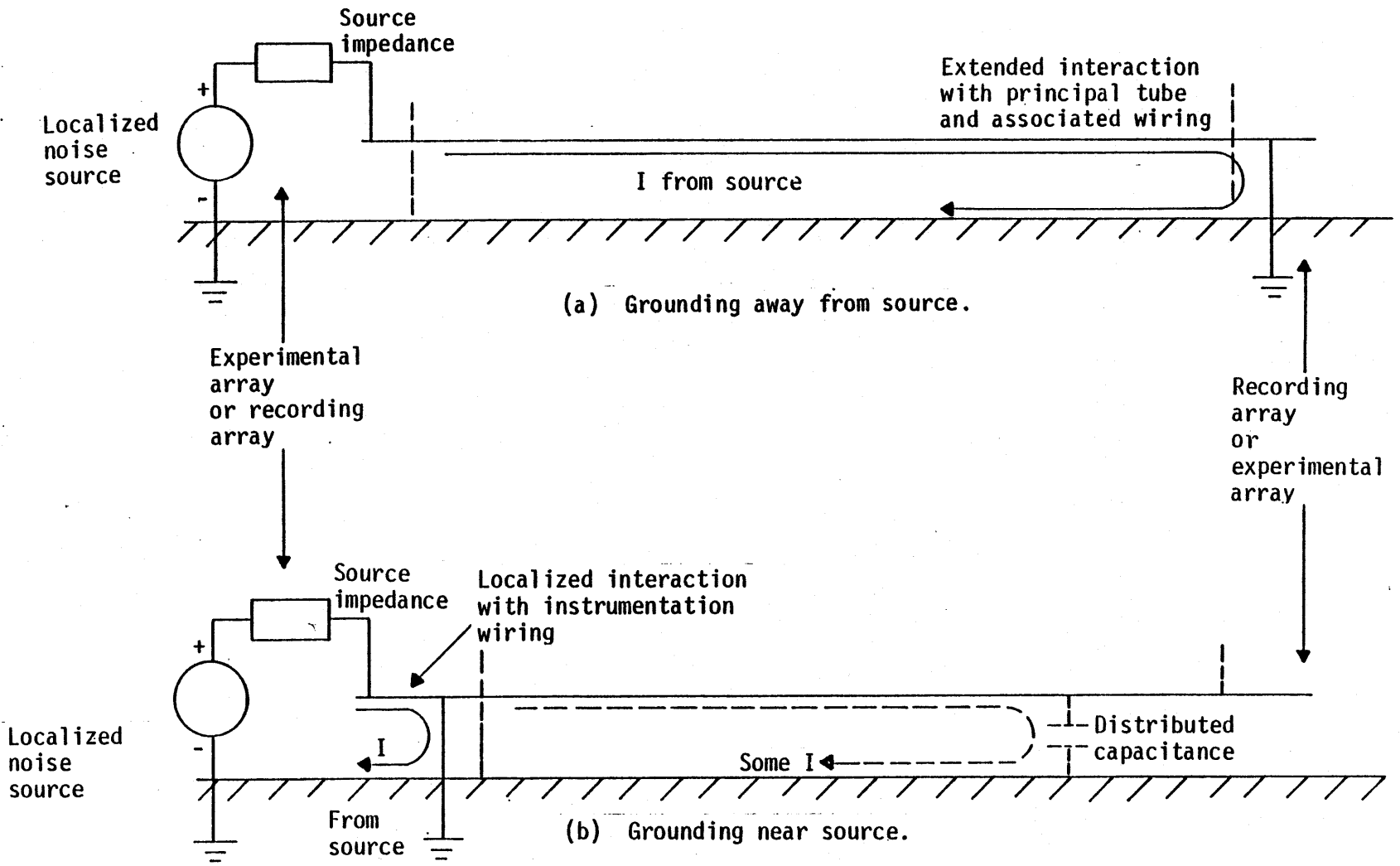


Figure 2. Tree network.

source (in this case, in the vicinity of the test bed), then the noise source will have some effective impedance tying it to ground and to the outer shield of the cable. Thus, currents will be induced on the shield, and these will cause noise on the gathered data. The system can be improved by placing the ground near the source (Fig. 3b) and thus attenuating the currents on the shields. This method, however, is extremely difficult to implement on an operation like HAVE HOST because (1) grounding at the transducer would yield a number of widely spaced grounds, causing possible loops, and (2) the possibly significant potential difference between the grounds at the test bed and those in the earth next to the van introduces a safety hazard. This danger has been observed at the Nevada Test Site, where the described grounding system is sometimes used. It is overcome by rubber mats placed next to the van to eliminate the shock hazard.





6

Figure 3. Single-point grounding.

A third type of grounding system overcomes the difficulties associated with the single-point ground. This is a distributed, or continuous, ground (Fig. 4). In this system the shield is grounded at as many places as are physically and economically practical. The maximum spacing between the grounds is much less than the wavelength, in the cable, of the maximum frequency of interest. In this case the shield currents decrease in an exponential manner as they propagate down the cable. Because the exterior shield is kept closed whenever physically possible, the transducer case is grounded. This method appears to this author to be much better than the method normally used by the OLAG detachment of the Air Force Weapons Laboratory (AFWL), in which the transducer case is floated with respect to the shield, because if the case is grounded to the shield through hot ionized gases or by motions, then the single-point grounding system becomes a two-point system whose points are widely separated. The resulting ground loop will introduce significant 60-Hz and 120-Hz noise. With the continuous grounding system, on the other hand, the possibility of low-frequency ground loops is negated because all ground loops are required to be of such high frequency that they do not affect the data band of interest.

It seems obvious that in designing an experiment, one should take care to design the topology of the shield in such a way that it can be described as a tree network. One does not simply pull cable and wonder where the noise is coming from. It should also be recalled that the van is an integral part of the shield. Therefore, excessive noise emitters should not be allowed in the van, and penetrations of the shield should not be allowed to bring noise in. Thus power, IRIG time, fiducial (FIDU) signals, externally controlled closures, and communications should be isolated by either transformers or relays. Power leads should be shielded from signal leads, but the two should be kept within the same topology. The grounding should be continuous or distributed, not single-point, because of the obvious advantages offered by the former system.

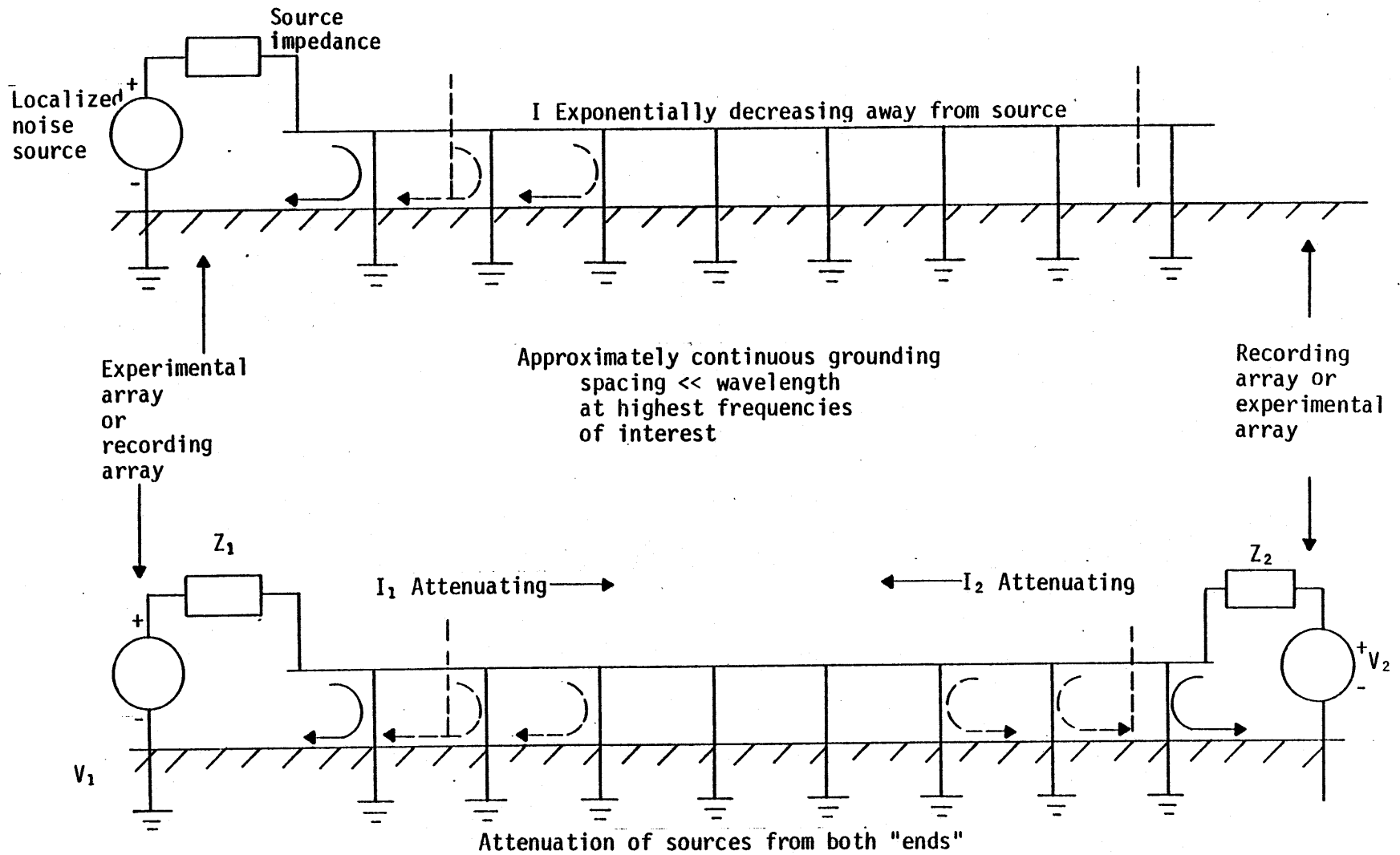


Figure 4. Distributed (continuous) grounding of external conductor.

## SECTION III

### TEST PROCEDURES AND RESULTS

The considerations discussed in Section II prompted NMERI to field two experiments in order to demonstrate the efficacy of the principles described. In both experiments, a small Air Force experimental van (E-8) was used to record some select channels of data. These data were then compared to data taken by the methods normally used by the AFWL/OLAG Detachment. The comparative data were recorded by gages identical to, and located similarly to, the E-8 gages.

The first experiment was performed in conjunction with HAVE HOST Event SIMCAL III. The shielding used on this experiment was far more complete and probably more expensive than anything previously attempted in the way of high-energy (HE) blast and shock tests. The results were impressive, but the cost of full-scale implementation was thought to be too high.

The second experiment, performed in conjunction with HAVE HOST VST, was an attempt to show that even a low-cost, simplified version of the experimental shielding system used on SIMCAL III could radically improve the quality of the data obtained. The cost was lowered by the simple expedient of placing the van close to the test event so that cabling costs were cut radically. This two-part test was called the Close-In Data-Acquisition System (CIDAS) experiment. Again, the results were impressive.

#### SIMCAL III TEST

The purpose of the grounding and shielding experiment conducted in conjunction with SIMCAL III was to quantify the electrical noise introduced into the instrumentation system from sources other than the voltage modulation of the transducers. To this end, the data obtained from two sets of gages placed in symmetric locations on SIMCAL III were compared.

The first set of gages, four soil-stress gages and two accelerometers, was placed on the ground in front of the A-structure on SIMCAL III. The output of these gages was recorded in van E-3 at the HAVE HOST test site. The grounding and shielding system was the one normally used by AFWL/OLAG. It consisted of a single-point ground at the van and a single, shielded, 50-pair transmission line.

The second set of gages, of the same type and number as the first, was placed in the test bed in front of the B-structure, in a pattern like that of the first set. The output from these gages was recorded in van E-8. Two dummy gages were also installed so that any mechanical or electrical noise generated on them could be observed. The dummy gages consisted of 350- $\Omega$  carbon resistor bridges mounted in flexible copper pipe.

The grounding and shielding system used for the van E-8 gages was similar to that used by the Electromagnetics Division of AFWL (AFWL/NTM) on underground tests where the electromagnetic (EM) noise environment is extremely harsh. It consisted of a primary shield (zone 1) that was, for all practical purposes, homeomorphic with a unit sphere. This primary shield included an aluminum cable tray (3- to 4-KHz skin depth), the transducer housing, piping to the individual transducers, piping under the testbed, and the E-8 van itself. This shield was grounded at maximum intervals of 15 m. The next shield (zone 2) consisted of the outer shield of the 20-pair cable, which was connected to the primary shield by a short at the transducer end and through a 75- $\Omega$  resistor at the van end. The 75- $\Omega$  resistor was chosen because it was close to the characteristic impedance between zones 1 and 2. The similarity was determined experimentally by the use of a Tektronix time domain reflectometer to excite the two shields. The rate of attenuation of the reflections was then observed, and it appeared that the reflections were terminated most effectively by the 75- $\Omega$  resistor. As was previously mentioned, van E-8 was an integral part of the shielding system and was connected to the rack containing the recording equipment only through the previously mentioned 75- $\Omega$  resistor. The third shield was that around the individual twisted pairs. The shield was shorted to the outer cable shield at both ends. (See Figure 5.) The power for the recording equipment was isolated from the van by means of an isolation transformer (not shown in Figure 5).

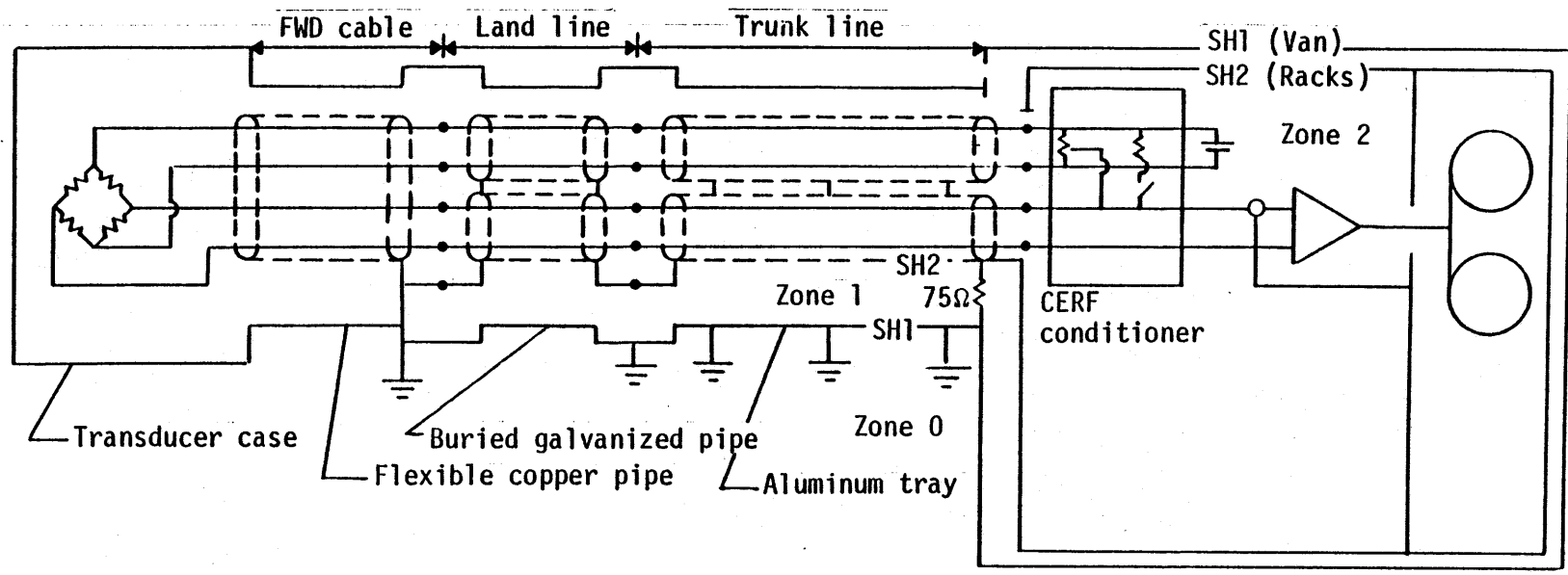


Figure 5. Grounding and shielding topology.

As another part of the experiment, van E-8 was entirely automated in a failsafe manner. The recording instruments were turned on by a closure from the timing-control center at T - 2 min. An alarm circuit was connected to the "reproduce" channel of the tape deck, on which the IRIG signal was recorded, so that if the recorder were turned on and not recording, a buzzer would sound and a red light would indicate that the system was not operating. This system is exactly the same as that used at the Nevada test site and was, in fact, borrowed from there. The purpose of this secondary experiment was to ensure that human involvement would be limited to monitoring and that the critical time and turn-on functions would be automated.

Returning to the primary experiment, the object was to compare the single-point, single-shield grounding system to the triple-shield continuous-grounding system. For the first, the shield is simply connected to the van; for the second, the primary shield is connected to the van in such a manner that there are no holes, and it is impedance-matched to the inner shields. Cabling for the first system is simply connected to a patch panel and run to the electronic system. For the second system, the cable must be routed carefully so that noise is minimized. These differences have given rise to the comment that the experiment was unfair. The response to this criticism has been and will always be that of course, it was unfair. It is always unfair to compare systems planned with extreme care with less carefully planned systems. In any well-thought-out grounding and shielding scheme, in fact, the source of noise within the topology must be eliminated, and external noise must be prevented from entering the system. When one designs a grounding and shielding system, one must consider the data-gathering system as a whole, not just the cable to be used and the location of the ground or grounds. The mathematical concept of topology explained previously formalizes this practice and provides a convenient way of mapping and representing the grounding and shielding system.

For instance, no direct penetrations were permitted through shield 1. FIDU, IRIG, and closures were isolated through transformers or relays. It has been suggested that it would have been fairer to run another cable into van E-8 and use the normal shielding practices on it. The noise figures on this

cable could then have been compared to those produced on the cable tray experiment. This procedure could not be used, however, because the second cable would have violated the topology of the shielding experiment and thus would have been a conduit for noise into the van.

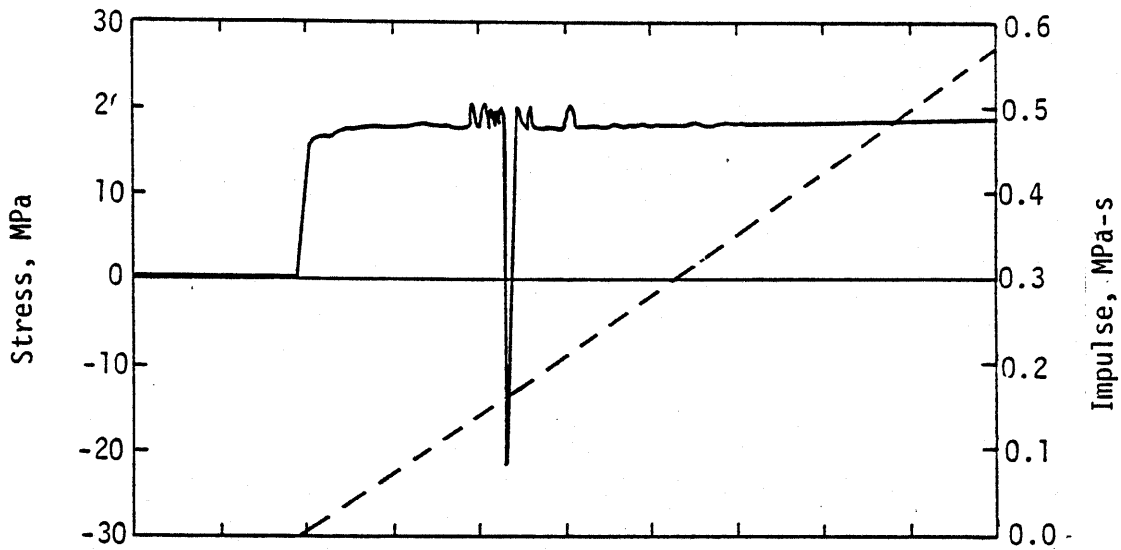
The motion data taken from the experiments are shown in Figures 6 and 7. The stress data for the various measurement numbers (MN) appear in Table 2. It should be noted that the accuracy of the gage that failed at shock arrival (MN 9043) had been questioned before the test because the bridge had a high-impedance ( $7\text{-M}\Omega$ ) leak to ground. The data appear to be quite reasonable in that the peak values taken in van E-3 agree well (for stress data) with those taken in van E-8. This agreement averaged at  $\pm 8$  percent with the mean at a given depth in SIMCAL III.

The difference in the amount of noise recorded on the two sets of measurements was considerable. The root mean square (rms) peak signal-to-noise ratio was determined by a comparison of the peak signal value with the rms noise just before shock arrival. The average value for the data taken from van E-3 was slightly less than 20 and for the data taken from van E-8, greater than 200.

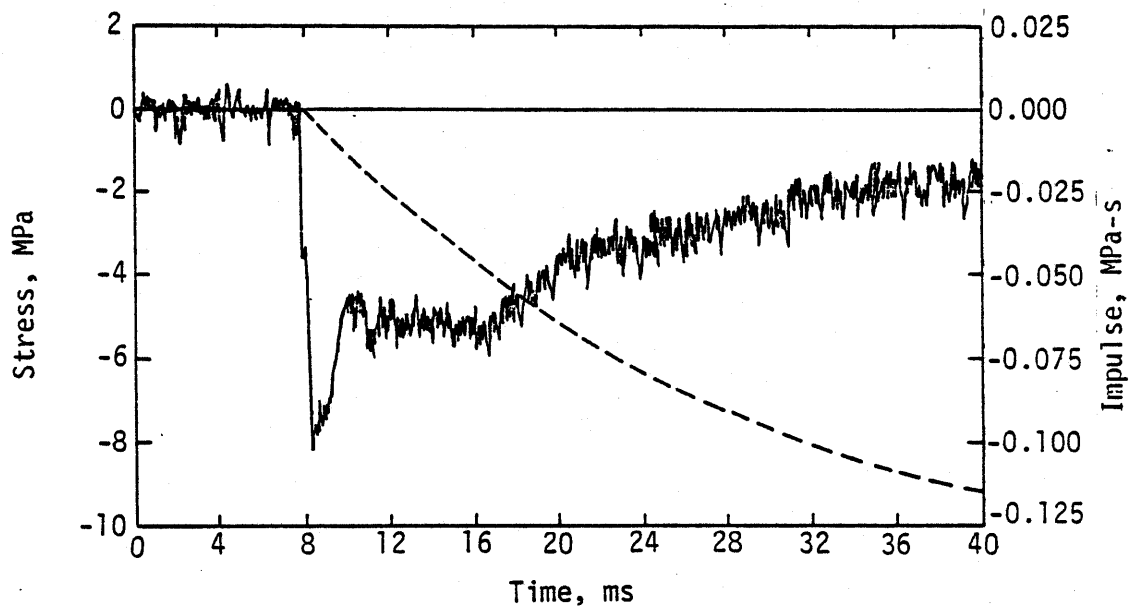
Of course not all of the noise in van E-3 can be attributed to the exterior topology of the grounding system, but the noise value was probably influenced significantly by what was allowed inside that topology. The reader should recognize, however, that no shielding system will protect against noise generated inside the shield. Thus, it is extremely necessary to take into account all possible noise generators when designing an experiment and to either eliminate them or isolate them from the experiment.

The only other noise specification that was measured was what the author chooses to call quiescent noise; namely, the noise produced at the van end when neither the van nor the gages is powered. In van E-8 the quiescent noise was not measurable with the available equipment because it was less than 0.2 mV, the line width of the available oscilloscope trace.



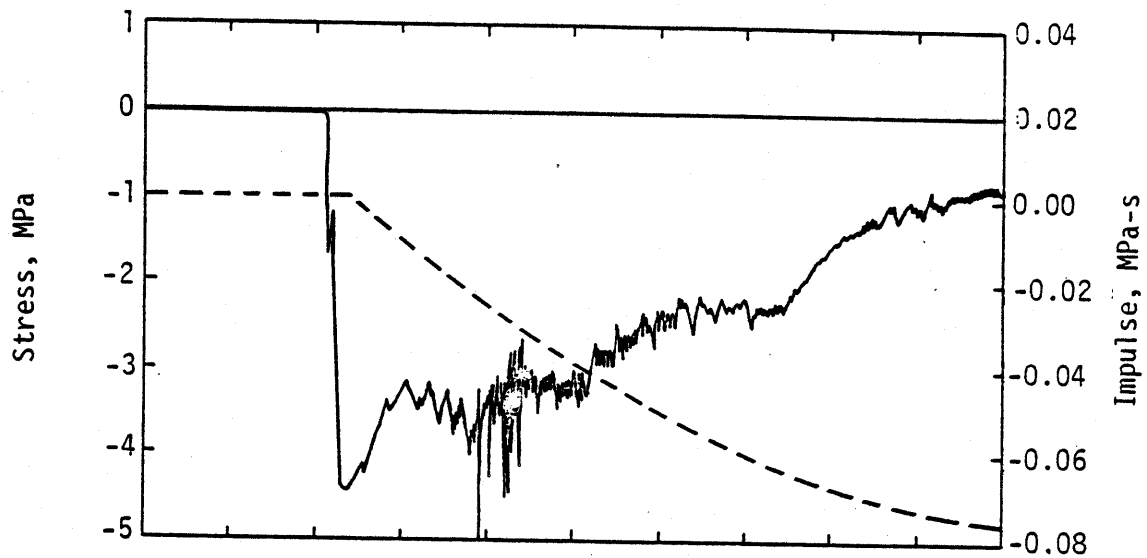


(a) Van E-8, MN 9043.  
(gage failed at shock arrival)

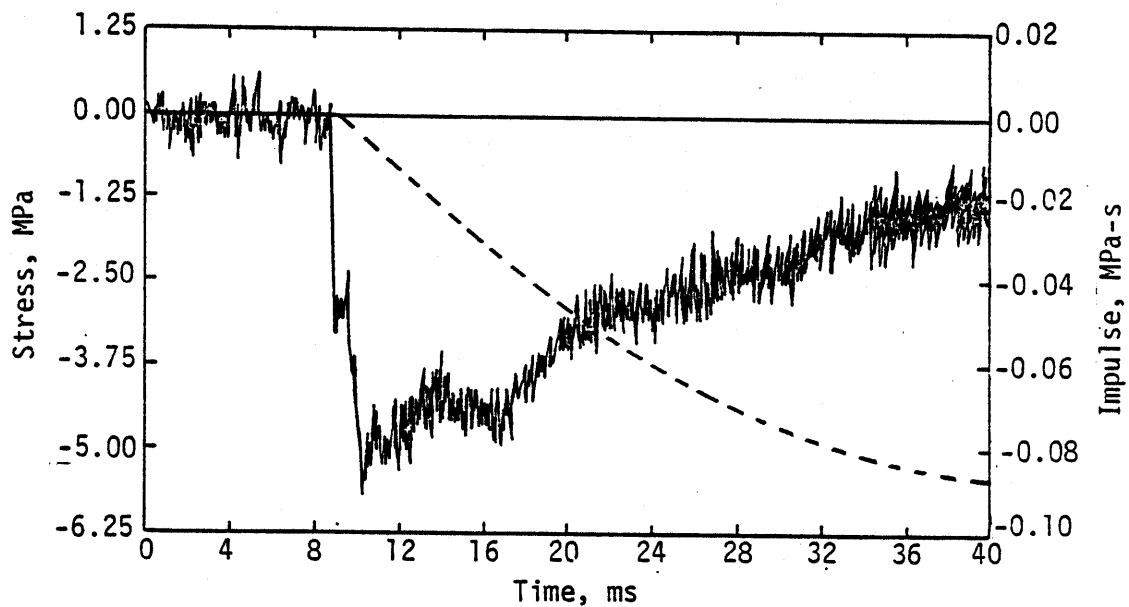


(b) Van E-3, MN 9047.

Figure 6. SIMCAL III motion data.

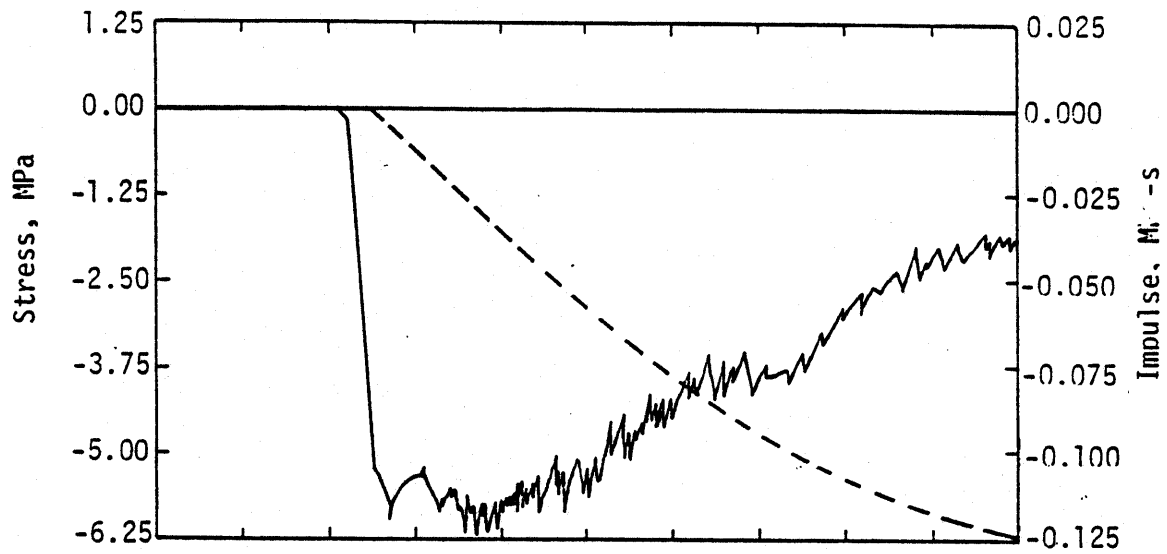


(c) Van E-8, MN 9041.

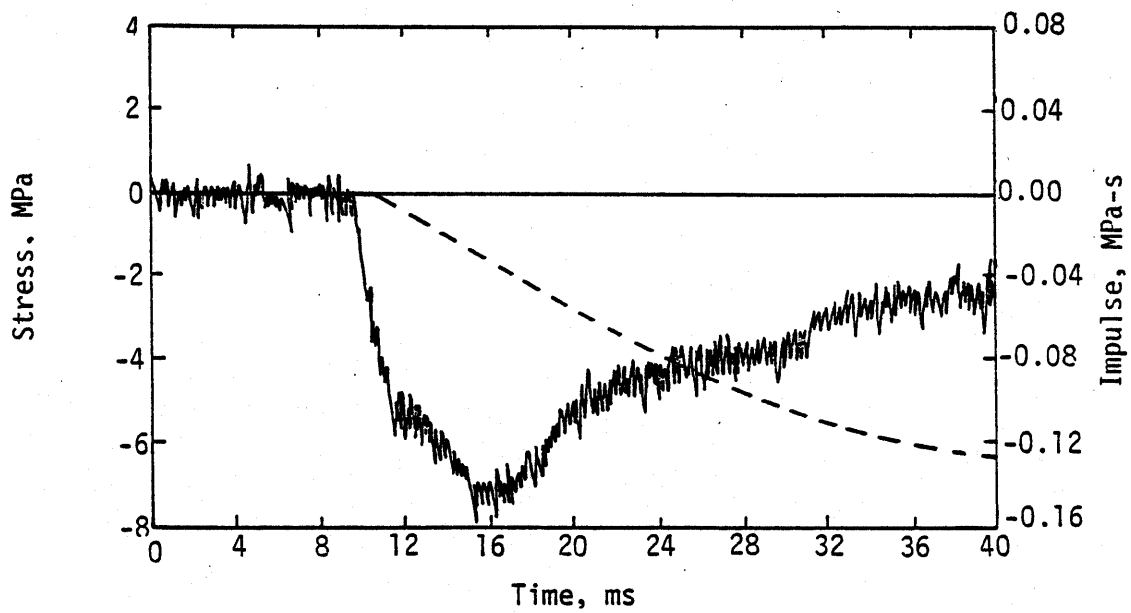


(d) Van E-3, MN 9045.

Figure 6. Continued.

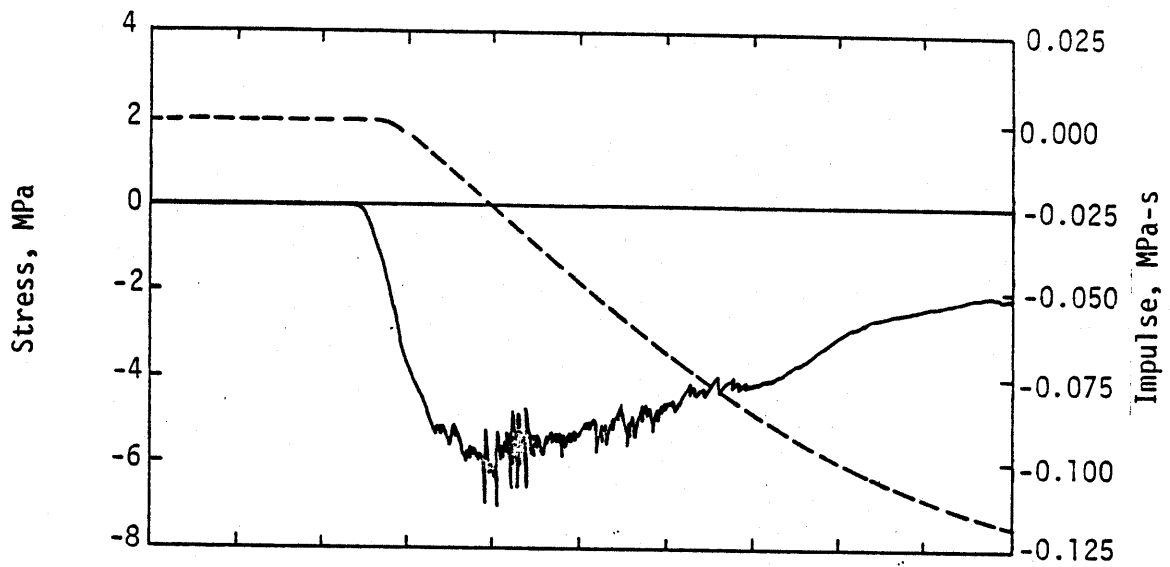


(e) Van E-8, MN 9042.

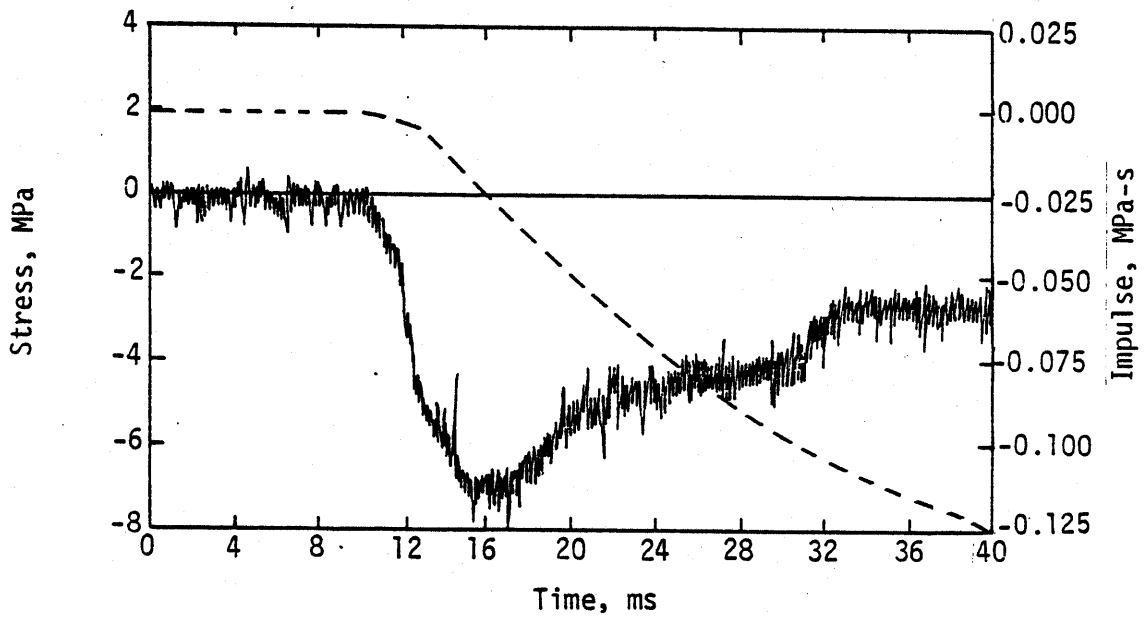


(f) Van E-3, MN 9046.

Figure 6. Continued.

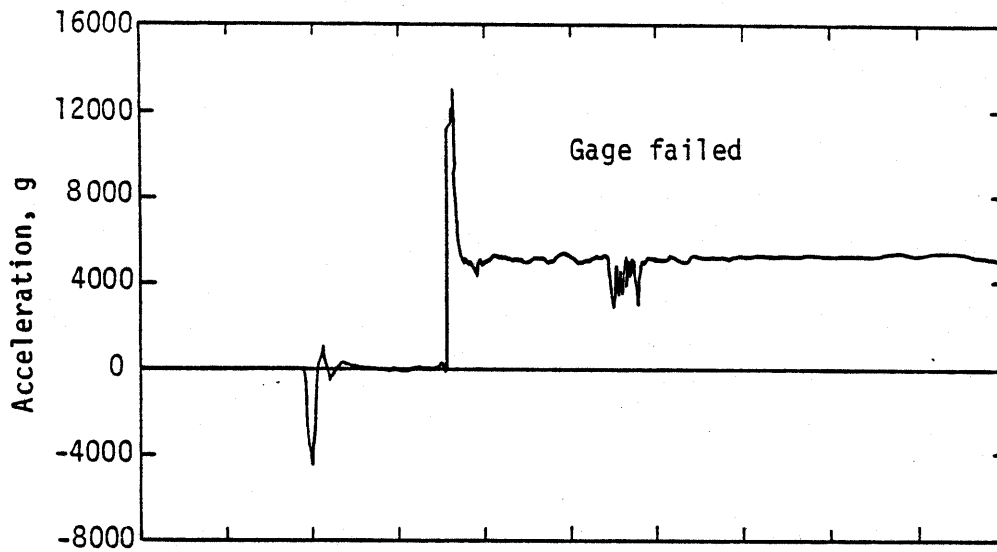


(g) Van E-8, MN 9044.

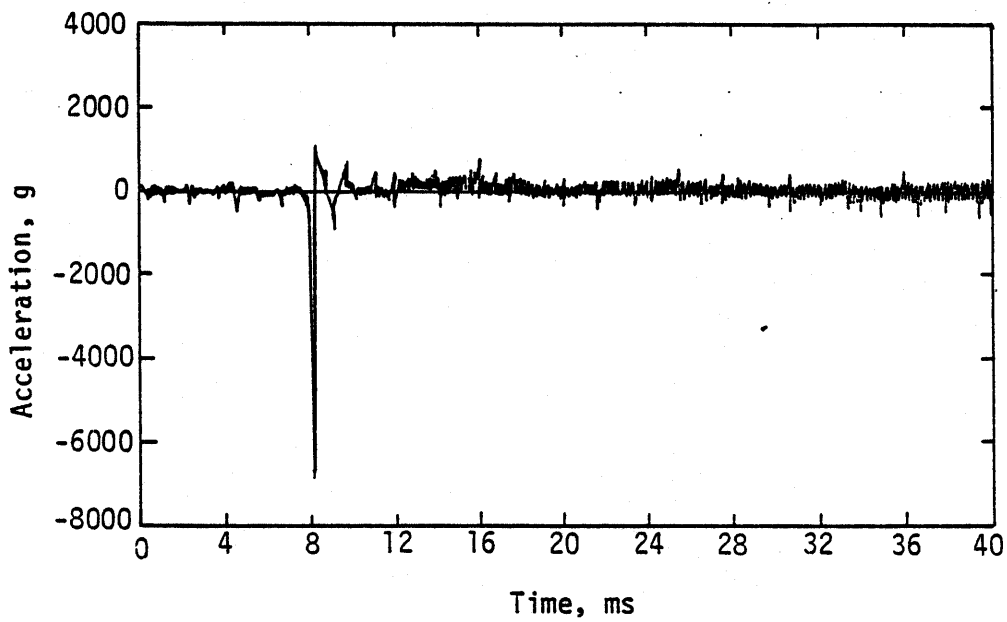


(h) Van E-3, MN 9048.

Figure 6. Concluded.

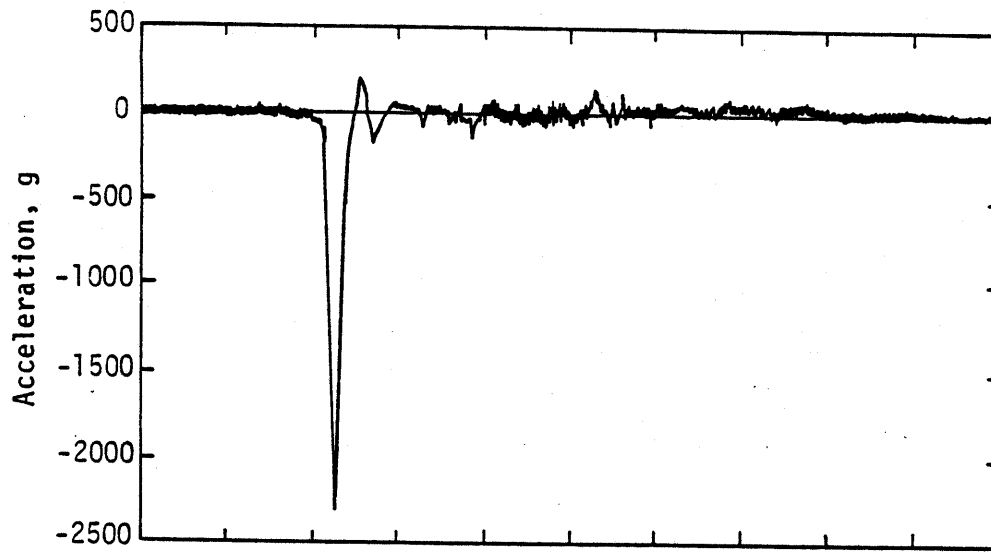


(a) Van E-8, MN 9015.

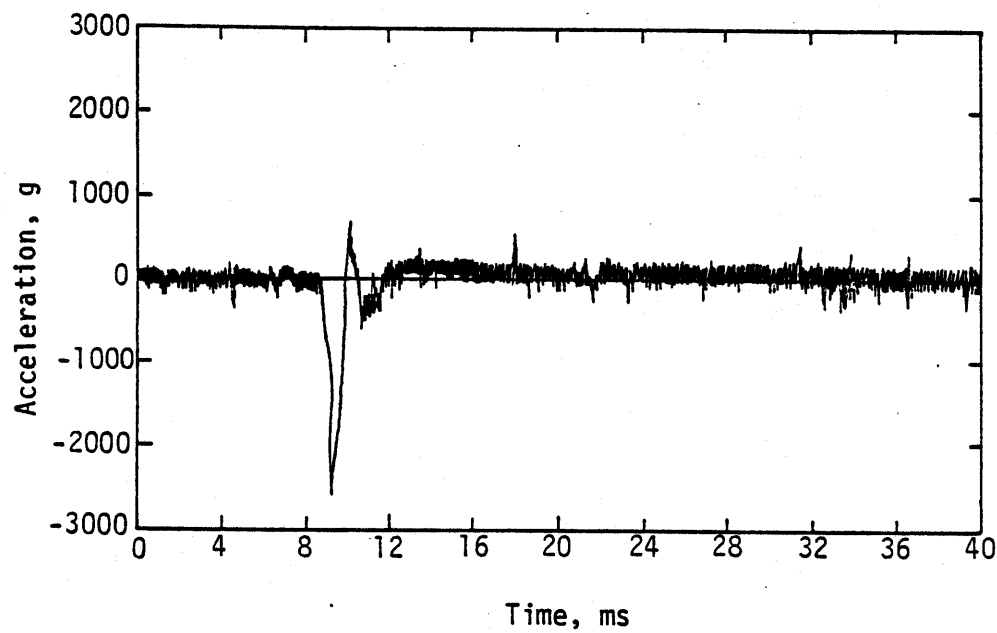


(b) Van E-3, MN 9016.

Figure 7. SIMCAL III acceleration data.



(c) Van E-8, MN 9017.



(d) Van E-3, MN 9018.

Figure 7. Concluded.

TABLE 2. STRESS-GAGE RESULTS

Depth, m	MN	Peak stress, MPa
0.150	9043	Gage failed at shock arrival
0.150	9047	8.0
0.300	9041	4.4
0.300	9045	5.0
0.600	9042	5.8
0.608	9046	7.0
1.035	9044	5.8
1.013	9048	7.0

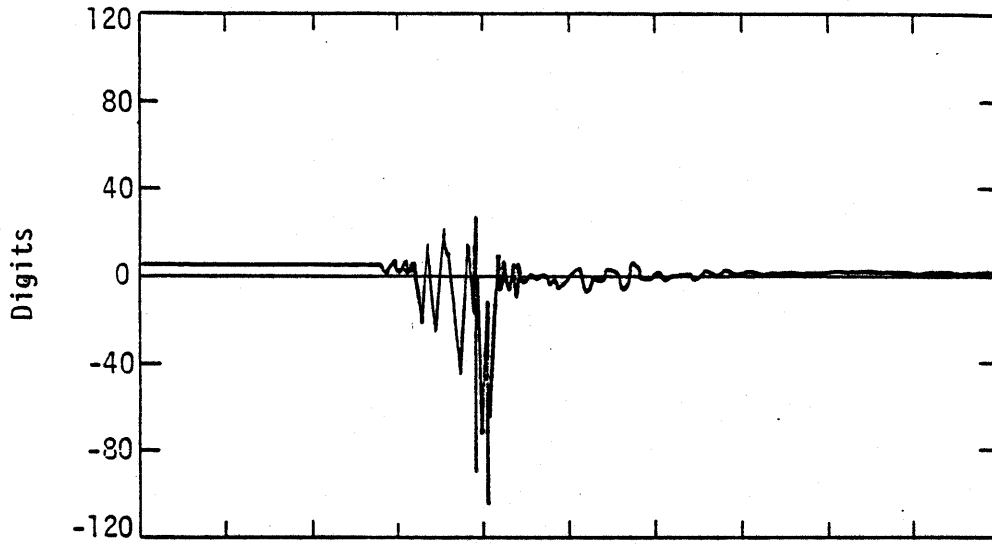
The reported value of this quiescent noise in the other vans was 2 mV to 5 mV peak to peak. The apparent noise burst around 16 ms was either due to electrical causes or the result of mechanical effects on the junctions. The author speculates that the latter was the cause because noise appears at the other gages at nearly but not exactly the same time.

The dummy bridge outputs are shown in Figure 8. These gages behaved somewhat like accelerometers when the shock arrived at their location.

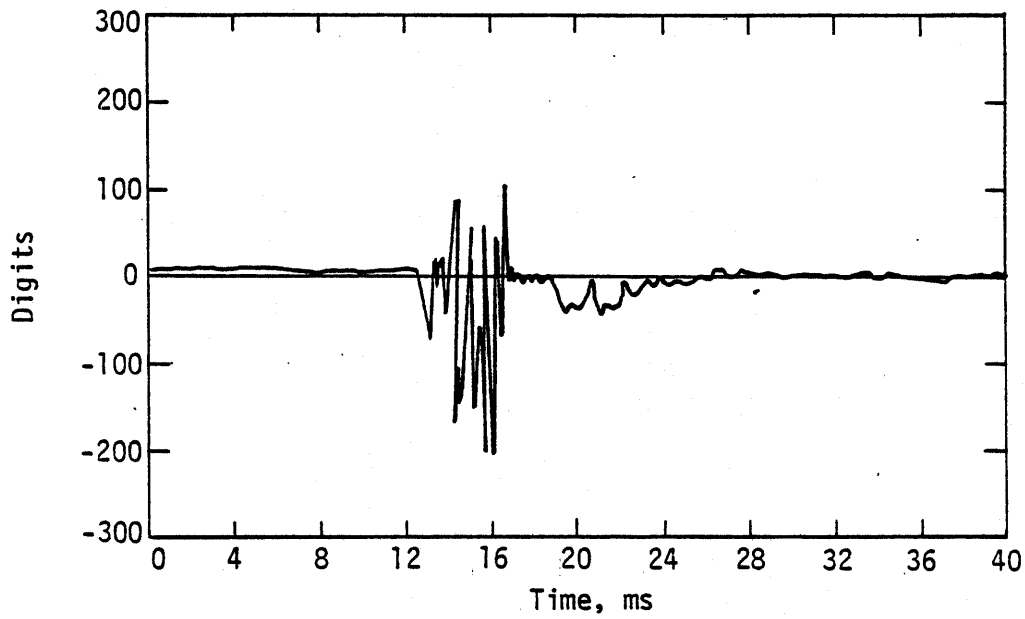
The conclusion can be reached that the data obtained in van E-8 were much cleaner than those obtained in van E-3 because of the exterior cable shield (as demonstrated by the quiescent noise) and the care taken within the topology. It was therefore decided that this philosophy of grounding and shielding should be considered for future applications and that an effort would be made to improve the ease of installation and to lower the cost of the outer shield. It was also recommended that van E-3 be analyzed and that it be considered for upgrading.

#### CLOSE-IN DATA-ACQUISITION EXPERIMENTS

The results of the SIMCAL III experiment led to the conceptualization of ways in which the cost of implementing the SIMCAL III type of grounding and shielding could be reduced. Since the cost of the shield increases



(a) MN 9019.



(b) MN 9020.

Figure 8. Dummy bridge data.



linearly with the length of the cable, one obvious solution was to shorten the cable. Another was to reduce the thickness of the shield while maintaining a good low-impedance ground.

Consequently, an experiment was performed in conjunction with the HAVE HOST VST for the purpose of demonstrating the efficacy, practicality, and economy of using an improved grounding and shielding system in conjunction with a data-acquisition van placed relatively close to the test bed. This experiment was called the Close-In Data-Acquisition System (CIDAS). The experiment consisted of two parts: (1) to ascertain how much the quality of the data could be improved by the use of an improved grounding system and shorter signal cables (VST Grounding and Shielding Experiment), and (2) to determine the amount of airblast and ground shock received at the protected van location (Van Environment Experiment).

VST Grounding and Shielding Experiment--The grounding and shielding scheme used in this experiment was considerably different from that used to take other measurements on the HAVE HOST VST. The ground was a continuously buried, bare no. 4 copper wire that was connected to the outer shield of the cable every 6 to 7 m ( $\approx 8$  MHz). The connection used was bus wire soldered to the outer drain wire on the 20-pair shield and to the bare copper wire. A tree map of this scheme is shown in Figure 9.

The actual experiment employed two triax gages (six channels of data) and two strain gages, all recorded in van E-8. Data from these gages were compared to those obtained from other similarly located gages in the B-structure, recorded in van E-1. There were other differences, in addition to the grounding and shielding, in the way in which the signals were handled. For the comparable measurements recorded in van E-1, the signal was amplified by close-in amplifiers. This means that the signal level was of the order of 200 to 1200 mV at van E-1, while the signal levels at van E-8 were of the order of 4 to 19 mV. The cable used for the comparable measurements was Madison 4 conductor between the transducer and the amplifier and 20-pair trunk line connecting into van E-1. For CIDAS, the cable was a continuous 20-pair to the splices in the structure.

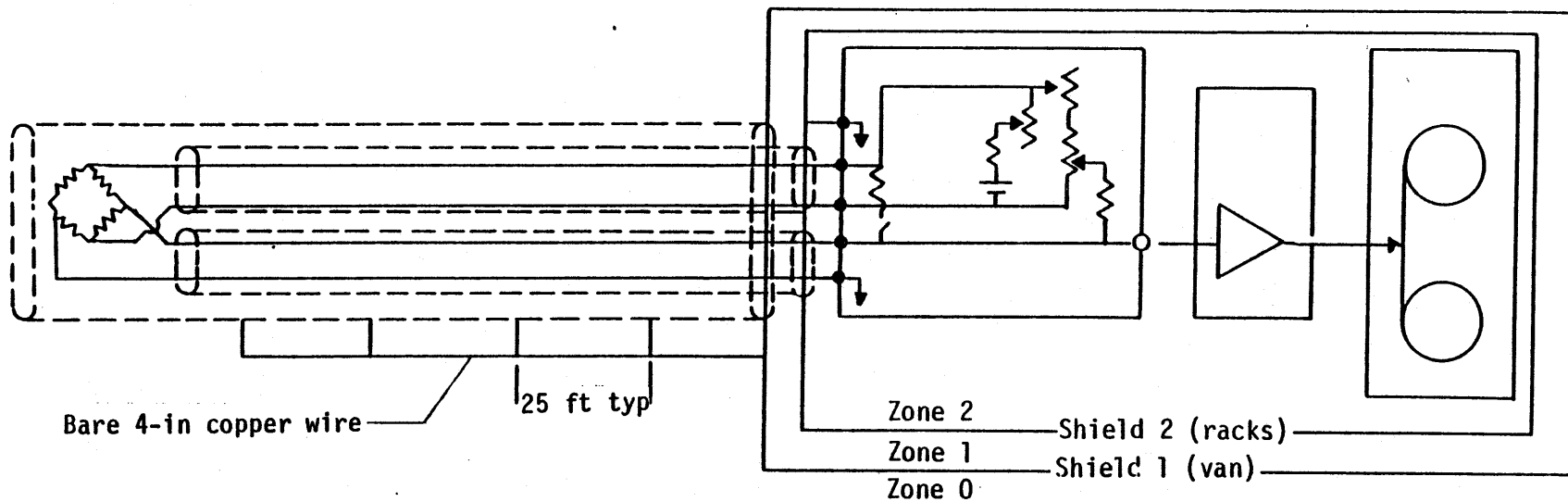


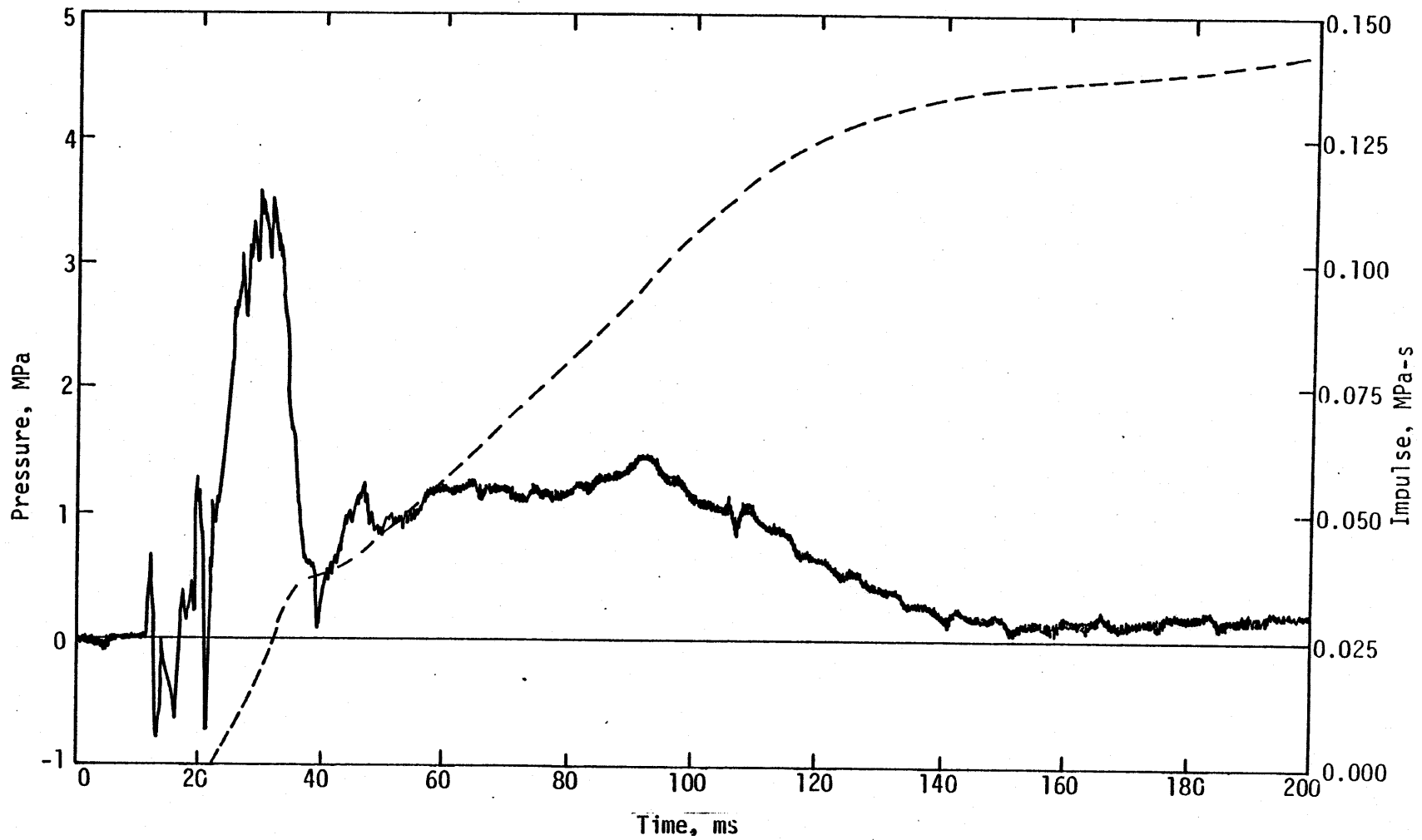
Figure 9. Partial tree map showing one channel of VST grounding and shielding experiment topology.

The signals received in the experimental van and the comparable measurements from the B-structure are shown in Figures 10 through 16. The noise on the comparable measurements is of two types: noise bursts, probably induced by EM sources; and steady-state noise, induced by cable ring or pickup within the signal conditioning equipment. With the notable exception of the noise that appears on virtually every channel at between 20 and 25 ms, the data obtained by means of the CIDAS grounding and shielding system was clearly and significantly of better quality than that obtained when a single-point ground and open shields were used. A quantitative signal-to-noise figure is not given because both transient and continuous types of noise were evident, the methods of quantification are as numerous as the quantifiers, and it is obvious to the naked eye that the CIDAS data are much quieter than the data from the B-structure gages. Thus the author will leave it as an exercise for the reader to use whatever quantification procedure he chooses.

The low-frequency noise that appeared on both the CIDAS and the comparable measurements at between 20 and 25 ms is due to one of two things: (1) channels 6719 (Fig. 10c) and 6720 (Fig. 12c) failed at that time, which may have caused a  $\dot{B}$ -coupling to the other channels; or (2) triboelectric noise was possibly induced when the shock wave arrived at the exterior cable trench.

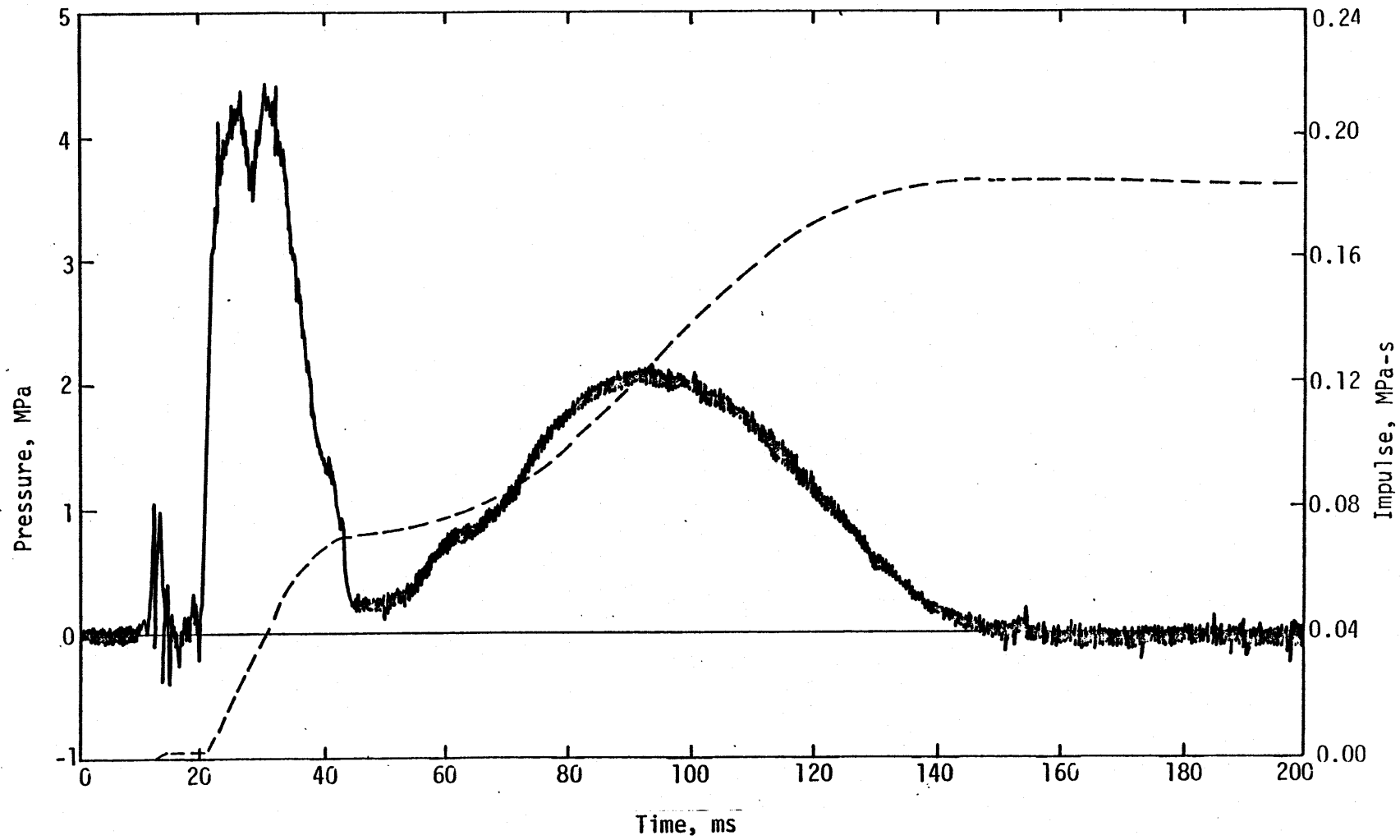
The one spike on measurement 3733 (Figure 16a) at 47 ms most likely came from mechanical sources as it does not appear on even adjacent channels. However, it should be noted that in the case of the strain gages, the shielding topology was violated because the gages had been emplaced in the vertical shelter with no shields around them, and it was of course impossible to shield them after they had been cast in concrete.

In summary, one may say that insofar as noise is concerned, CIDAS significantly improved the quality of the signal. In other words, paying careful attention to the topology of the shielding system and using a good distributed or continuous ground pays off in the form of better data quality.



(a) CIDAS normal pressure, MN 6713.

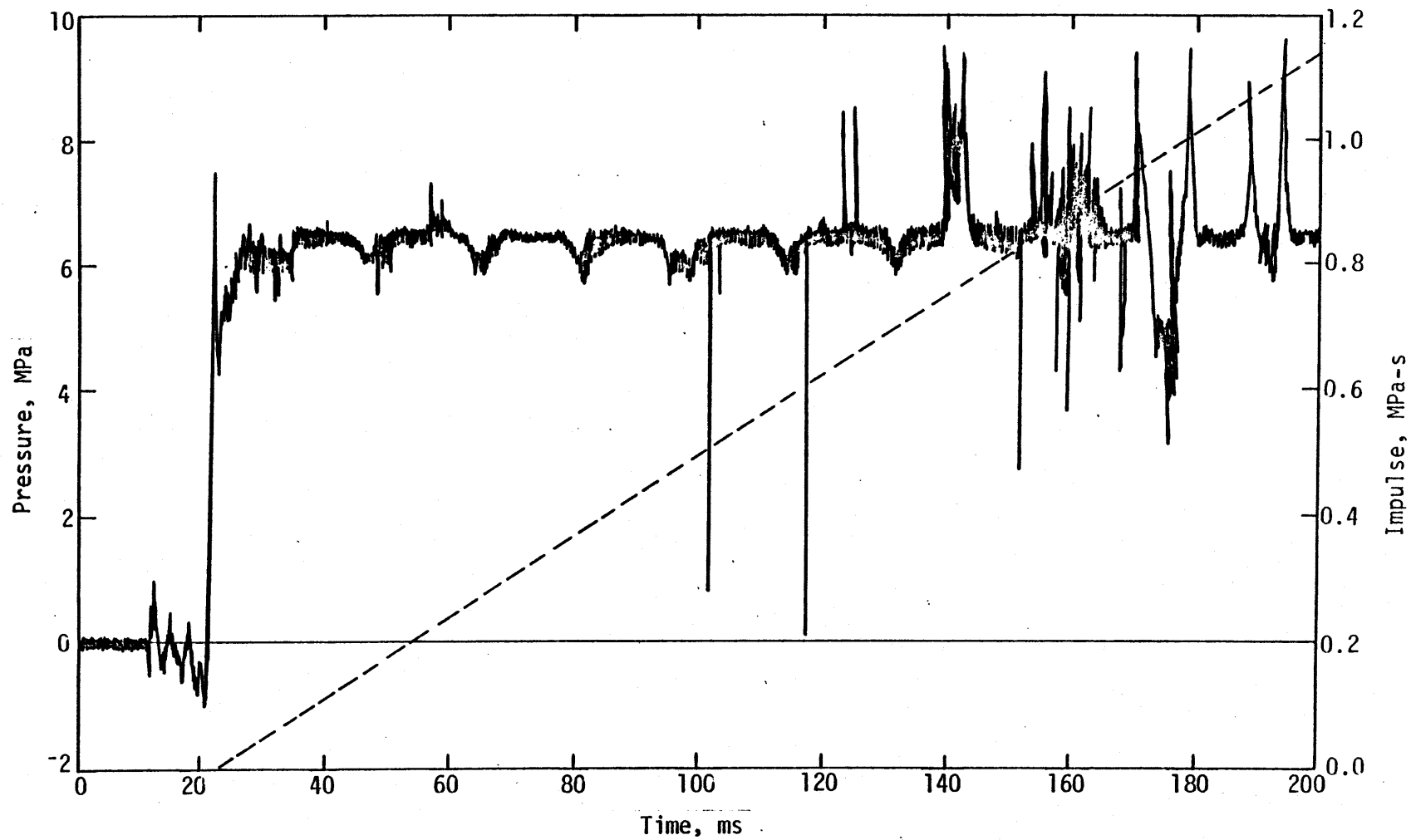
Figure 10. Comparative stress measurements, qage 1.



(b) Comparable measurement from B-structure, MN 6716.

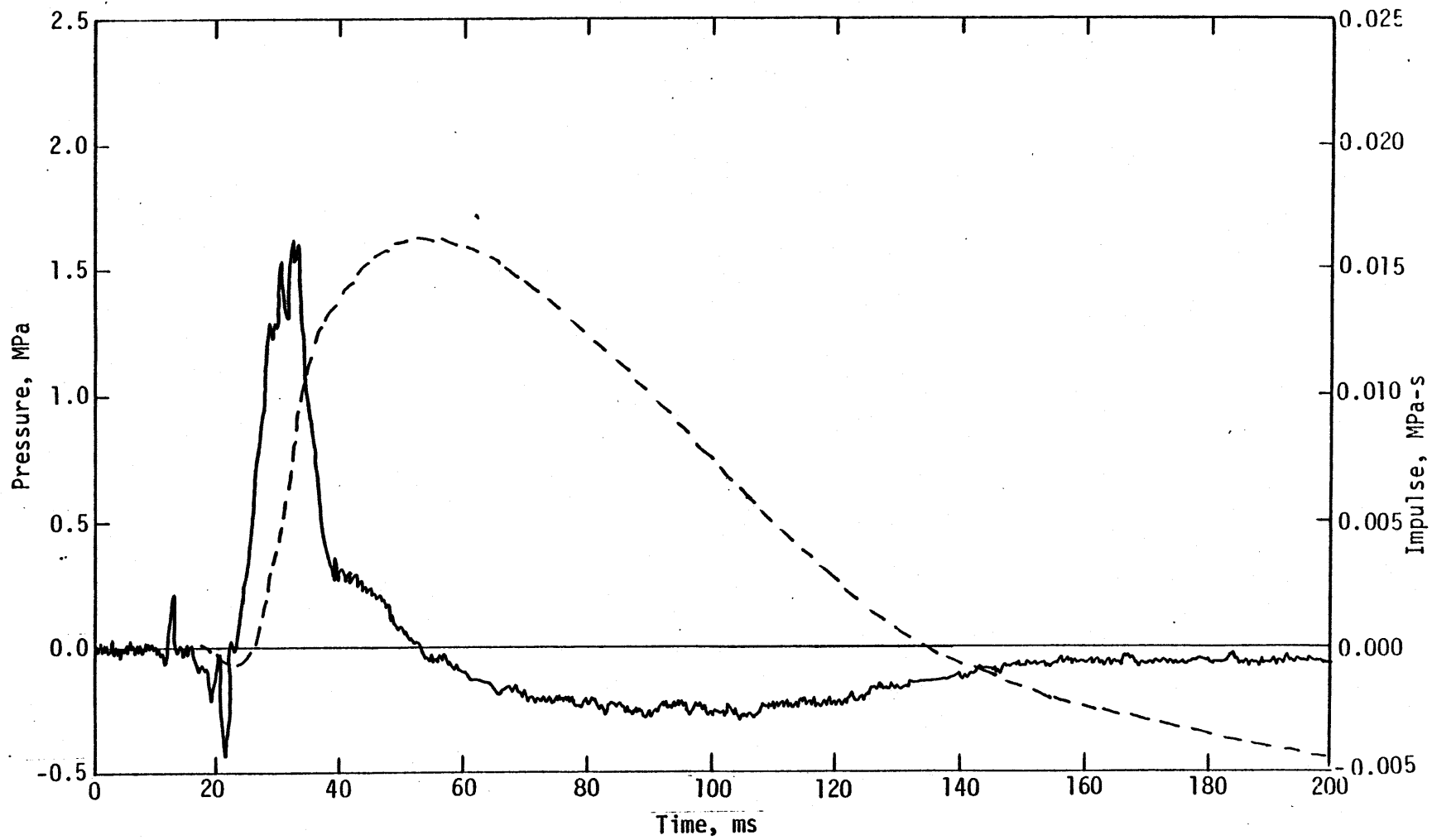
Figure 10. Continued.

30



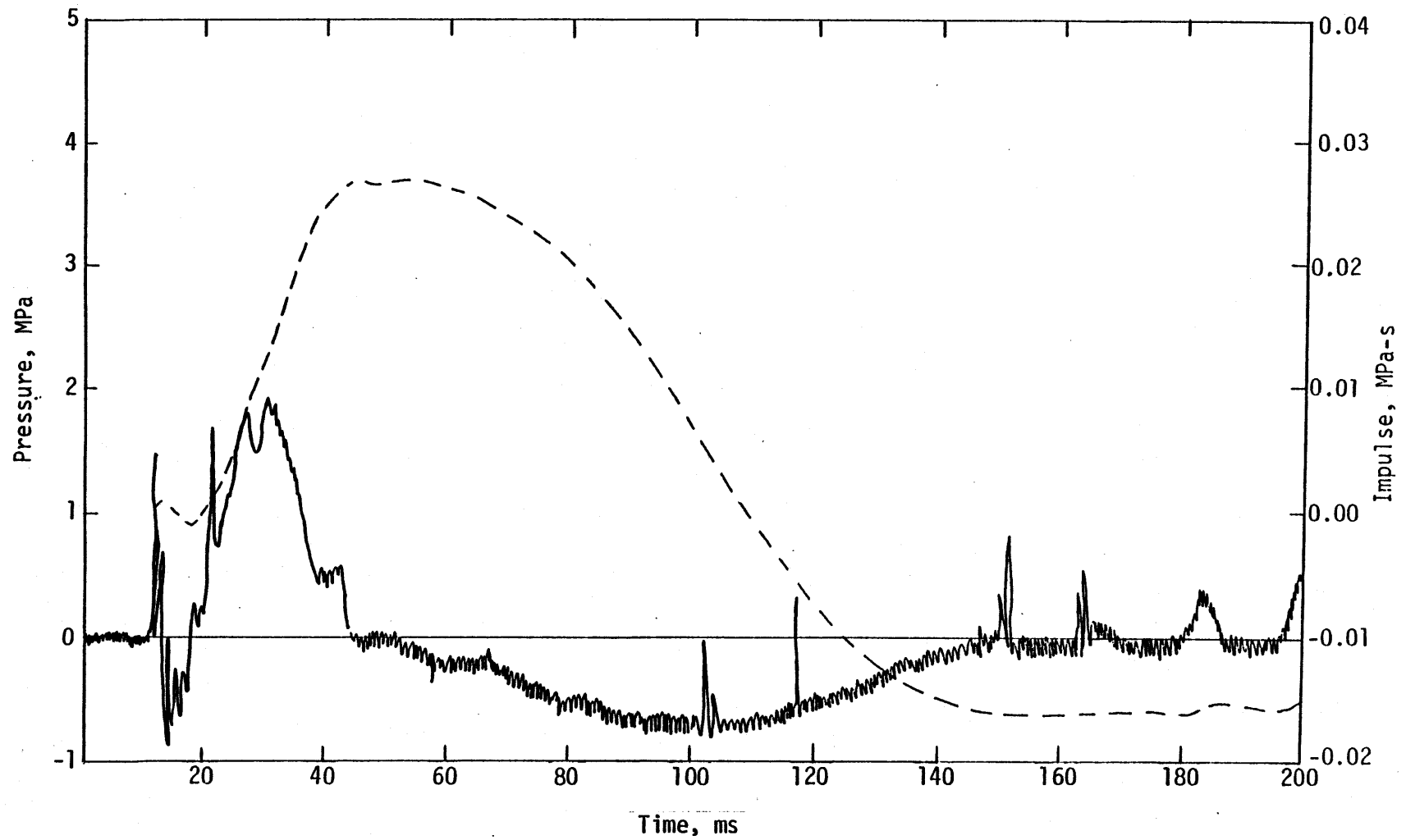
(c) Comparable measurement from B-structure, MN 6719.

Figure 10. Concluded.



(a) CIDAS, MN 6714.

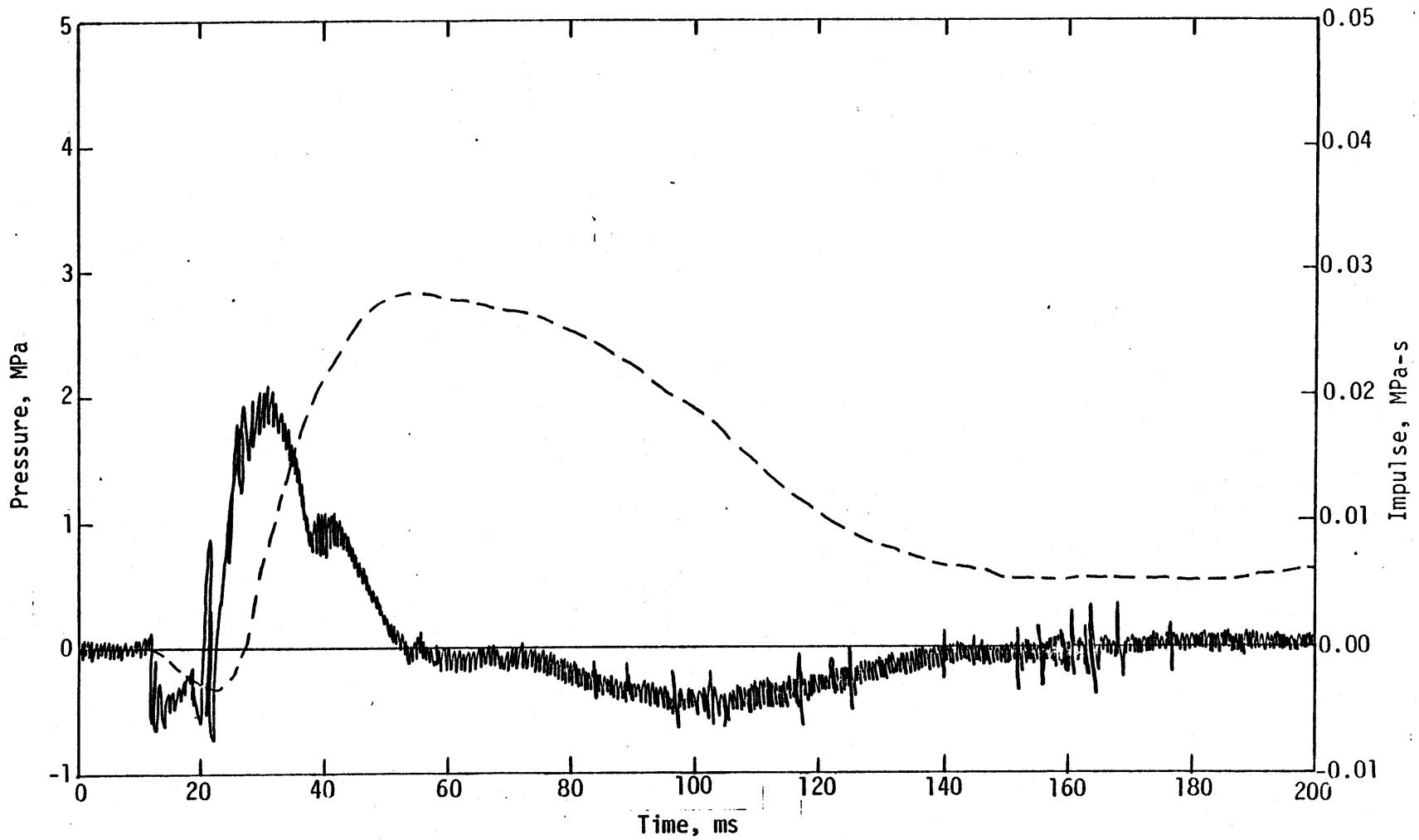
Figure 11. Comparative vertical shear measurements, gage 1.



(b) Comparable measurement from B-structure, MN 6717.

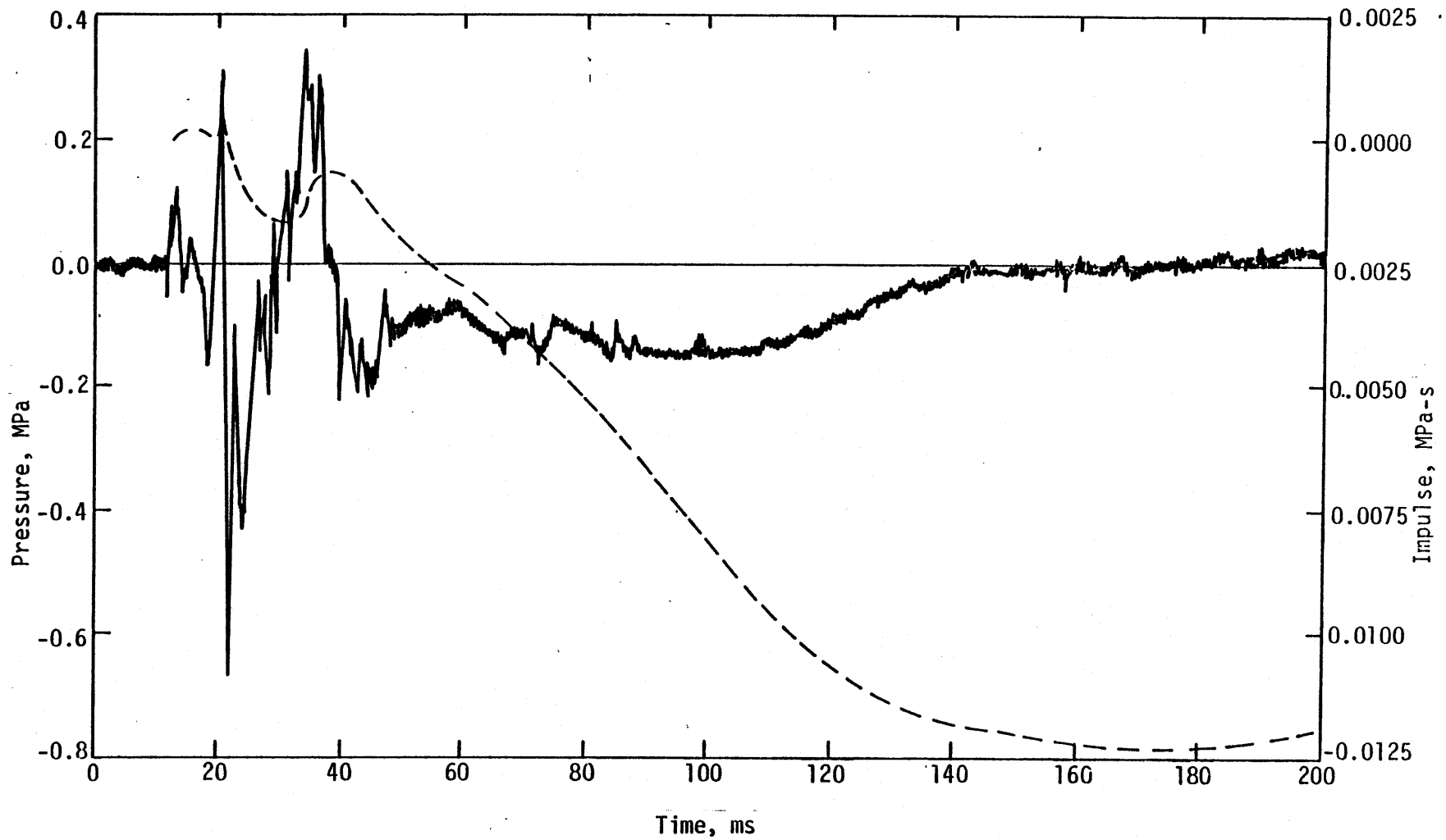
Figure 11. Continued.





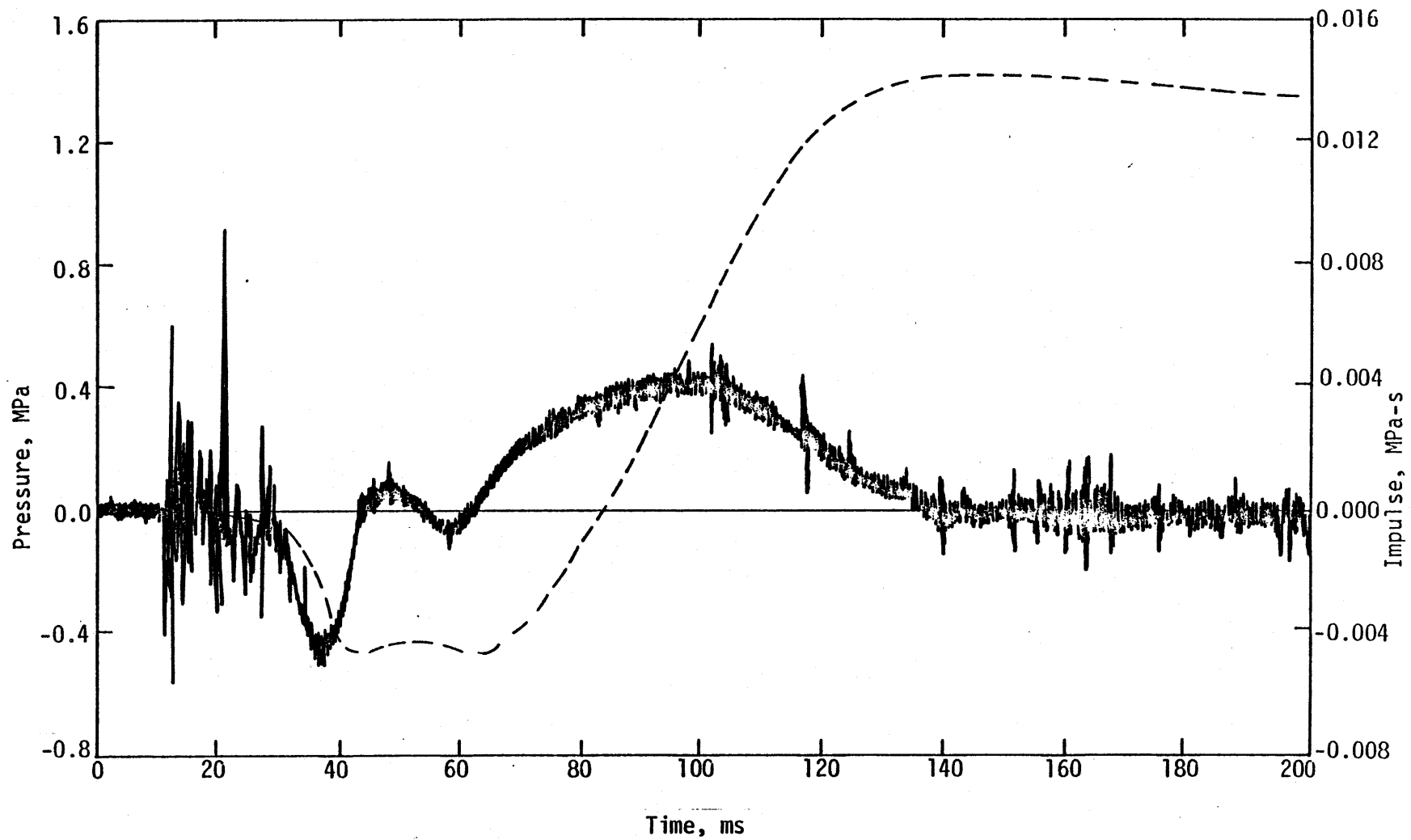
(c) Comparable measurement from B-structure, MN 6720.

Figure 11. Concluded.



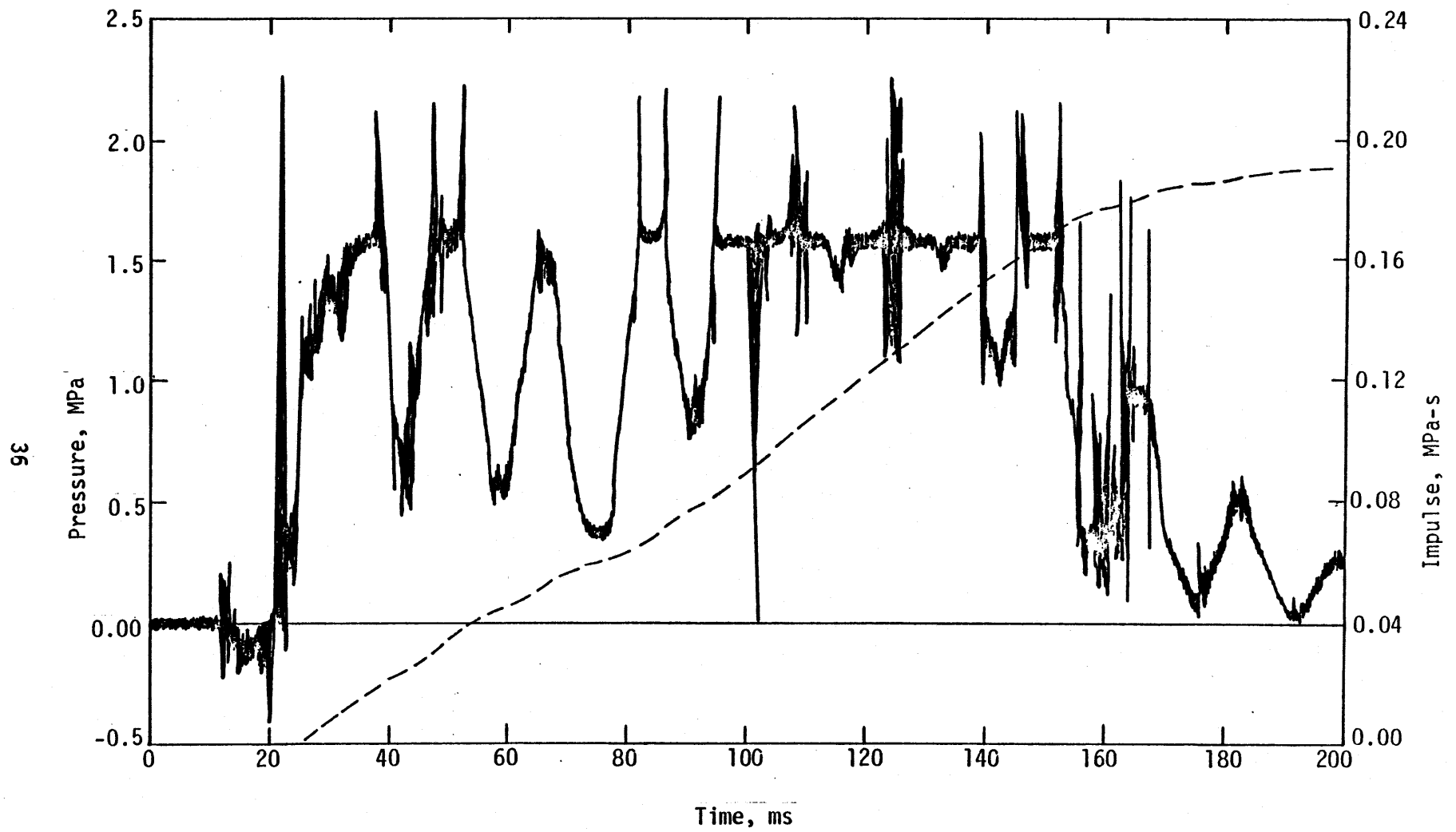
(a) CIDAS, MN 6715.

Figure 12. Comparative tangential shear measurements, gage 1.



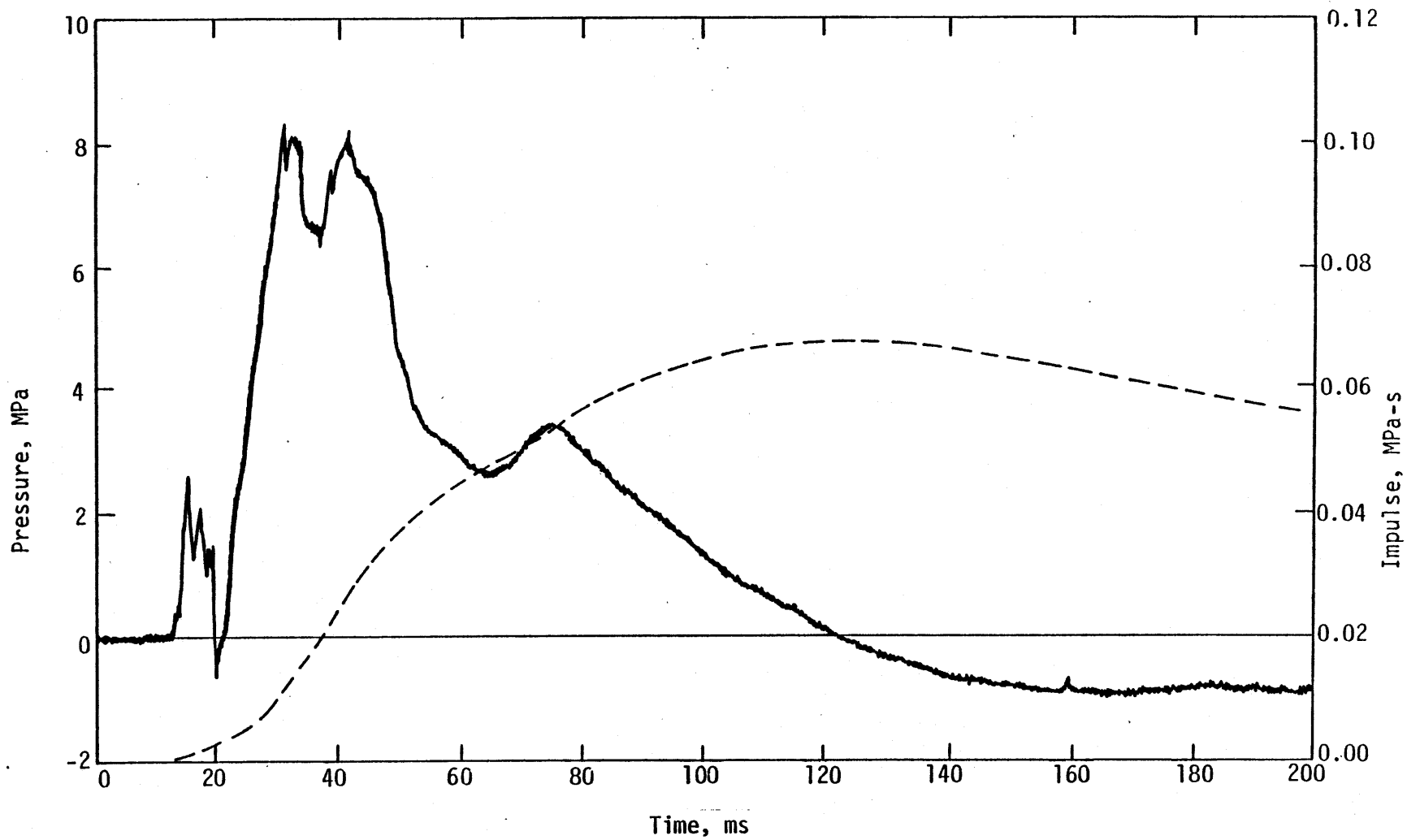
(b) Comparable measurement from B-structure, MN 6718.

Figure 12. Continued.



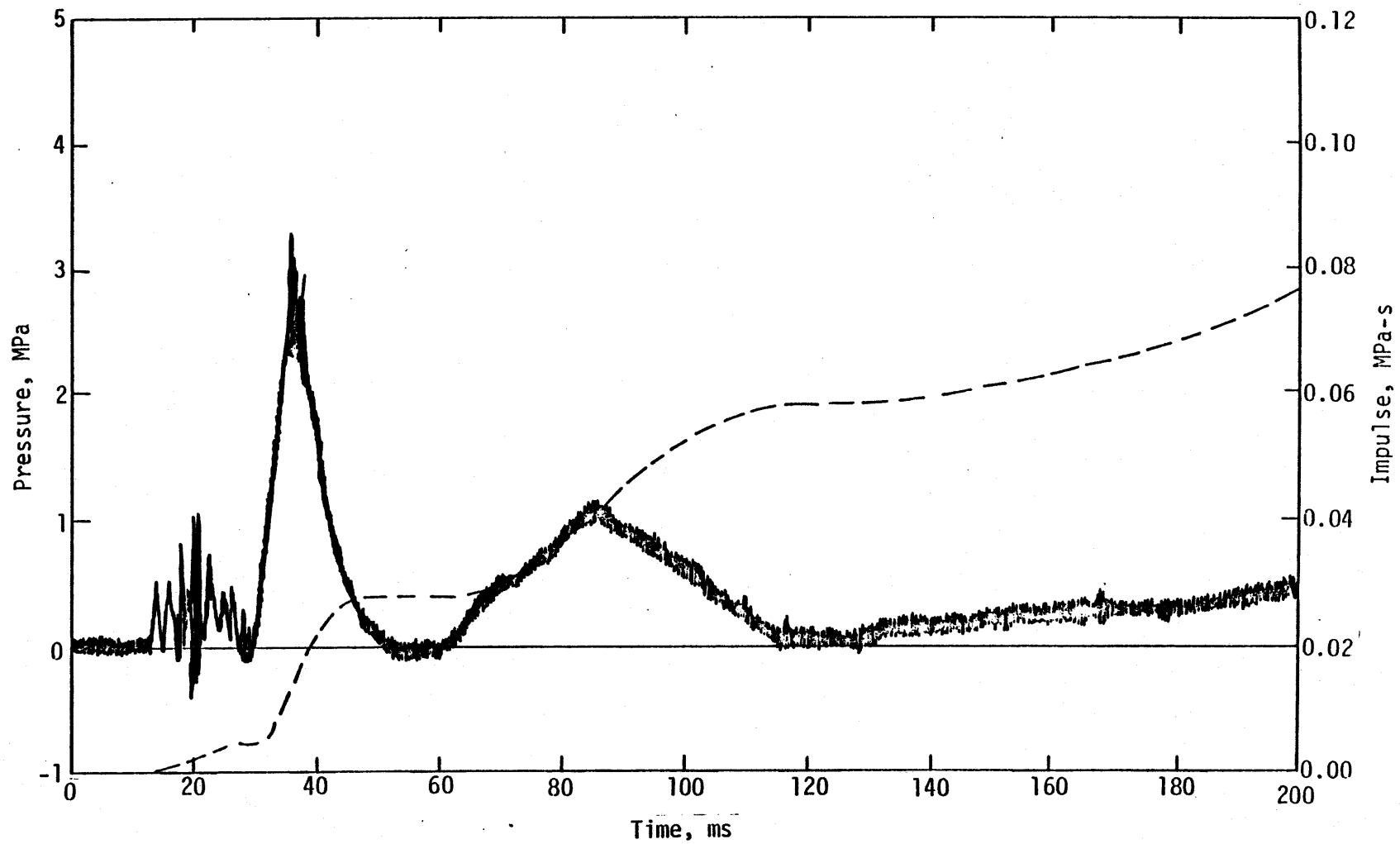
(c) Comparable measurement from B-structure, MN 6721.

Figure 12. Concluded.



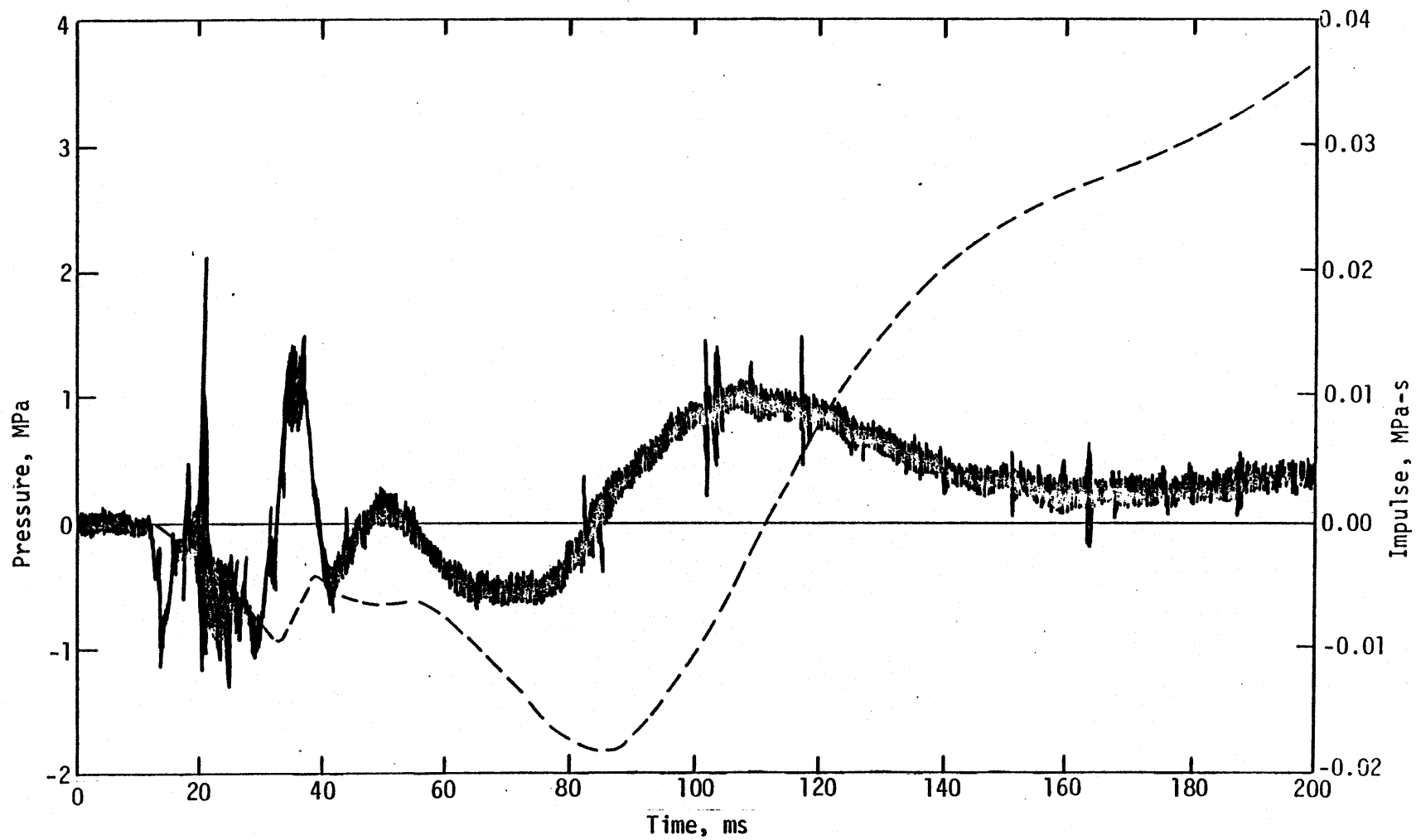
(a) CIDAS normal pressure, MN 6725.

Figure 13. Comparative stress measurements, gage 2.



(b) Comparable measurement from B-structure, MN 6728.

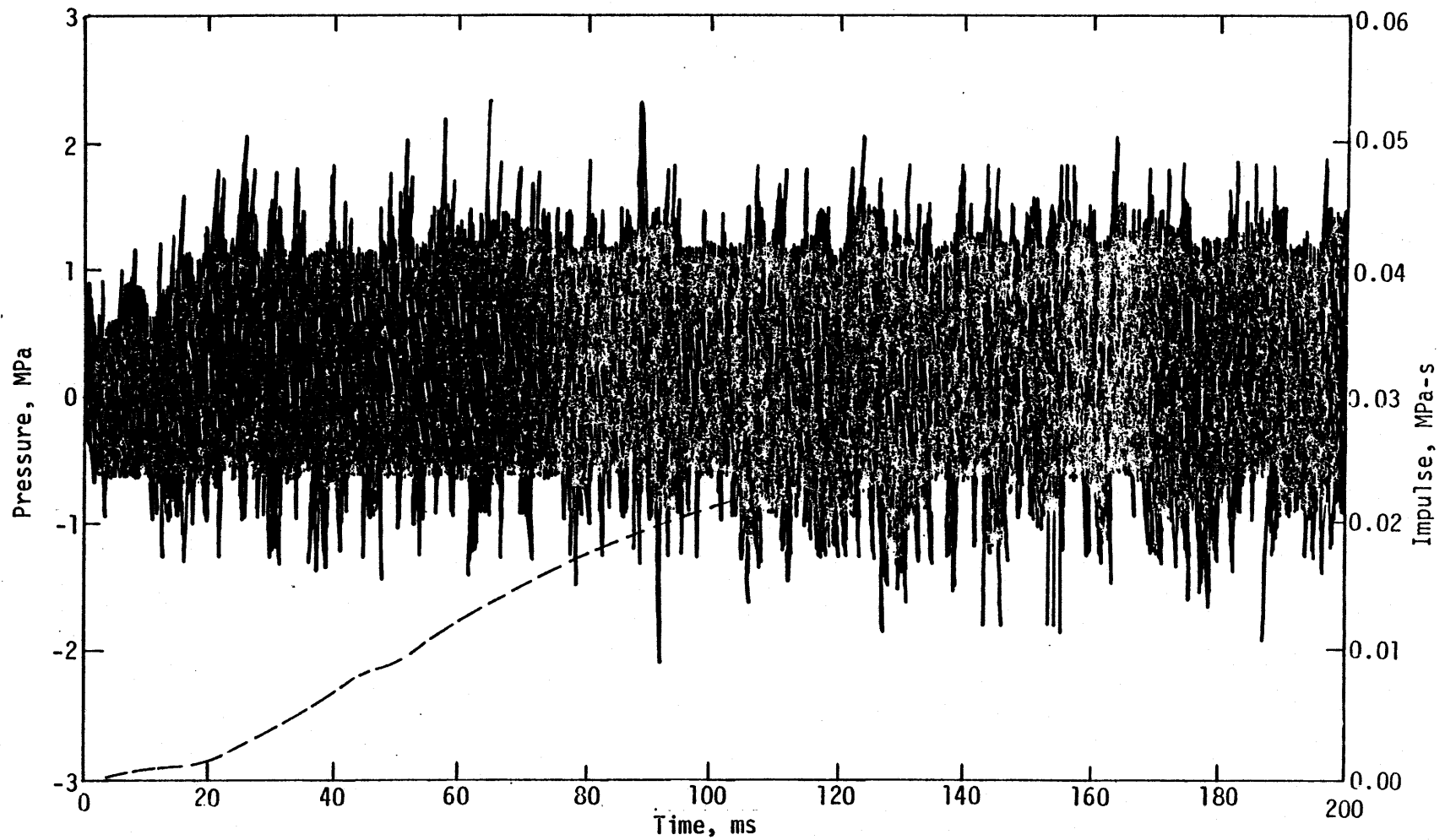
Figure 13. Continued.



(c) Comparable measurement from B-structure, MN 6731.

Figure 13. Continued.

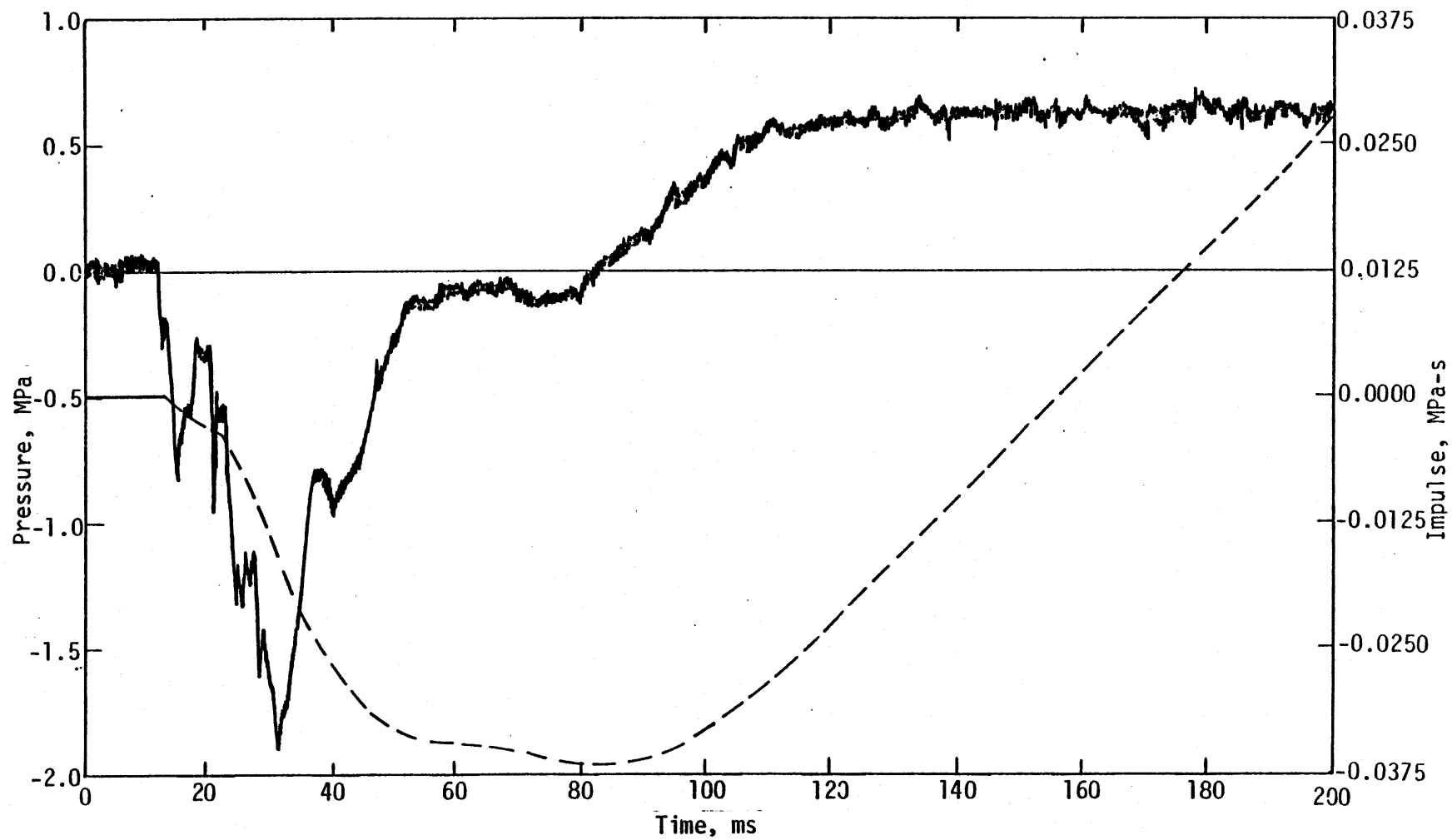
40



(d) Comparable measurement from B-structure, MN 6734..

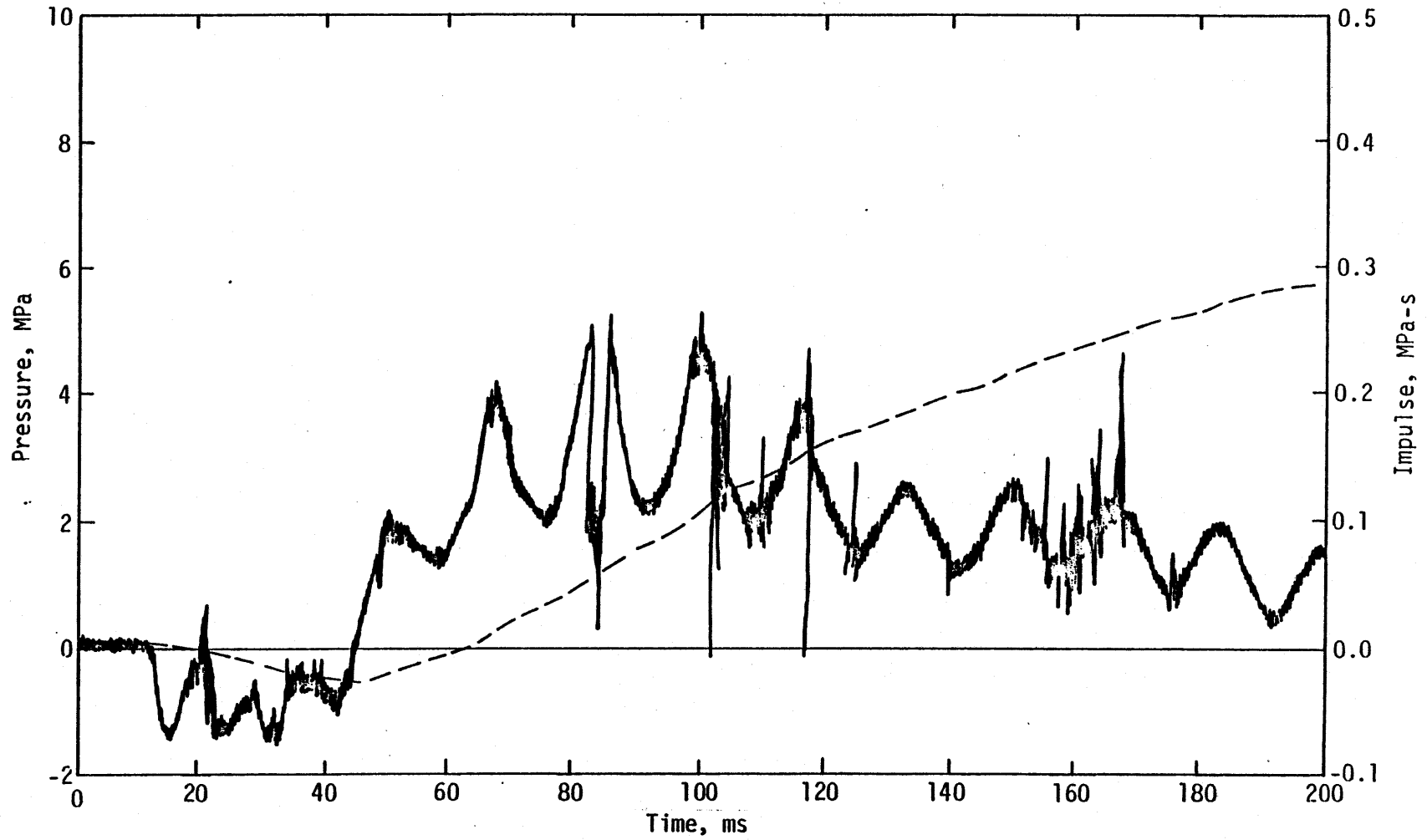
Figure 13. Concluded.





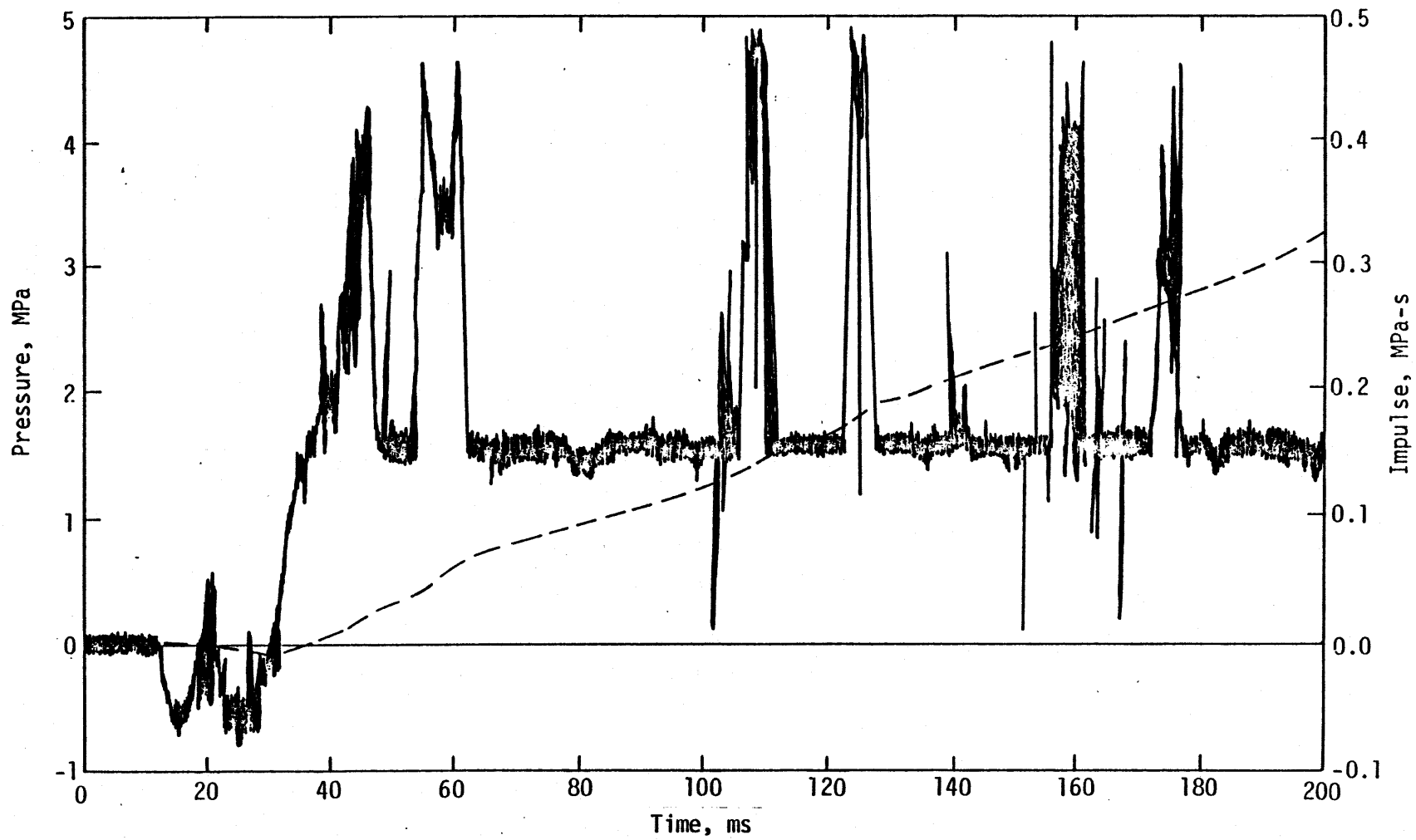
(a) CIDAS, MN 6726.

Figure 14. Comparative vertical shear measurements, gage 2.



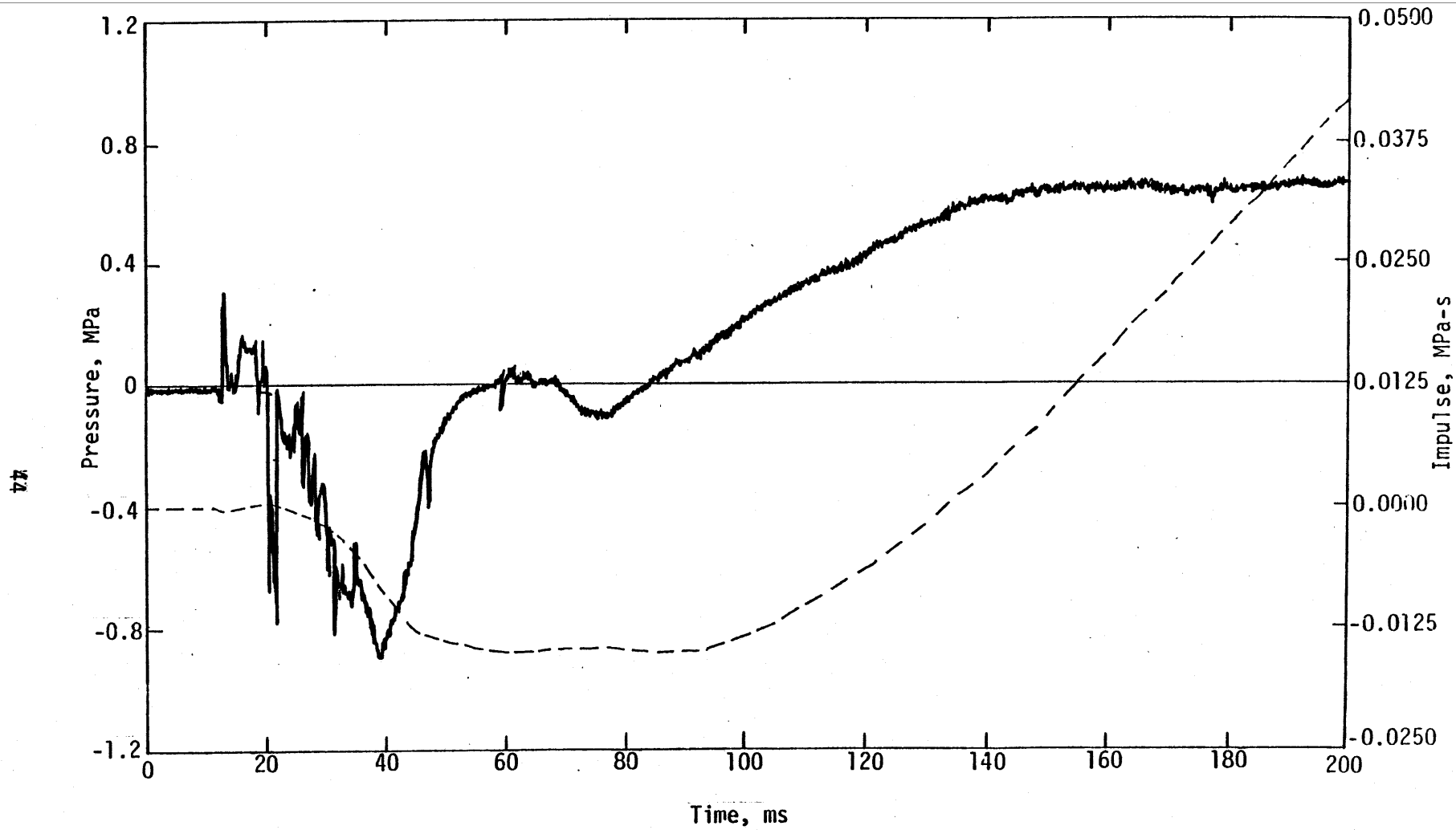
(b) Comparable measurement from B-structure, MN 6732.

Figure 14. Continued.



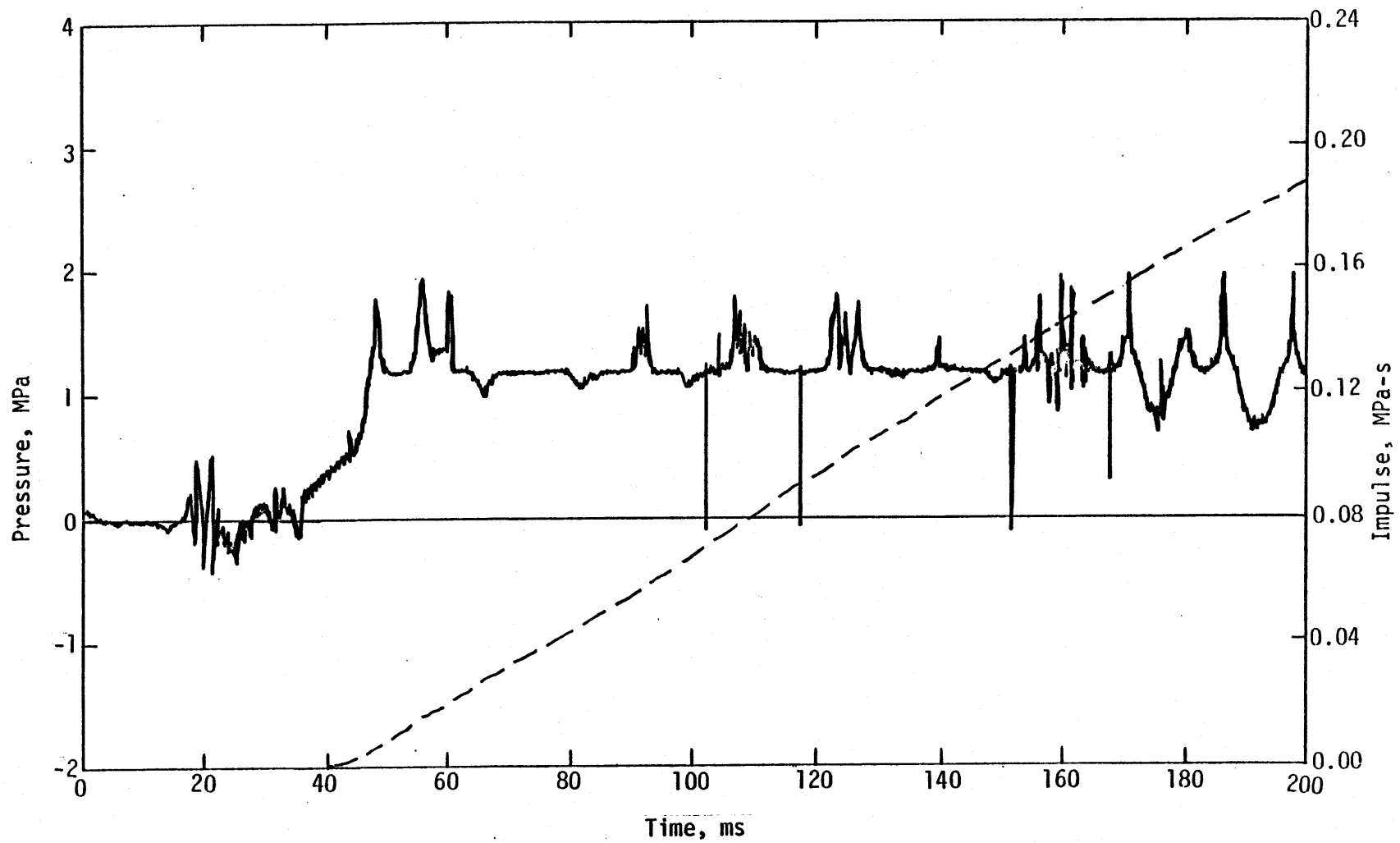
(c) Comparable measurement from B-structure, MN 6735.

Figure 14. Concluded.



(a) CIDAS, MN 6727.

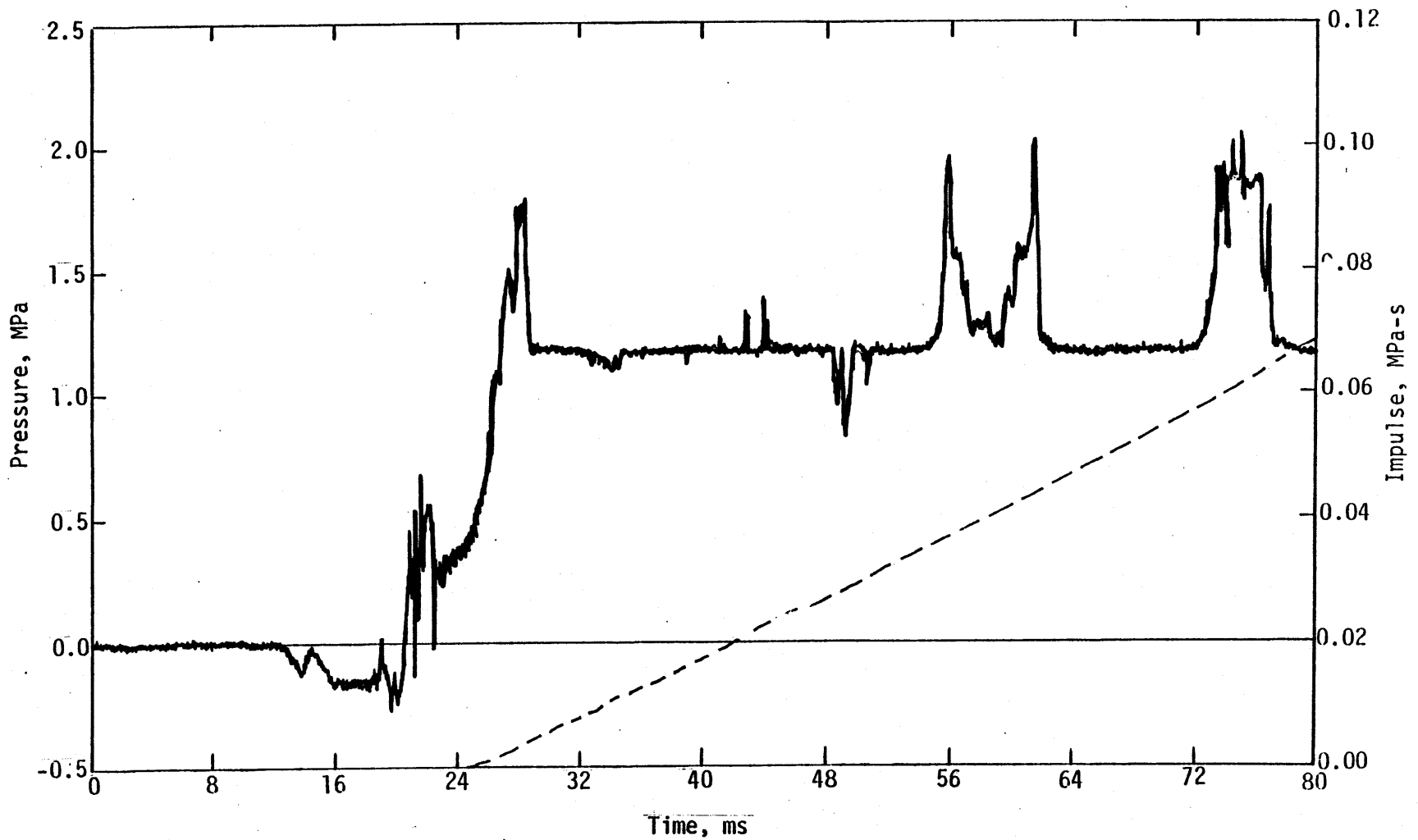
Figure 15. Comparative tangential shear measurements, gage 2.



(b) Comparable measurements from B-structure, MN 6730.

Figure 15. Continued.

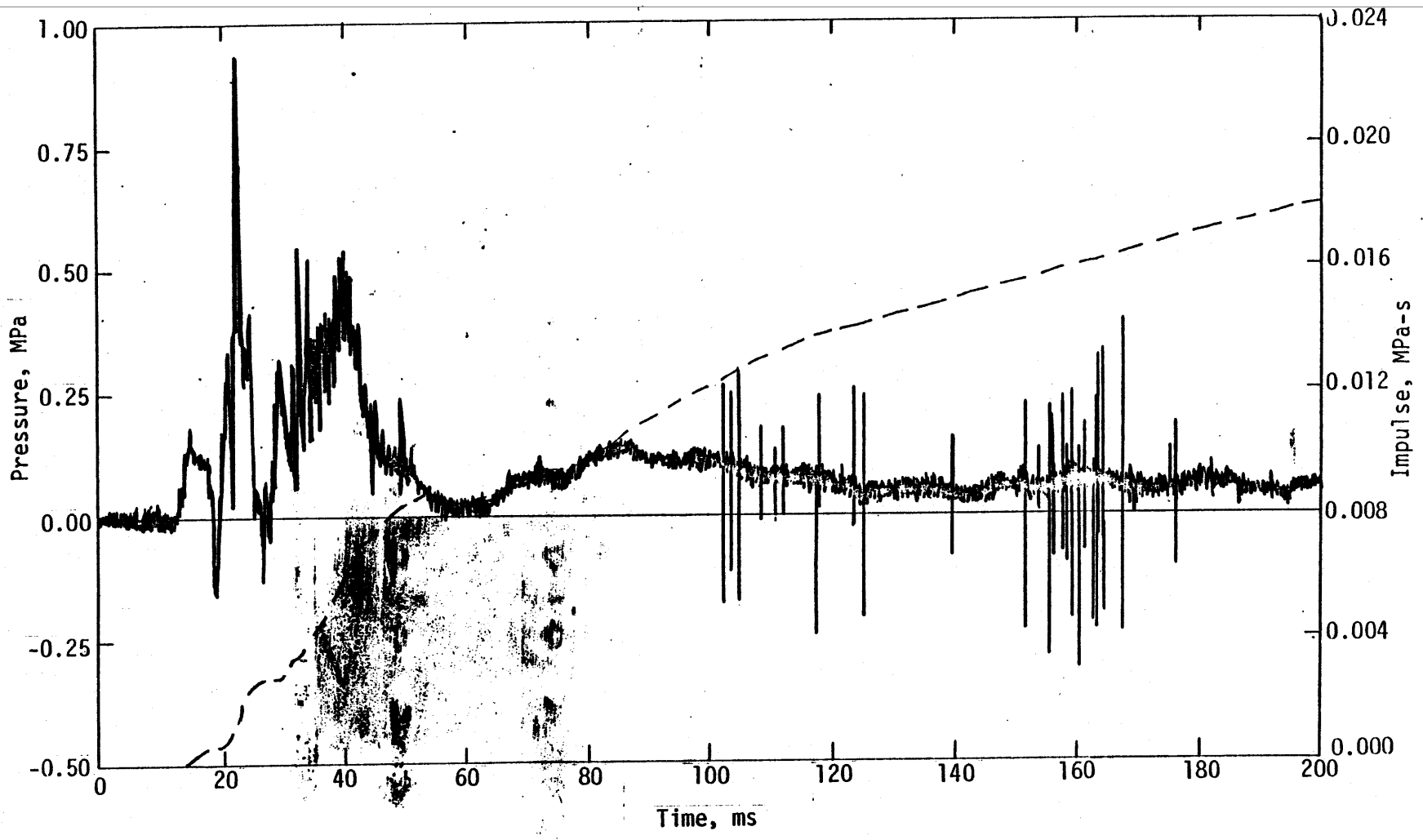
46



(c) Comparable measurement from B-structure, MN 6733.

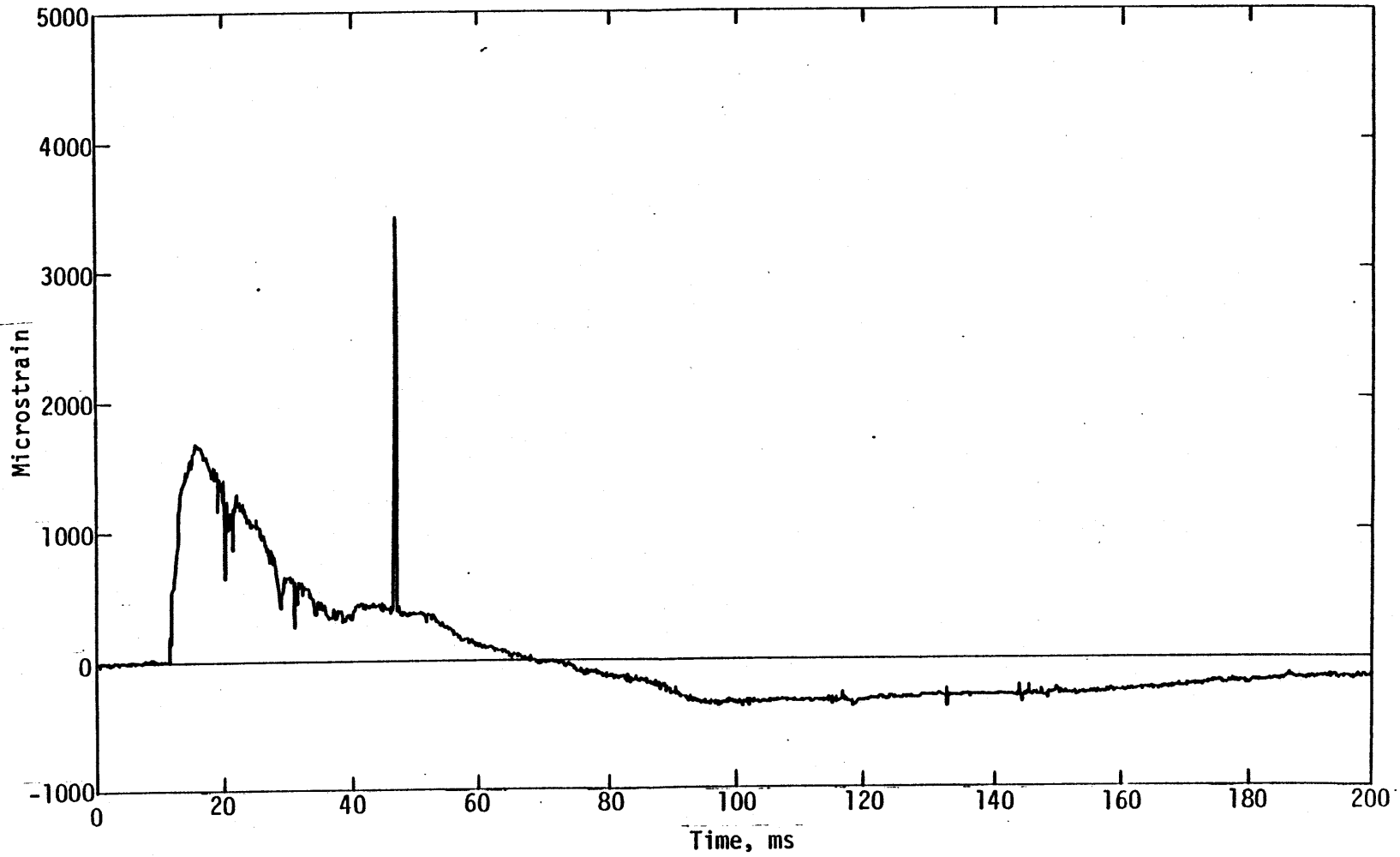
Figure 15. Continued.

47



(d) Comparable measurement from B-structure, MN 6736.

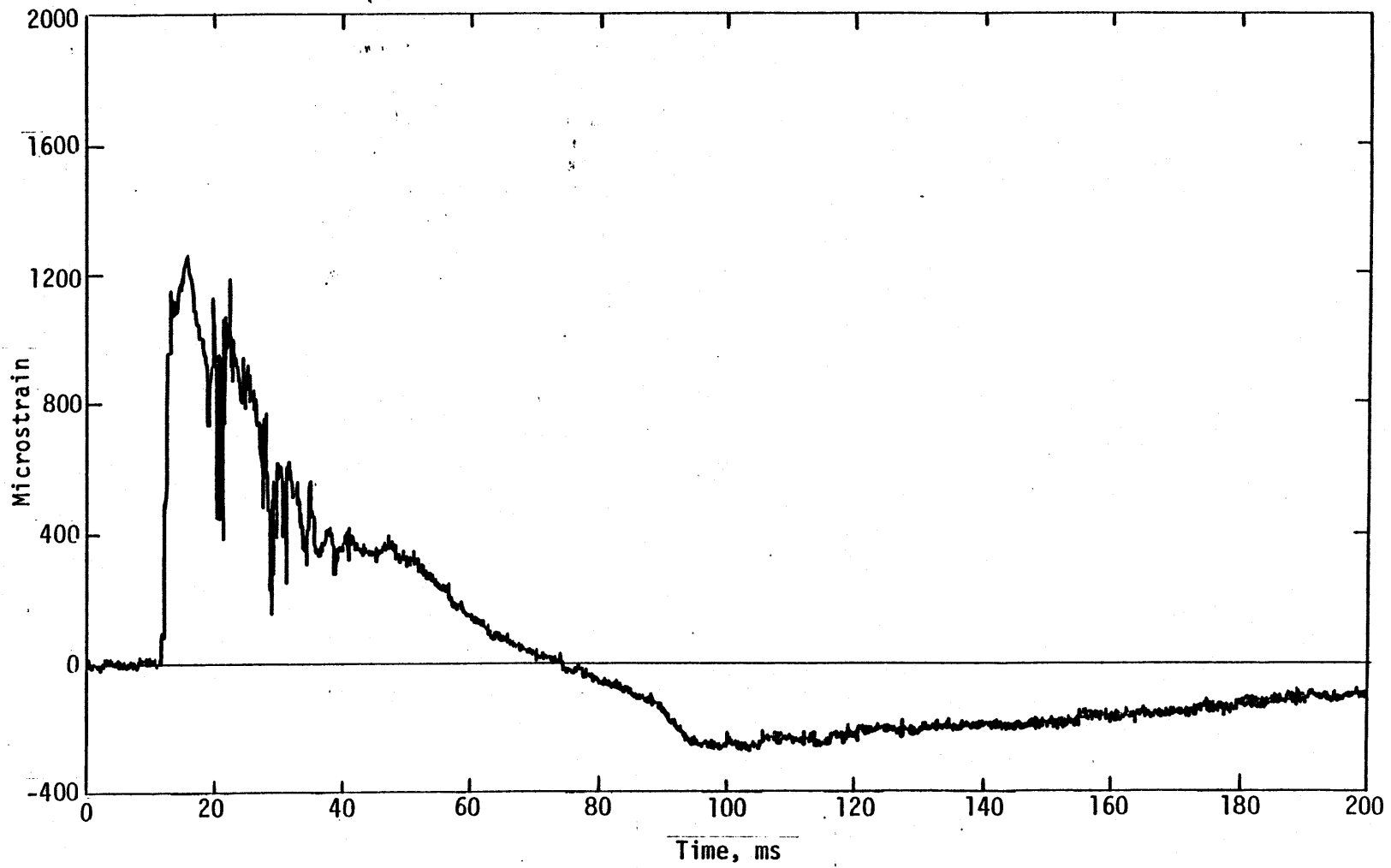
Figure 15. Concluded.



(a) CIDAS, MN 3733.

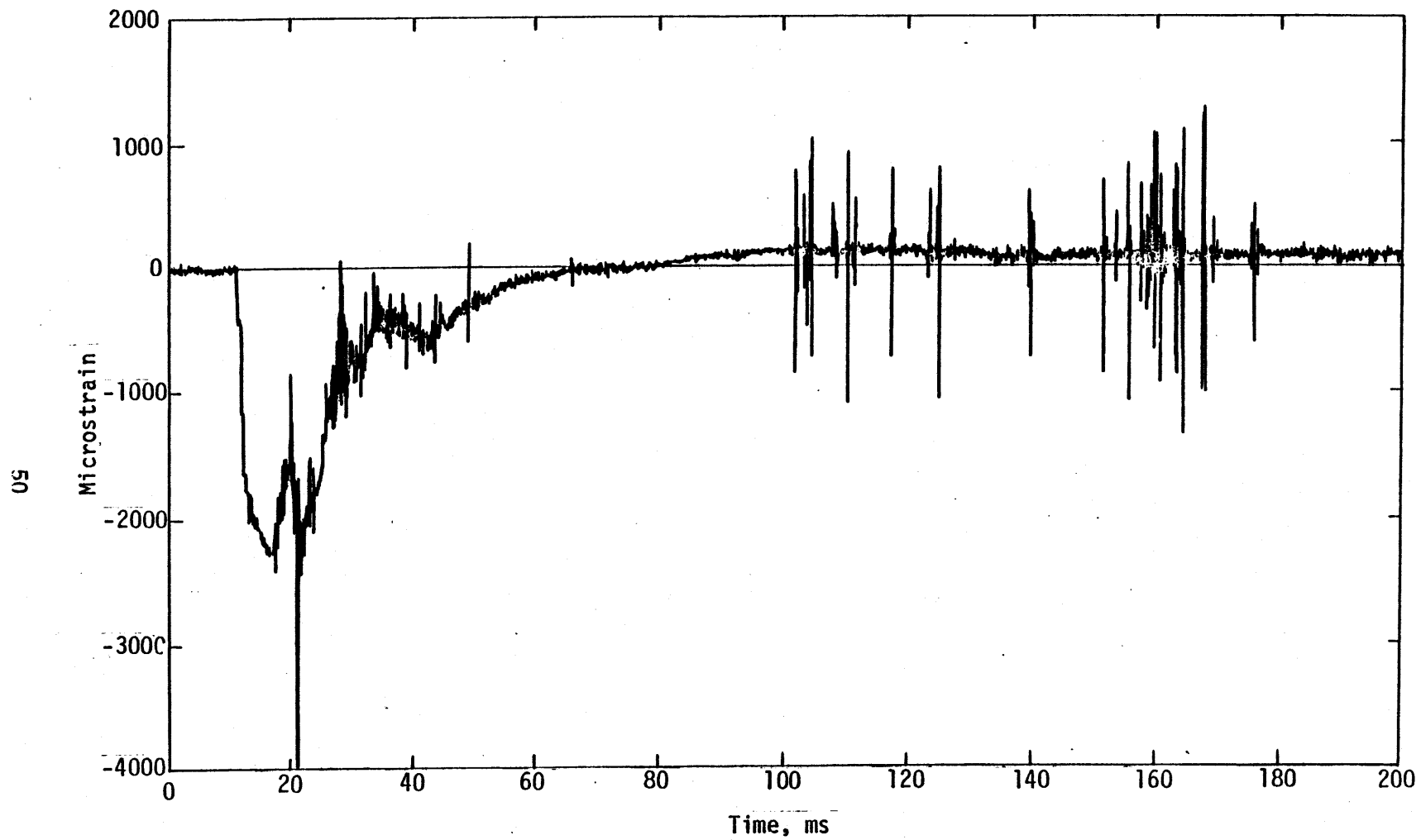
Figure 16. Comparative rebar strain measurements, gage 2.





(b) CIDAS, MN 3734.

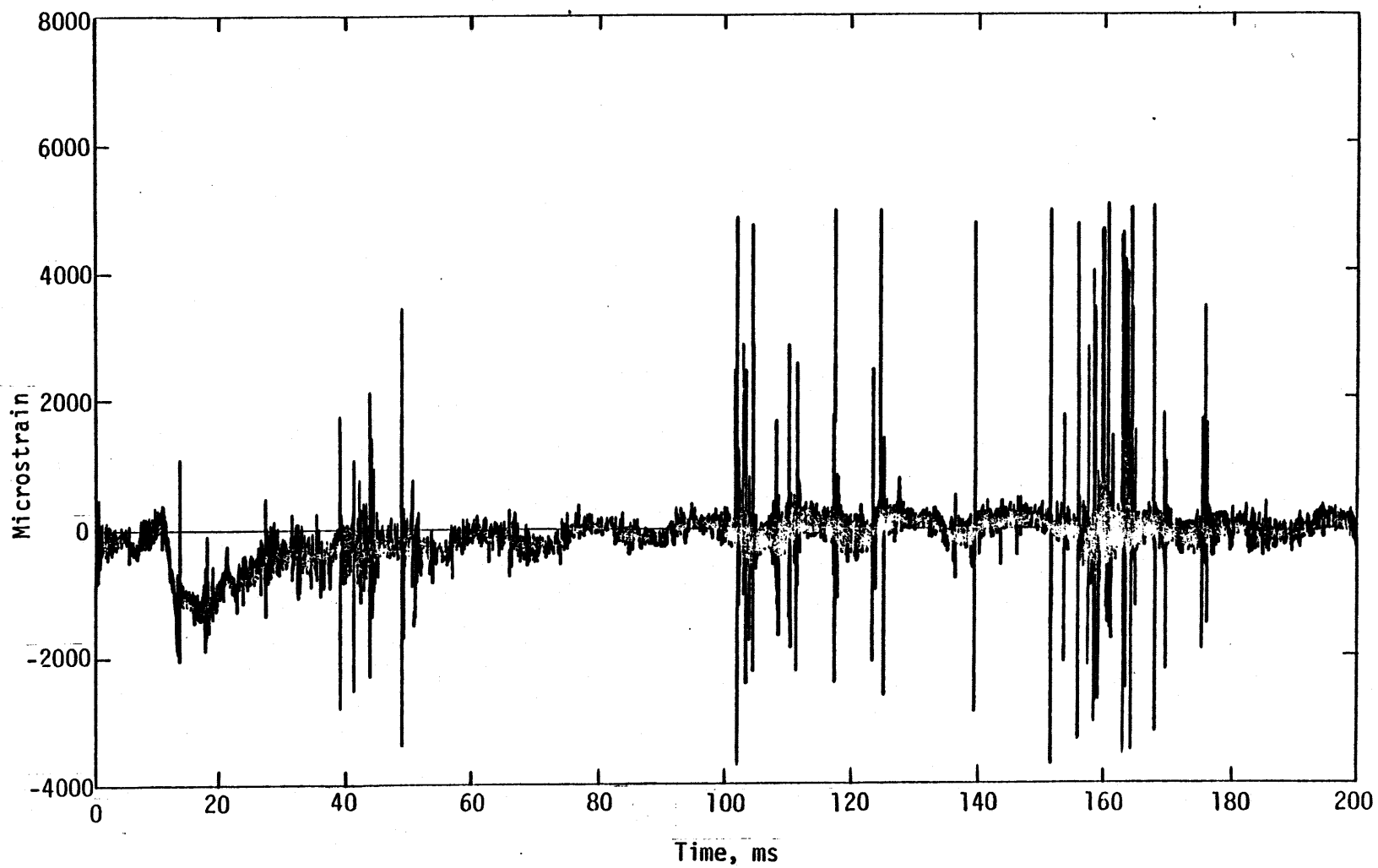
Figure 16. Continued.



(c) Comparable measurement from B-structure, MN 3735.

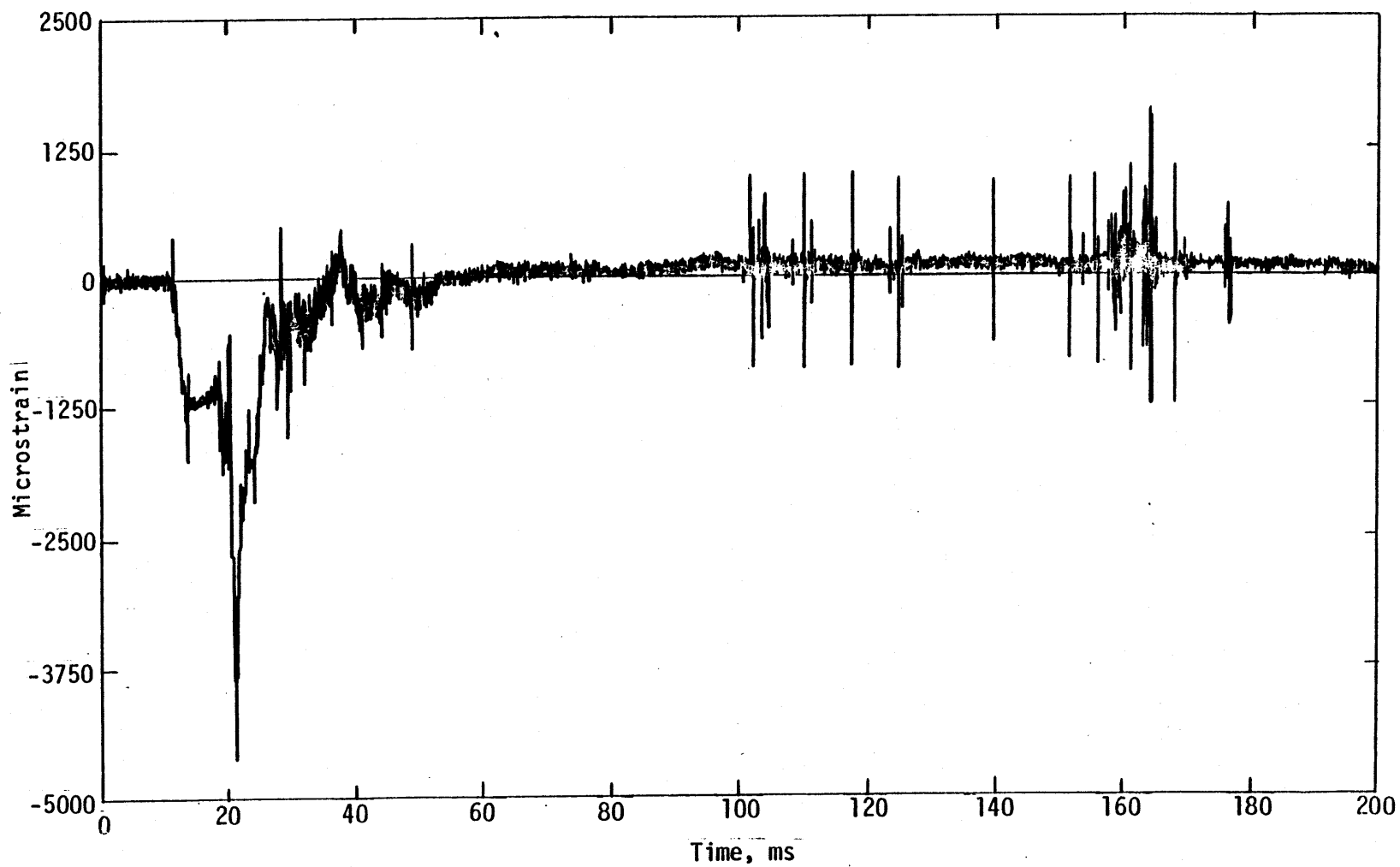
Figure 16. Continued.

51



(d) Comparable measurement from B-structure, MN 3731.

Figure 16. Continued.



(e) Comparable measurement from B-structure, MN 3732.

Figure 16. Concluded.

Van Environment Experiment--The second part of the CIDAS experiment was an attempt to determine whether the shock and blast environment at the close-in van was too severe for normal equipment and vans. Van E-8 was placed in a buried structure approximately 100 m from the edge of the test bed (see Figs. 17 and 18). The roof of the structure, which was level with the ground surface, consisted of 2-in x 12-in structural fir rafters spaced 410 mm (16 in) apart and covered with 3/4-in plywood and 150 mm (6 in) of soil. The sole purpose of this roof was to protect the van from damage due to debris from the test. Because it was felt that the principal threat was ground motion, however, the roof was designed to take the loads induced by a 3-g acceleration.

The primary shock-isolation system for the van was its own suspension. Additional vertical isolation was provided by placing the van on styrofoam pads with a load-distributing pallet. Horizontal isolation was provided by placing the van transmission in neutral and allowing  $\pm 150$  mm of motion between the chocks blocking the front wheels.

The instrumentation layout is shown in Figure 19. The types of measurement employed in the test are listed in Table 3.

TABLE 3. MEASUREMENTS FOR CIDAS VAN ENVIRONMENT EXPERIMENT

MN	Measurement type
9032	Incident pressure at roof center
9033	Reflected pressure at van rear
9034	Vertical acceleration under van
9035	Vertical acceleration at front bumper
9036	Vertical acceleration at rear bumper
9037	Vertical acceleration at roof center
9038	Vertical acceleration adjacent to shelter
9039	Vertical acceleration adjacent to shelter
9040	Vertical acceleration adjacent to shelter
9041	Vertical acceleration adjacent to shelter
9042	Horizontal acceleration of front wall
9043	Vertical velocity under van

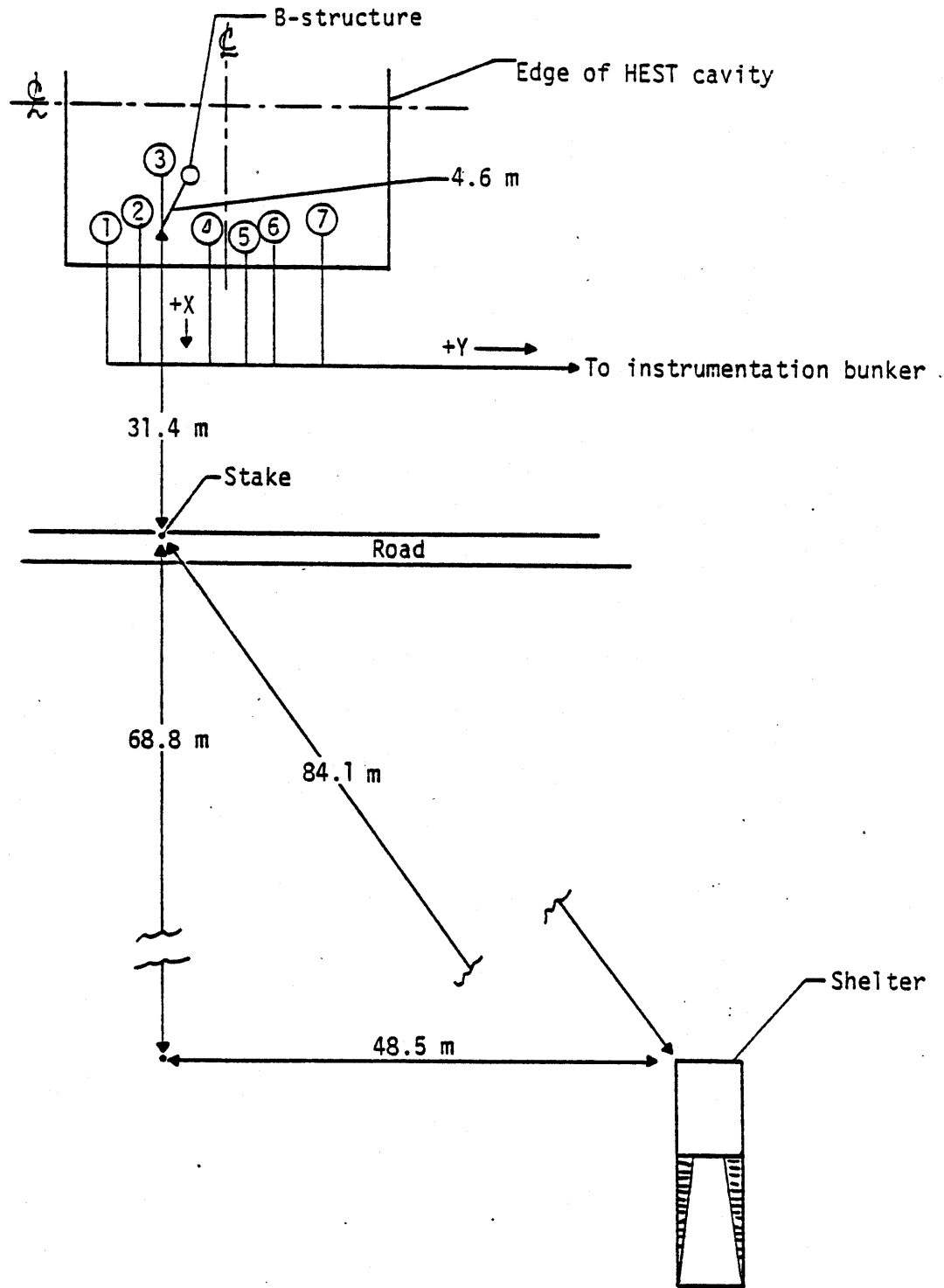


Figure 17. CIDAS test-bed layout, HAVE HOST VST-1.

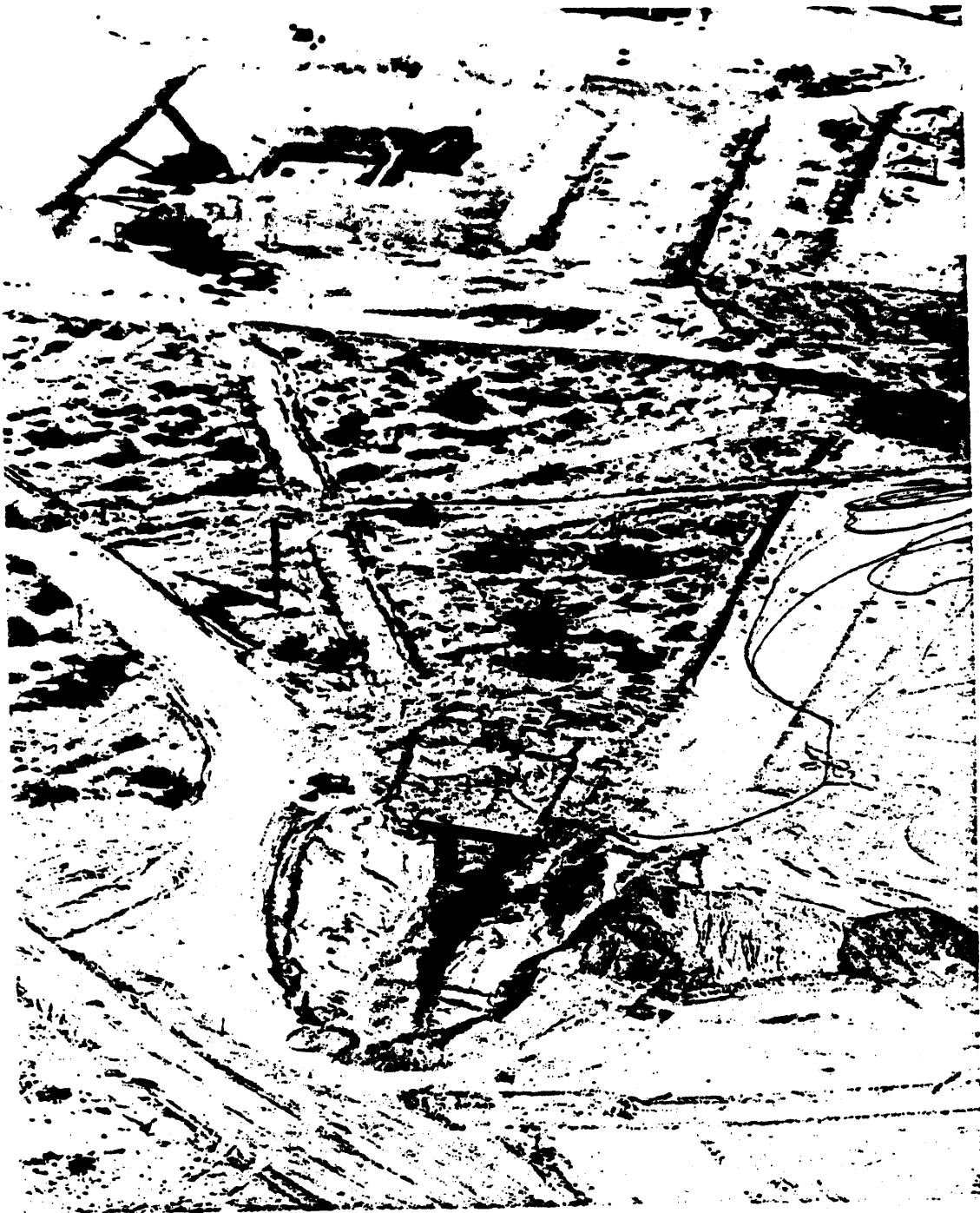


Figure 18. Photograph of Van E-8 and test bed.

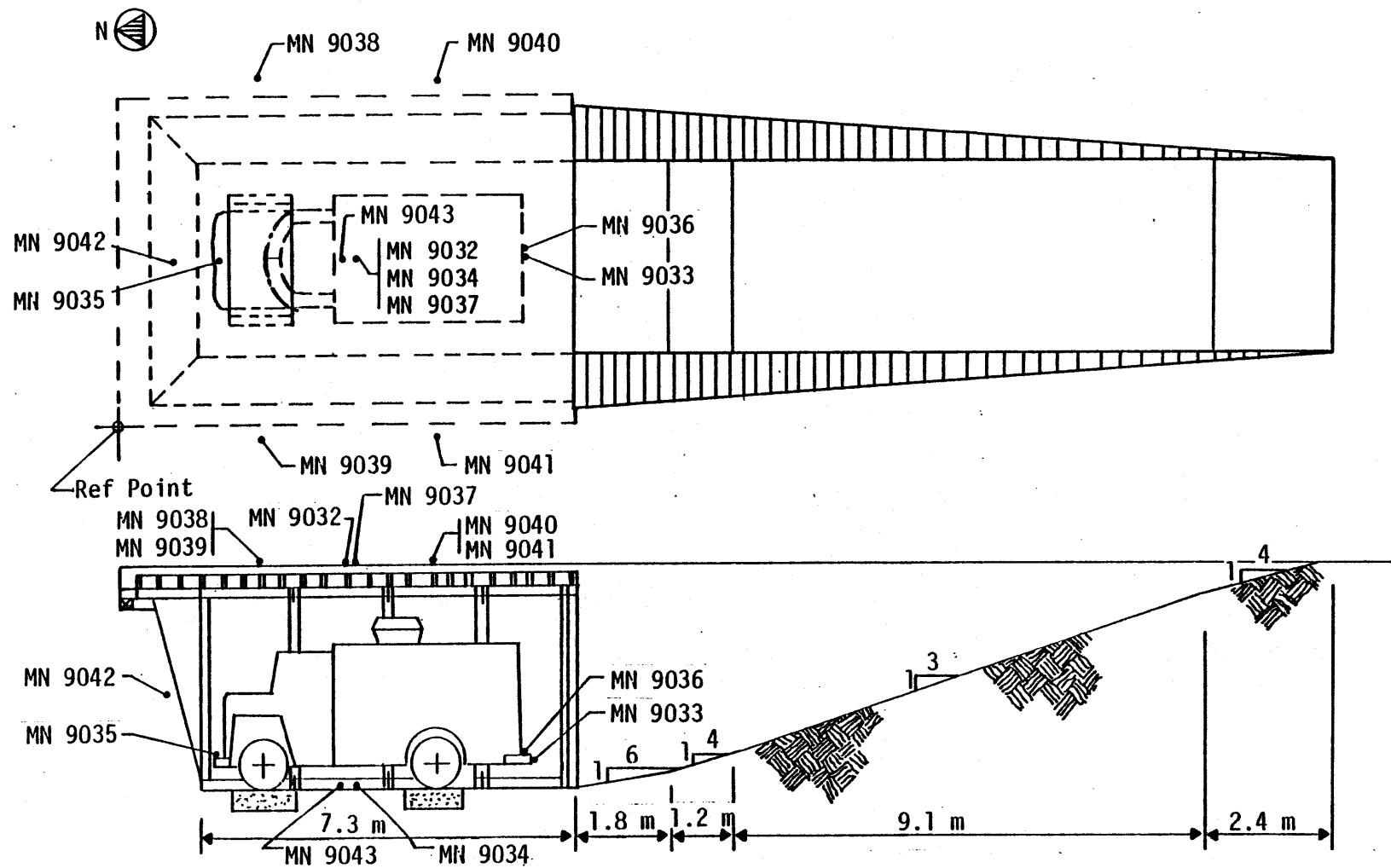


Figure 19. Environmental measurements, CIDAS experiment, HAVE HOST VST-1.



Sample results are presented in Figures 20 through 22 (complete results are given in Appendix B). The results can be summarized as follows:

1. peak overpressure, 0.8 kPa ( $\approx 1/8$  lb/in<sup>2</sup>)
2. peak g-input, 0.27 g
3. effectiveness of shock isolation, 40 to 50 percent
4. peak vertical displacement under van,  $\approx 8$  mm

As the data presented in Appendix C show, the predictions were somewhat low, probably indicating that the high-explosive simulation (HEST) structure vented early or that the pressure wave was not symmetrical. However, the overpressure was still so low that it presented no hazard to the van and equipment. In other words, the environment at the van was fairly mild, and in fact there was no evidence of any debris other than dust at the location. However, when one recalls HAVE HOST Event T-1, where debris showered at a similar distance, and when one takes into account the worst-case prediction in Appendix C, it is apparent that steps must be taken to protect the van against impacting debris.

Also because of the danger from debris, personnel cannot be allowed in the van during the test, and the data must be taken by remote control or automation. Therefore, the tape deck in van E-8 was turned on at T - 2 min, and the nonessential power was turned off at the same time. To ensure that the tape deck was recording, a monitor of the reproduced IRIG signal, supplied by the Defense Nuclear Agency (DNA), was used to actuate a warning-light system in the timing-control center for the shot. The entire remote-control system worked correctly. The only known disadvantage to this type of system is that any hold imposed after T - 2 min, will be an extensive one because the charge must be disarmed before personnel can safely enter the area to reload the tape decks.

The only instrument that did not perform properly was the velocity transducer, and this failure occurred because the input was too low. The rest of the experiment was an outstanding success and demonstrated that instrumentation systems of this type can be fielded easily.

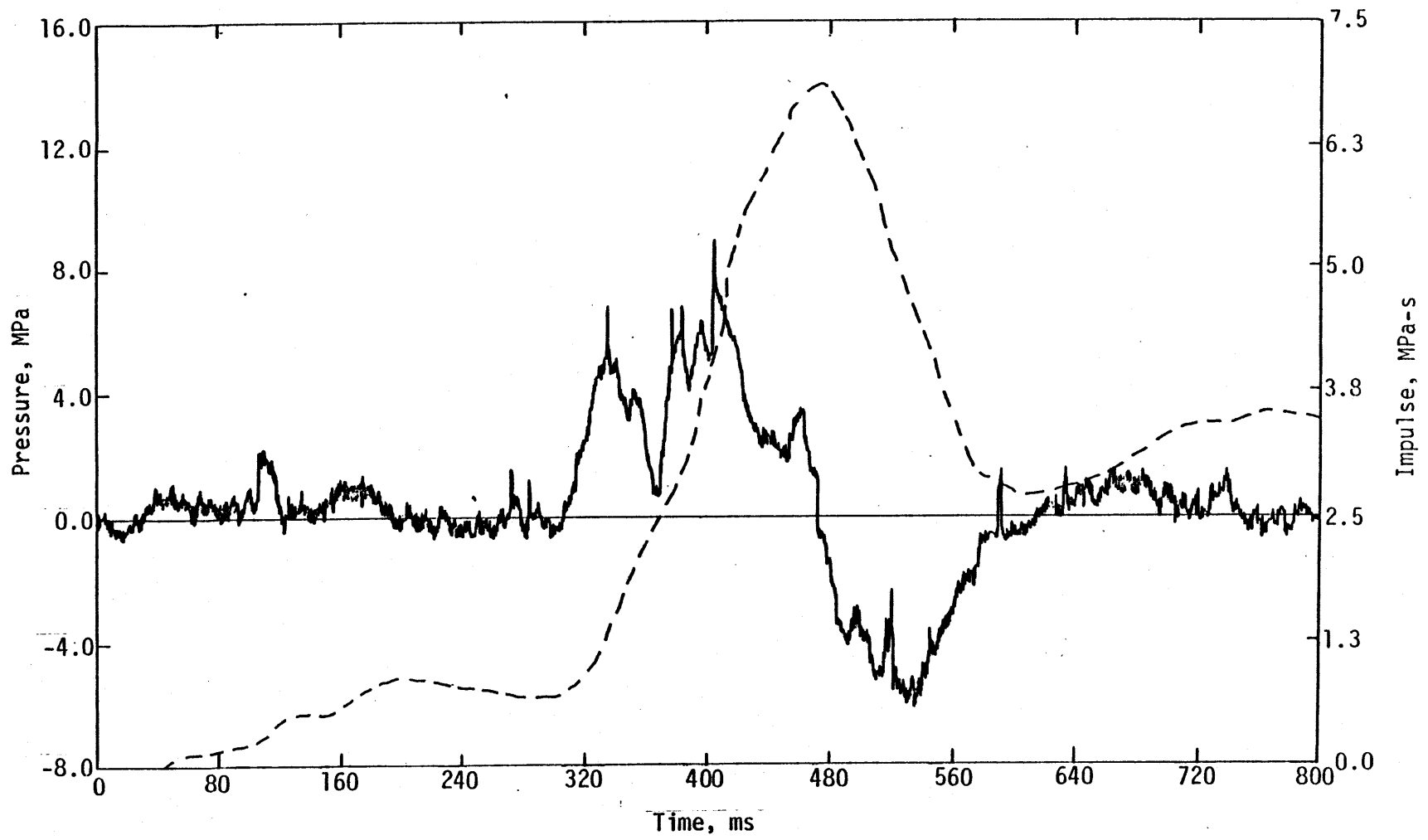


Figure 20. Incident pressure at roof center.

69

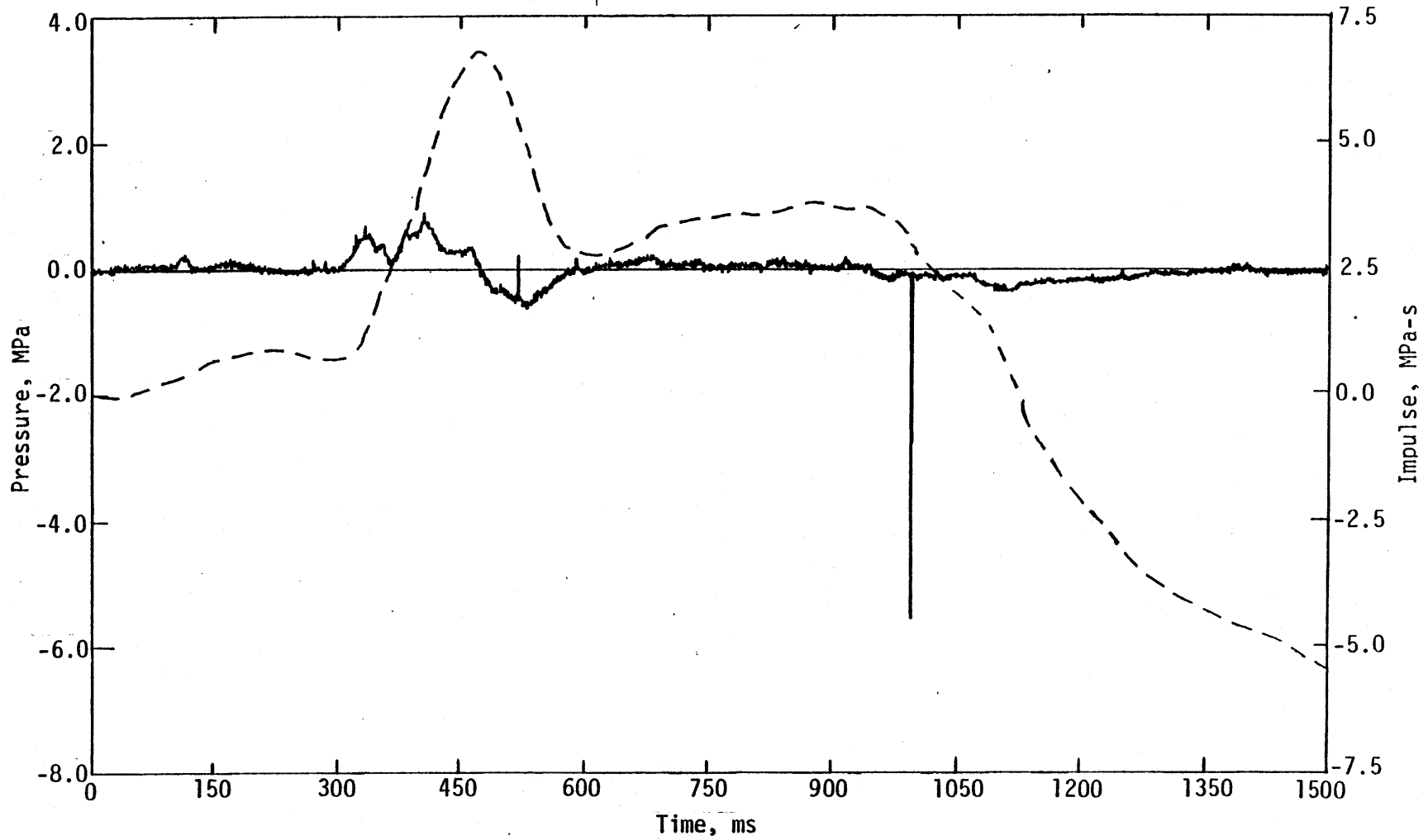


Figure 21. Reflected pressure at van rear.

09

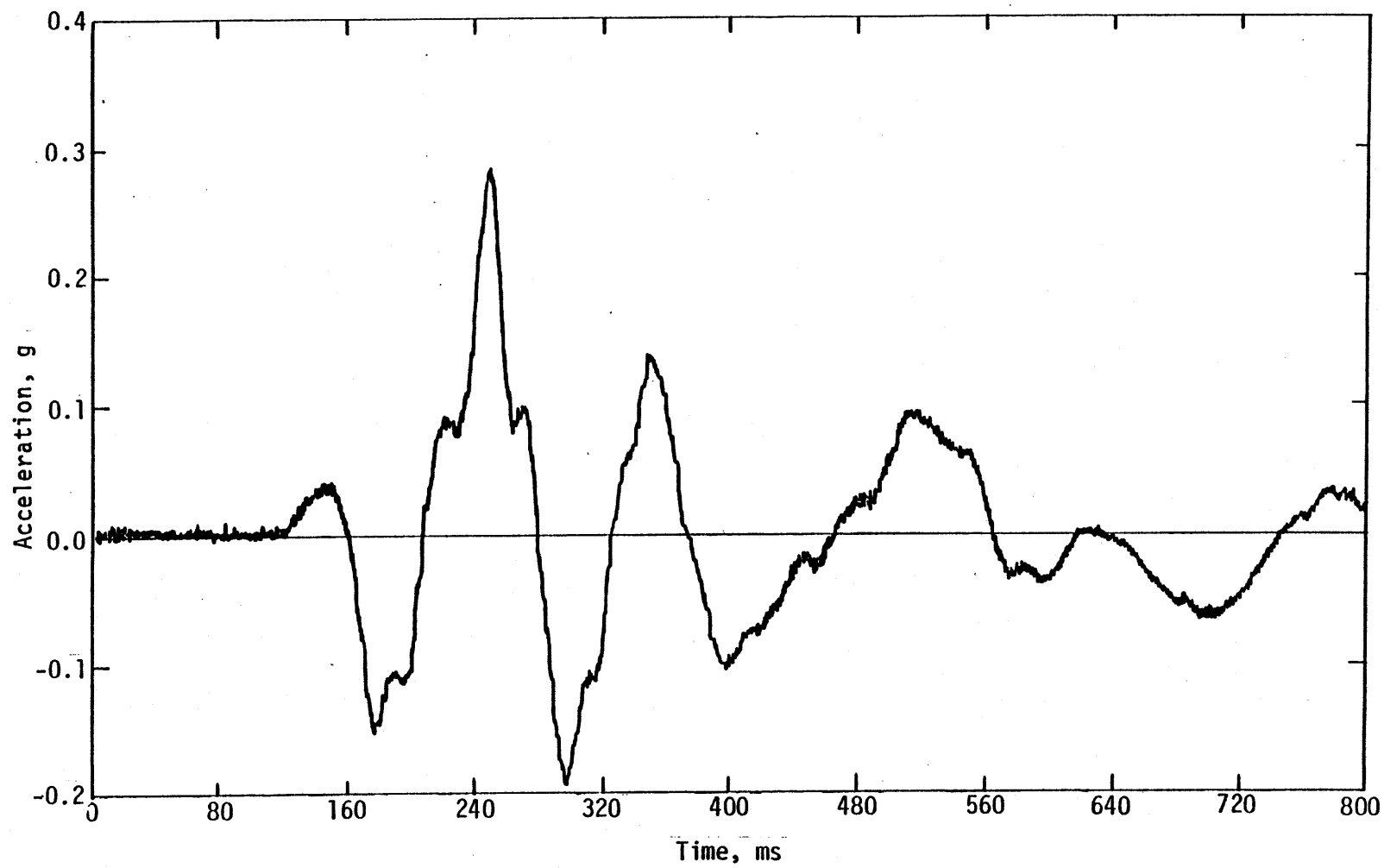


Figure 22.. Vertical acceleration under van.

## SECTION IV

### CONCLUSIONS AND RECOMMENDATIONS

#### CONCLUSIONS

The system of continuous or distributed grounding, combined with careful planning of the topology of the shielding system, is effective in reducing observed noise in test data. While the CIDAS shielding was not as good as that used on SIMCAL III, with its extra exterior shield, it certainly was effective in reducing both cost and noise.

The instrumentation van may be placed close to the test bed and protected in a relatively easy manner from the effects of a test of the type and size of VST.

An automation system can be installed in the van with relative ease and can be made to function in a dependable way.

#### RECOMMENDATIONS

The following recommendations based upon the results of the CIDAS and the SIMCAL III experiments relate to grounding and shielding, van operation, and van placement. They are presented in order of relative importance.

Grounding and shielding--It is recommended that the entire cabling system and the instrumentation lines used to transfer electrical data at the HAVE HOST site be changed from a single-point grounding system to a continuous or distributed ground. An engineer at the HAVE HOST site should be authorized to ensure that the topology of the shielding system is not violated. This recommendation implies changing to metal junction boxes, isolating the vans from power, and grounding the transducer cases.

---

\*This includes photo closures and consideration of the firing system on each shot.

Van operation-- It is recommended that the vans be automated. If it is possible to have operators in the vans during the shot, then their only function should be to ensure that the automated system is operating correctly. This procedure would radically improve the reliability of the data-recording system.

Van placement--It is recommended that the sites for all tests scheduled for 1980 (where the environment is to be of the order of or less than that of VST) be located within 100 m of a given (van) location if geologically possible. The vans would then have to be hardened only to debris, and this could be done economically by using one berm constructed of styrofoam and wood or steel. In addition to improving data quality, the close-in location of the van would save money. The cost of 20-pair cable is currently \$1.30/ft. Projecting next year's cost to \$1.50/ft and presuming that one 20-pair cable can handle six to eight channels, close-in location of the van could save about \$750,000 in the cost of cable for an 1800-channel shot.

The CIDAS test and the signal-isolation experiment on SIMCAL III have demonstrated the efficacy of these recommendations. These experiments have also shown that there is no reason AFWL and NMERI engineers cannot require, as an arbitrary standard, that signal-to-noise ratios (peak to peak) of less than 100 to 1 be justified in each individual case. A standard such as this would eliminate virtually all grounds for user complaint.

This recommendation is not meant to imply that signal-to-noise ratios of less than 100 to 1 would not be tolerated. Extremely low signal levels, the experimental nature of some measurements, and other such conditions may negate the possibility of obtaining the desired ratio. In such cases, however, the cause of the noise must be identified and eliminated where physically and economically practical.

APPENDIX A  
MECHANICAL CABLE-HARDENING ON UNDERGROUND TESTS

The mechanical hardness of cables can be made consistent with the electrical topology discussed in the body of this report. Cable hardening usually involves one of two things: impedance and flow matching or enclosing the cable in a material that mechanically shields it from the ground shock environment. The first method involves orienting the cable with respect to the flow in such a way that either the cable is always in compression or the strains are minimized. CIDAS has shown that with minor modifications, one can use a tree network to incorporate normal cable shields into a topology that minimizes noise. The second method requires only a metallic shield around the cable to protect the cable from shears induced by material flow. The introduction of an extra metallic shield only improves the electromagnetic shielding when the shield is properly fitted into the electrical topology, as it was on the SIMCAL III test. Thus, one may refer, in a sense, not only to an electrical topology but also to a mechanical topology that protects the cable from failure and the introduction of triboelectric noise. The two concepts are complementary, not contradictory. In fact, one can discuss an electromechanical topology in which the properties of the shield are not only permeability, conductivity, and thickness but also ultimate strength, fracture toughness, modulus, and mechanical impedance. In the blast and shock field, after all, noise-free measurements that do not survive the stress pulse are about as useful as noisy measurements that do survive. Thus, engineers working in the blast and shock instrumentation area can only benefit from entrance into what has been described\* as "an unholy union between the slappers and the zappers."

The review given here of past work in the field of cable-hardening will be confined to underground test technology developed at the Department of Defense (DOD) and the Department of Energy (DOE). In the underground environment, the problems of both noise and survival are extreme; thus, the

---

\* By Donald Gage, Lt. Col. USAF/SAMSO.

cable-hardening schemes used on such tests are often viewed with hesitation as being too expensive and thus not practical for HE simulation work. As the SIMCAL III and CIDAS experiments showed, however, the concepts used on DOE and DOD tests may be applied in an economical way to other types of tests.

A report by Bruce Hartenbaum of H-Tech Company, which was completed at about the time the effort on this current task began, covers cable design on all relevant DOD and DOE tests prior to Hybla Gold (Reference A-1). To avoid repeating Dr. Hartenbaum's work, this author will summarize the DNA report, referring the reader to the original for additional details.

The following objectives for Hartenbaum's work are quoted from his report:

- a. Develop analyses, both mathematical and experimental, to assist in the rational design of subterranean instrumentation cables that will survive pressures of 2 to 3 kbar, large axial strains of the order of 40 percent and severe shear offsets, to allow the measurement of late-time displacements induced by large explosions.
- b. Review and analyze reports on underground tests and other pertinent literature to document cable design, cable performance, and cable problem areas.
- c. Establish both past and current cable practices by discussing cable techniques with experimenters involved in the fielding of underground tests.

To these ends, Hartenbaum gives a mathematical model for strains produced in an underground test; reviews the literature to determine what the appropriate experience has been on underground tests and close-in HE experiments; reviews the cabling practices of five agencies deeply concerned with the problem of cable survival on underground tests; gives a theoretical explanation of the factors affecting transverse loads on cables, such as those encountered at planes of weakness; and suggests experiments that may be used to resolve some of the uncertainties associated with given materials and cables.

---

A-1. Hartenbaum, Bruce, *The Design of Subterranean Instrumentation Cables to Survive Large Amplitude Ground Motion*, DNA 4636F, Defense Nuclear Agency, July 1978.



The theoretical study of the large strain fields covered in Hartenbaum's report shows that in a homogeneous material one can orient the cable with respect to any given radius in such a manner that the axial strain will be zero. Hartenbaum points out that if the cabling is to survive these strain fields, the entire geometry of the cable topology\* should be investigated for the purpose of estimating strain and determining whether the cable has a chance of surviving. This analysis is necessary on an underground test because the layout of the cable drifts almost never allows for ideal cable placement.

The types of ground motion of interest to Hartenbaum are orders of magnitude greater than those observed in a HAVE HOST type of test. In a HAVE HOST test, the maximum displacements are of the order of centimeters; whereas in the underground test, close-in permanent displacements often measure many meters. At HAVE HOST, the cables must survive megapascal pressures, whereas at the Nevada test site the cable must survive hundreds of megapascals of pressure. Consequently, techniques used in the high-stress area are often not appropriate for use in a HAVE HOST type of test. In large-scale motion experiments axial cable strain is to a great degree responsible for cable failure, but (as Hartenbaum points out) when peak pressures are less than 50 MPa, most failures are due to shear. It is in this region that there is some promise of possible technological overlap, but as Hartenbaum concludes, "At the present state of the art a workable method for protecting cables from shear failure at an unavoidable plane of weakness is uncertain."

The tests reviewed in the Hartenbaum report were Midi Mist, Diana Mist, Dido Queen, Hybla Fair, Dining Car, Husky Pup, Diamond Mine (HE), Mine Dust (HE), and Pre-DICE THROW II (HE). Hartenbaum also reviews a 1960 report discussing cable failure modes for near-surface communication cables and discusses practices used by Sandia Laboratories; Waterways Experiment Station; Systems, Science and Software; Physics International; and the DNA Field Command. His review shows that there are about as many cable-hardening schemes as there are experimenters and that the schemes have been used with varying degrees of success. For instance, Stanford

---

\* Dr. Hartenbaum uses the term *topology* in a different sense than does this author.

Research Institute fielded five different cable designs on the Husky Pup test in order to determine which was most suitable for large-strain field work. These were a "slip joint" design, "meander or slack aluminum conduit," "well logging cable" (two configurations), and "Sandia stretch cable." "All of the cables failed within 0.3 to 1.5 ms of shock arrival at the intersection of the bypass drift and cable bore holes," Hartenbaum reports. They also failed at the gas seal connectors. Hartenbaum gives this example to reinforce his statement that at the present state of the art, cable shear has yet to be overcome.

Hartenbaum then explains the mechanics of cable shear. He shows that the force per unit length (F) exerted on a cable by the backfill around it can be represented in the form

$$F = C S_0 d$$

where  $S_0$  is the maximum shear stress,  $d$  is the cable diameter, and  $C$  is the coefficient of shear loading.  $C$  is dependent upon the type of analysis used and is nominally between 2.00 and 3.14.

Table A-1 (Ref. A-1) gives the results of different theoretical approaches reviewed by Hartenbaum.

TABLE A-1. SUMMARY OF RESULTS FOR CABLE LOAD COEFFICIENT

Model	Coefficient	
Boussinesq "half buried cable"	$\pi/2$	1.57
Simple plasticity estimate	2	2.00
Karagozian shear estimate	2	2.00
Boussinesq "tangent buried cable"	$\pi$	3.14
Line force within material	$\pi$	3.14
Plastic punch on surface	$\pi + 2$	5.14

(Reference A-1)

Hartenbaum then suggests experiments that could be used to test the response of cabling systems to various environments. The first of these relates to shear and determines the factors effecting failure at a plane of weakness and the load induced by backfill flowing at appropriate

rates. The other experiments relate to axial loading; slip and buckling; tests of gas seal connectors, junction boxes, and canisters; and small-scale modeling.

Hartenbaum's first conclusion is truly worthy of note and should be emphasized:

The first step in designing a cable system is the laying out of the mechanical topology of the cables. The purpose of the cable topology is to minimize shear offsets and axial strains. Whether the cables are radial or non-radial is of lesser importance than avoiding planes of weakness.

With the understanding that Hartenbaum is using the word topology in a different sense than that employed by this author, his conclusion is in total agreement with the philosophy presented in the body of this report: that from the electrical standpoint one should pay attention to the shields, and from the mechanical standpoint one should take care where the shields are placed. This philosophy leads to the imposing of geometrical constraints on the topology, for it implies not only that the topology should be closed and simply connected, but also that its orientation with respect to shock propagation and geology is important.

Insofar as HAVE HOST is concerned, this philosophy implies that one does not design cable trenches with right-angle turns or rapid changes in elevation. If mechanical considerations dictate that metal conduits be used, Maxwell will only applaud and the good engineer will incorporate them correctly into his electrical topology.

What Hartenbaum is saying is that motions should be calculated and cable response and strength tested before any explosive event. Cabling plans should then be made in such a way as to reduce mechanically induced electrical noise and failure.

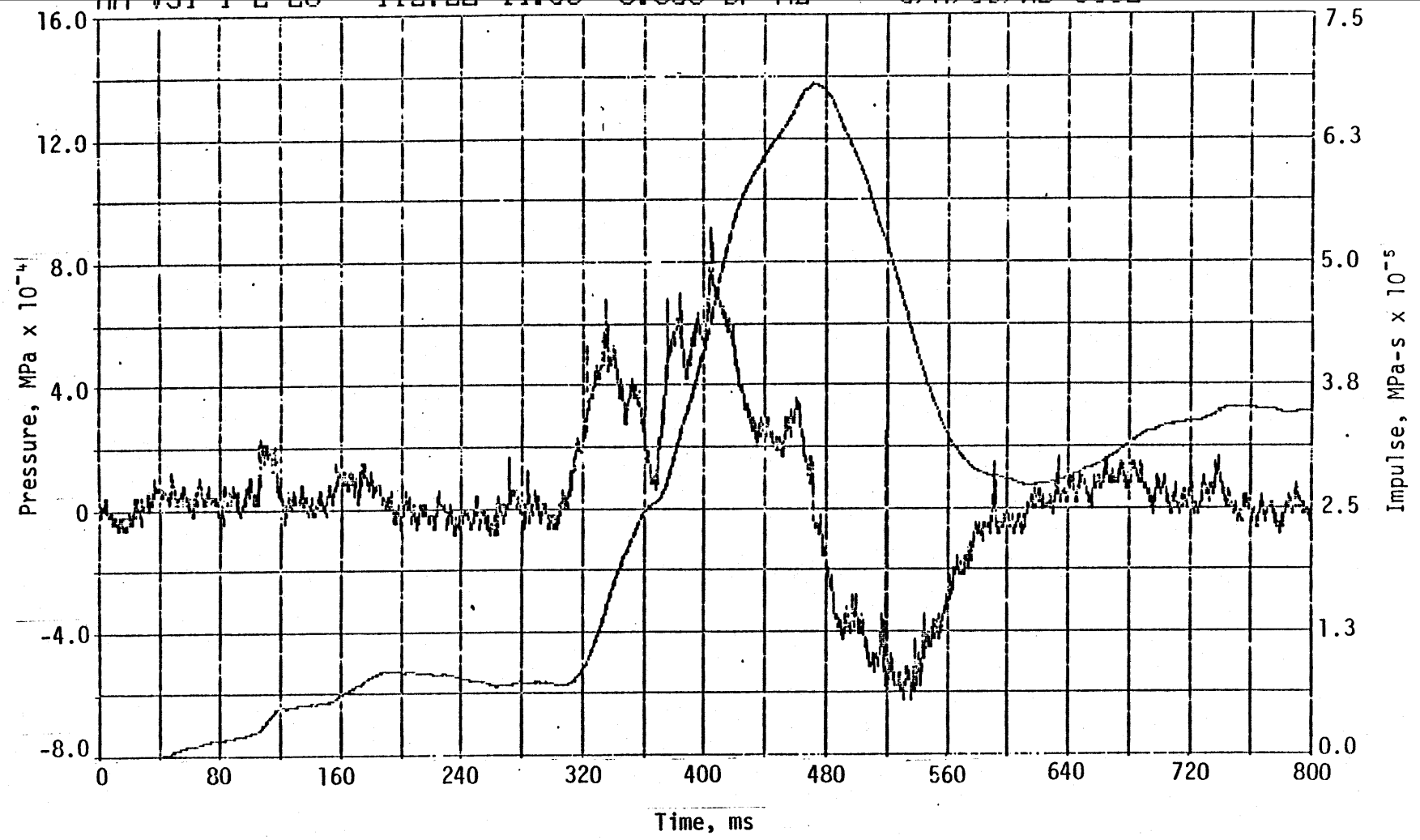
What Baum is saying is that similar care should be taken with the electrical configuration. The two concepts are complementary, not inconsistent, when correctly combined.

APPENDIX B  
CIDAS VAN ENVIRONMENT MEASUREMENTS

For documentation of the CIDAS experiments, a complete set of acceleration and van-environment measurements is presented here. Note that measurements 9033, reflected pressure at the van rear; 9034, vertical acceleration under the van; 9035, vertical acceleration at the front bumper; and 9036, vertical acceleration at the rear bumper either were attached directly to the van or were very close to it. The proximity caused an approximate 30-Hz apparent noise on these data. The apparent noise is particularly evident on the van-acceleration data. The cause of this disturbance was the real acceleration of the van due to oscillations caused by the operation of a generator within the van.

HH VST I-E-E8 112.22 44.86 0.000 BP HZ 8/A/09/WB\*9032

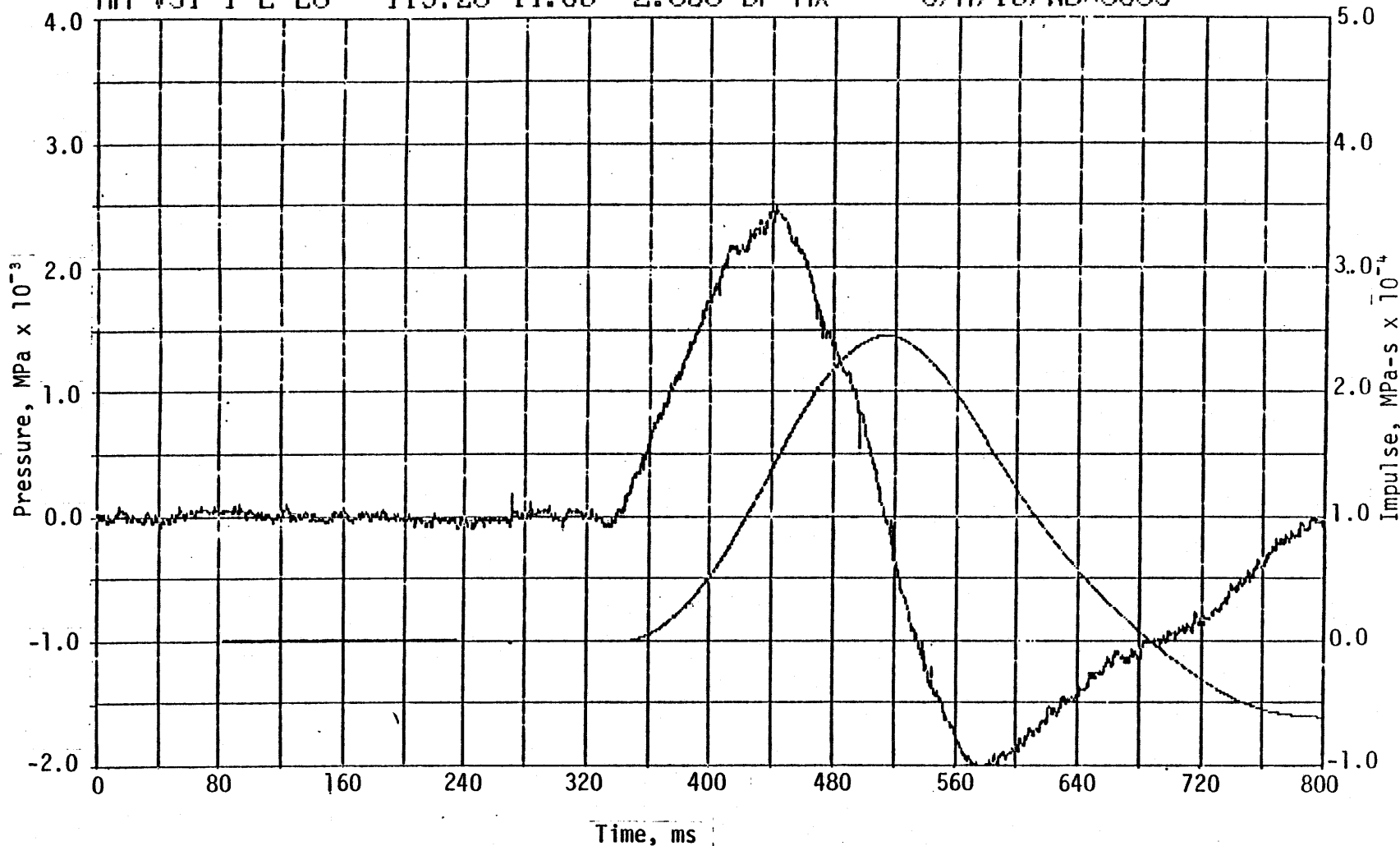
69



Incident pressure at roof center.

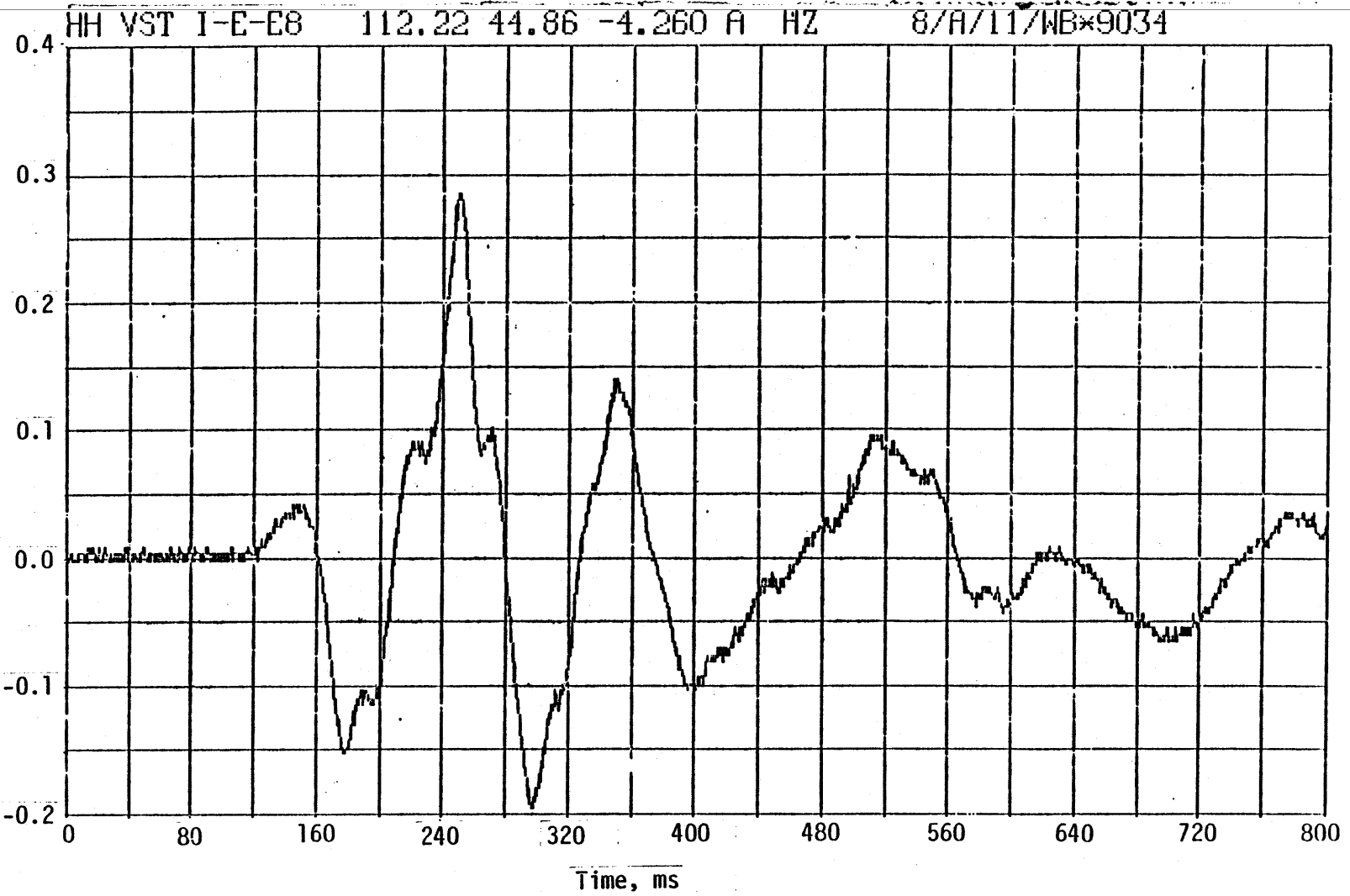
HH VST I-E-E8 115.26 44.86 -2.660 BP HX 8/A/10/WB\*9033

70



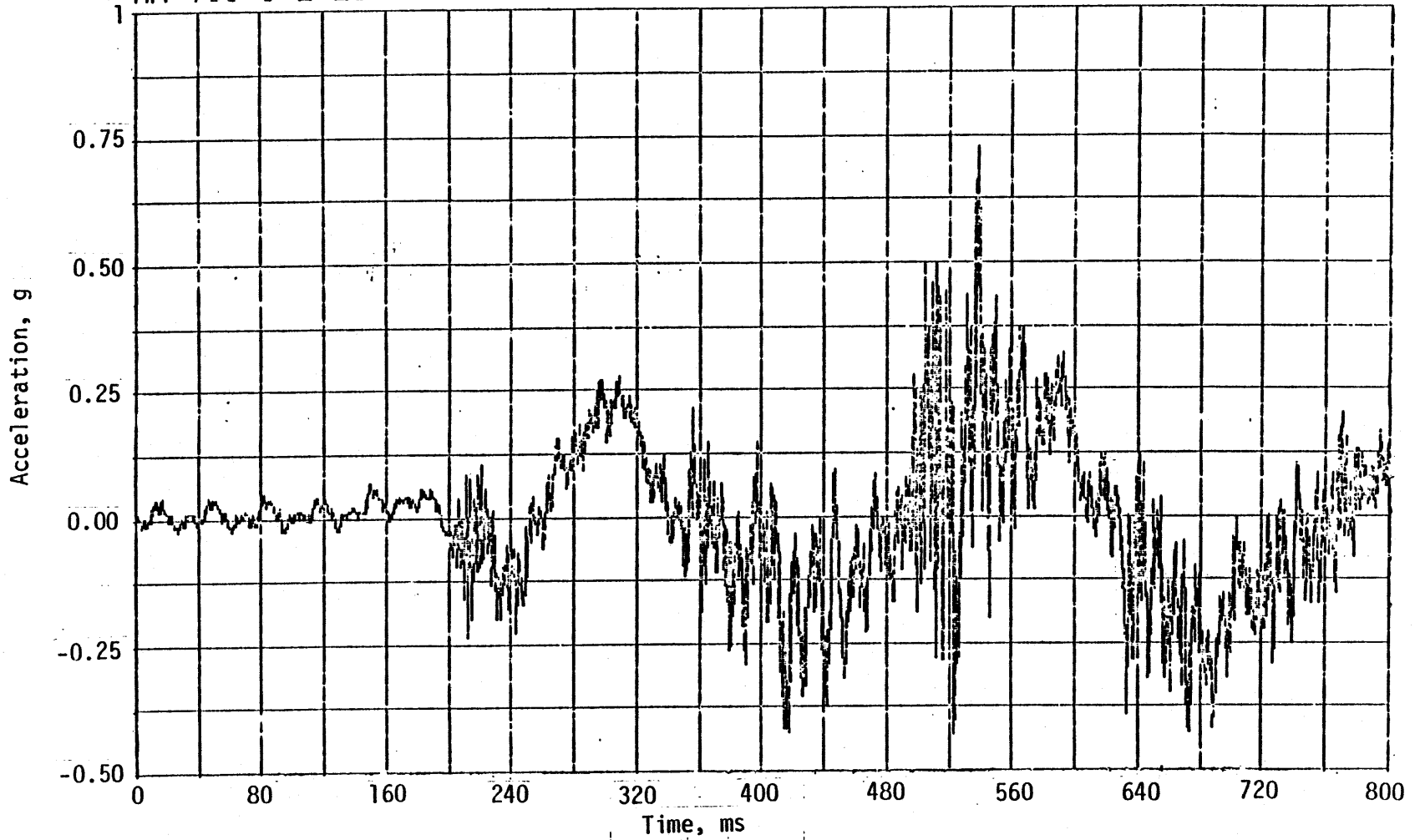
Reflected pressure at van rear.

71



Vertical acceleration under van.

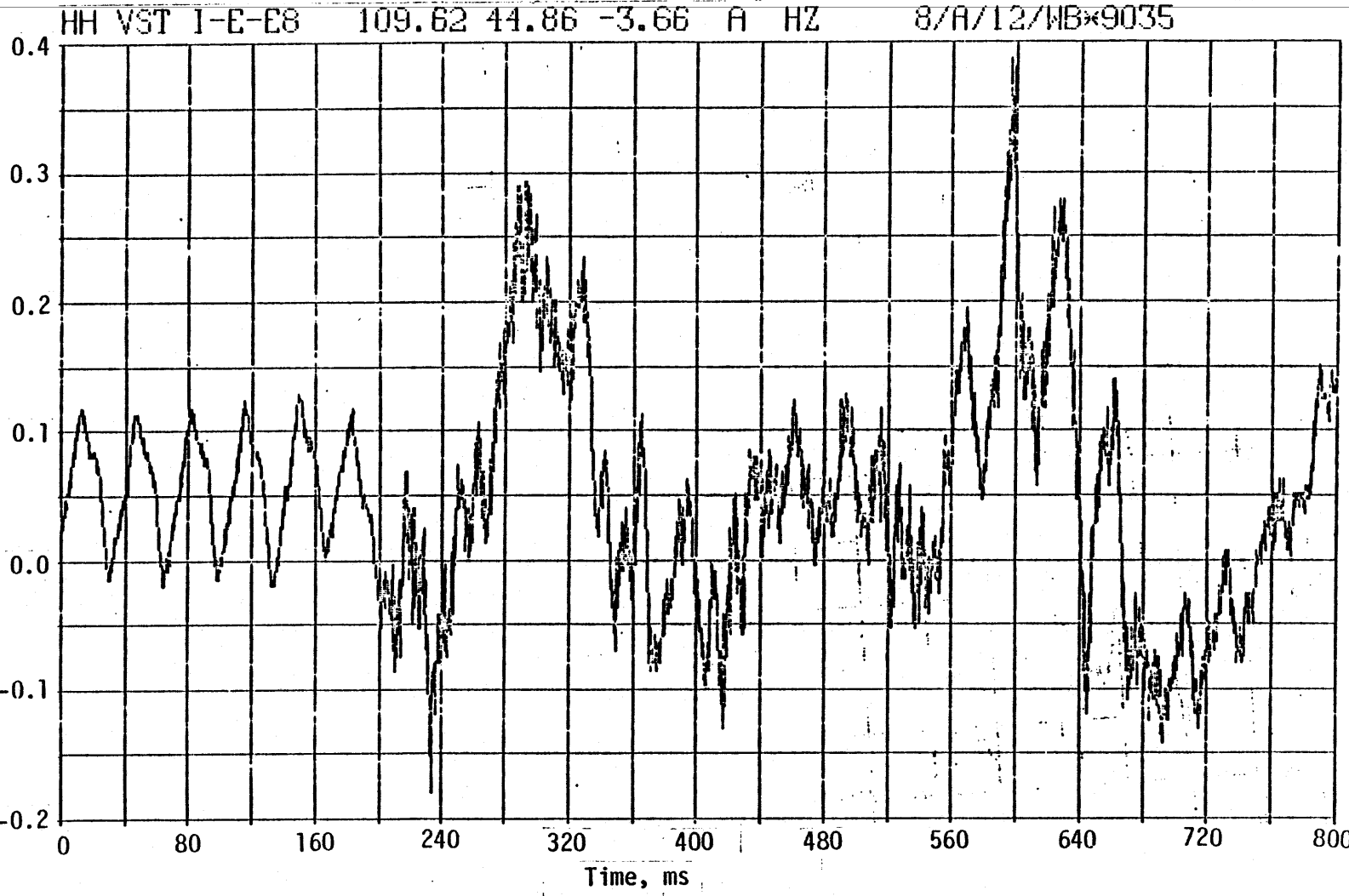
HH VST I-E-E8 115.26 44.86 -3.66 A HZ 8/A/16/MB\*9036



72

Vertical acceleration at rear bumper.

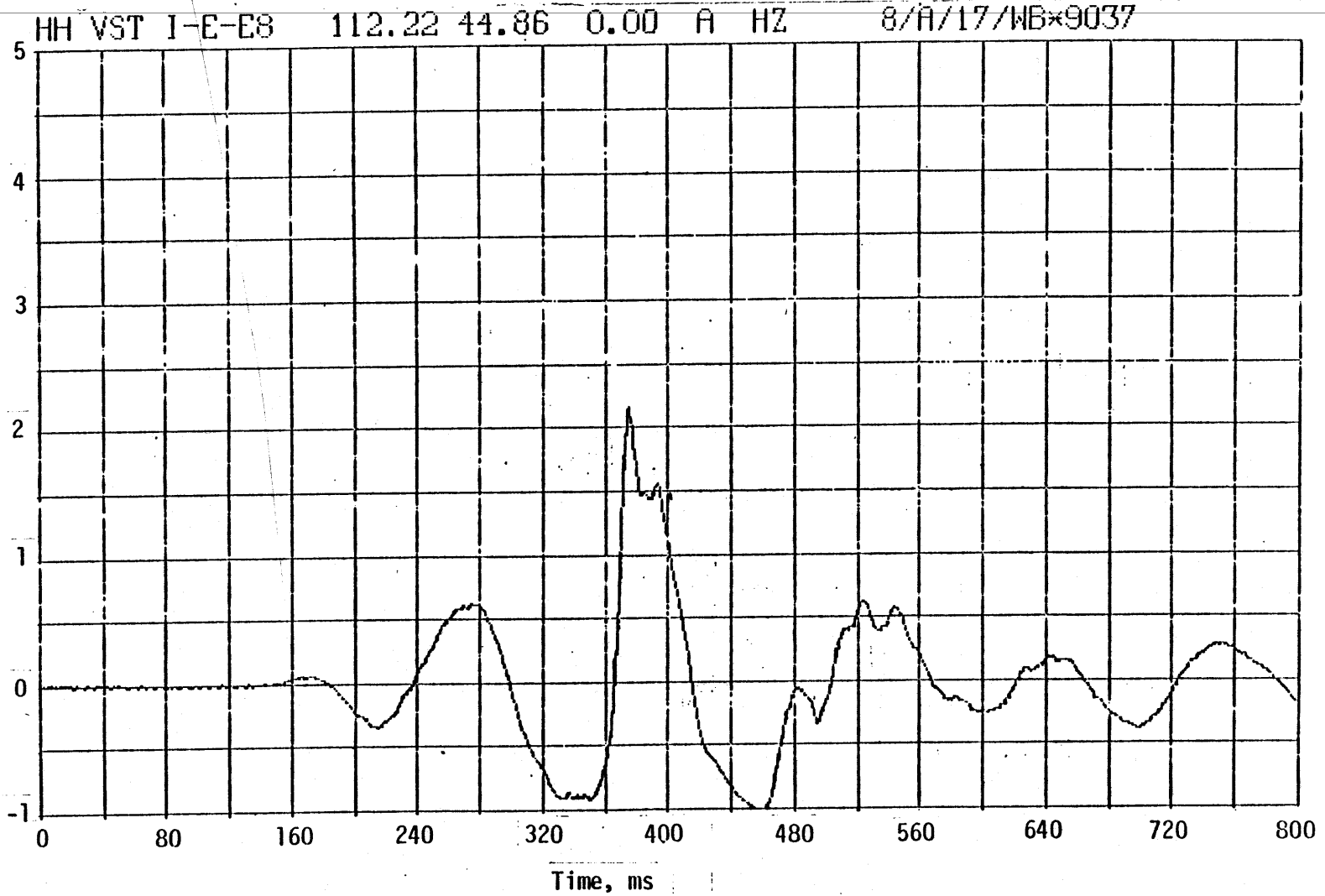




73

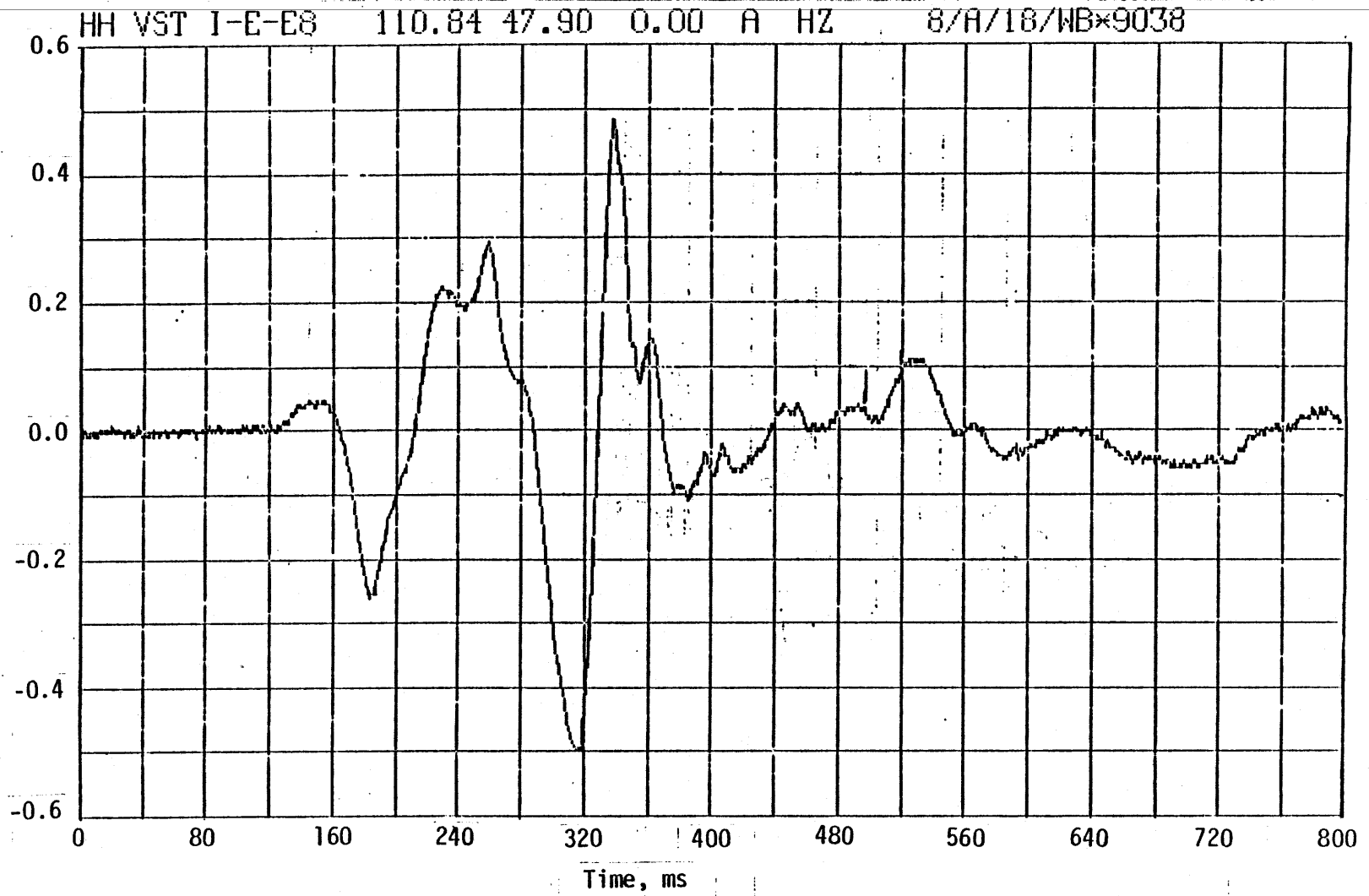
Vertical acceleration at front bumper.

Acceleration, g



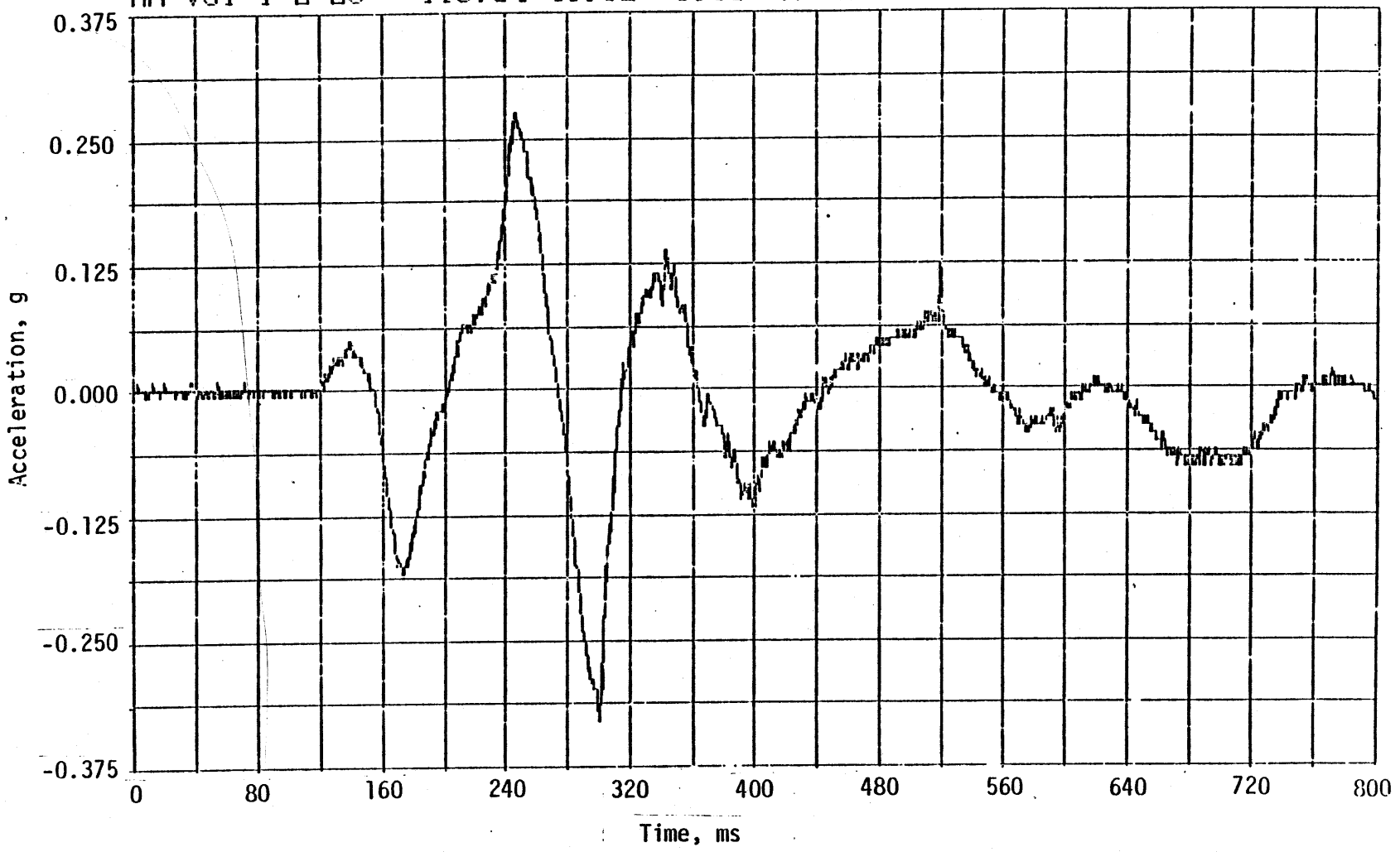
Vertical acceleration at roof center.

75



Vertical acceleration adjacent to shelter, MN 9038.

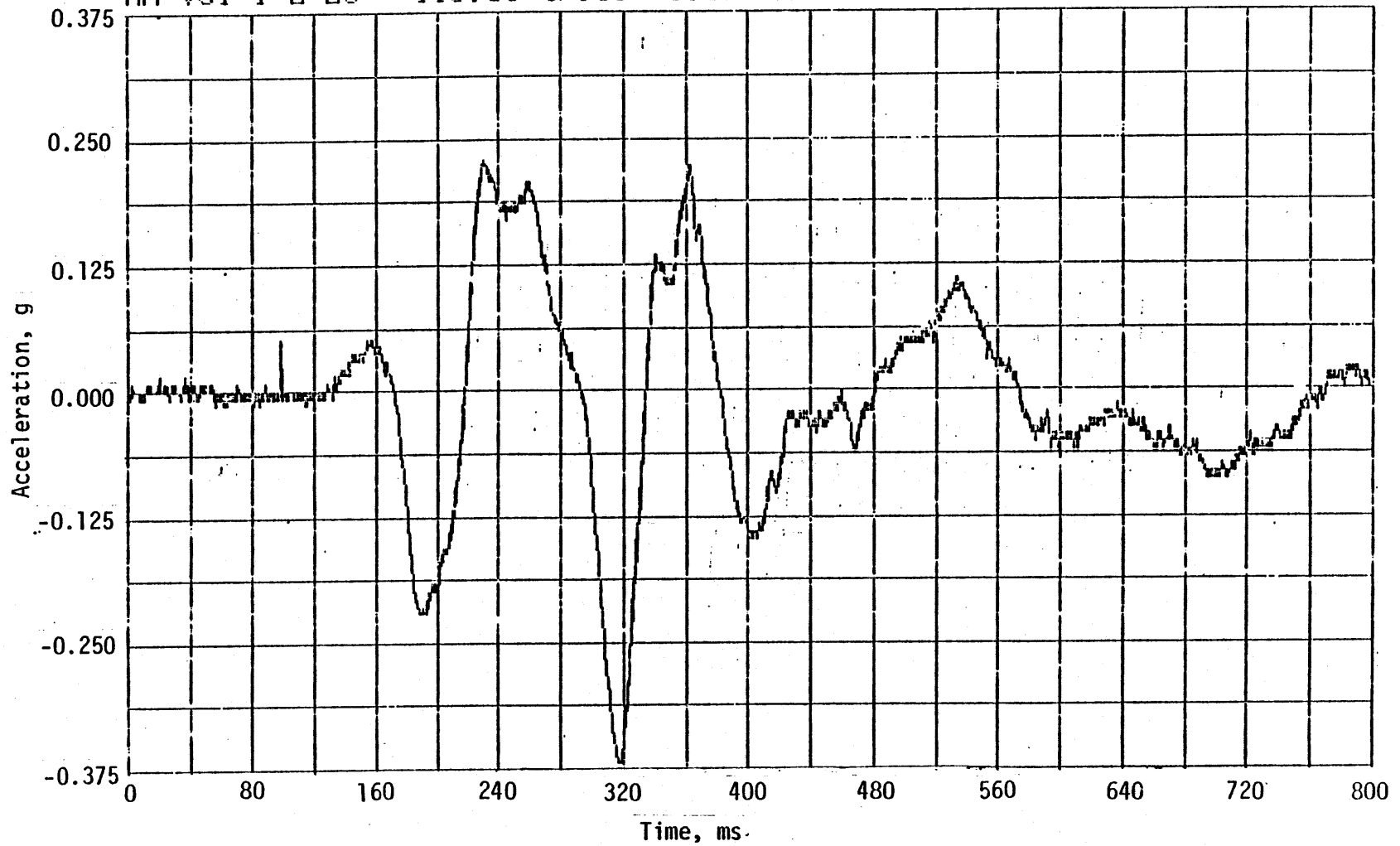
HH VST I-E-E8 110.84 41.82 0.00 A HZ 8/A/19/WB\*9039



76

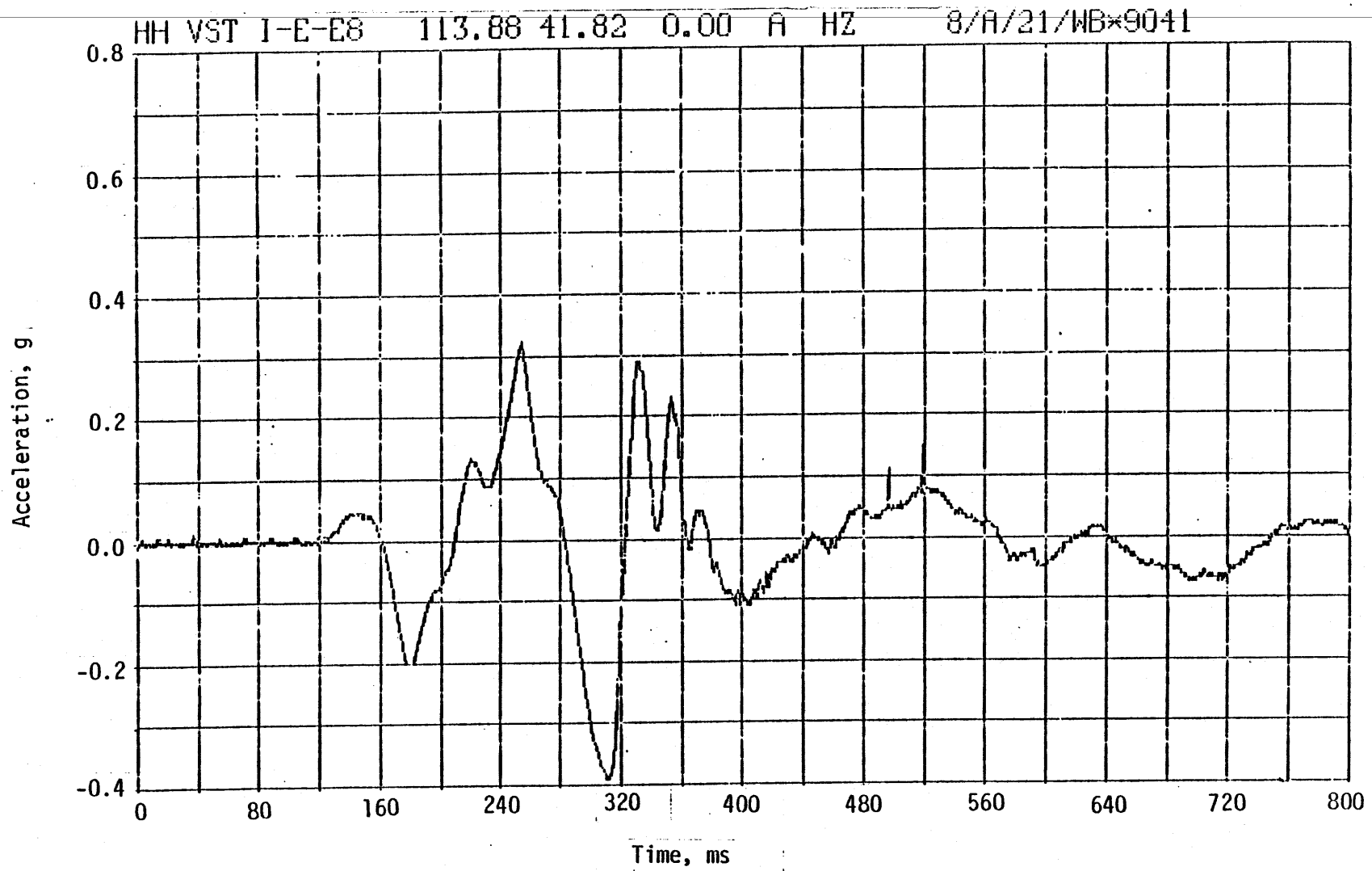
Vertical acceleration adjacent to shelter, MN 9039.

HH VST I-E-E8 113.88 47.90 0.00 A HZ 8/A/20/WB\*9040



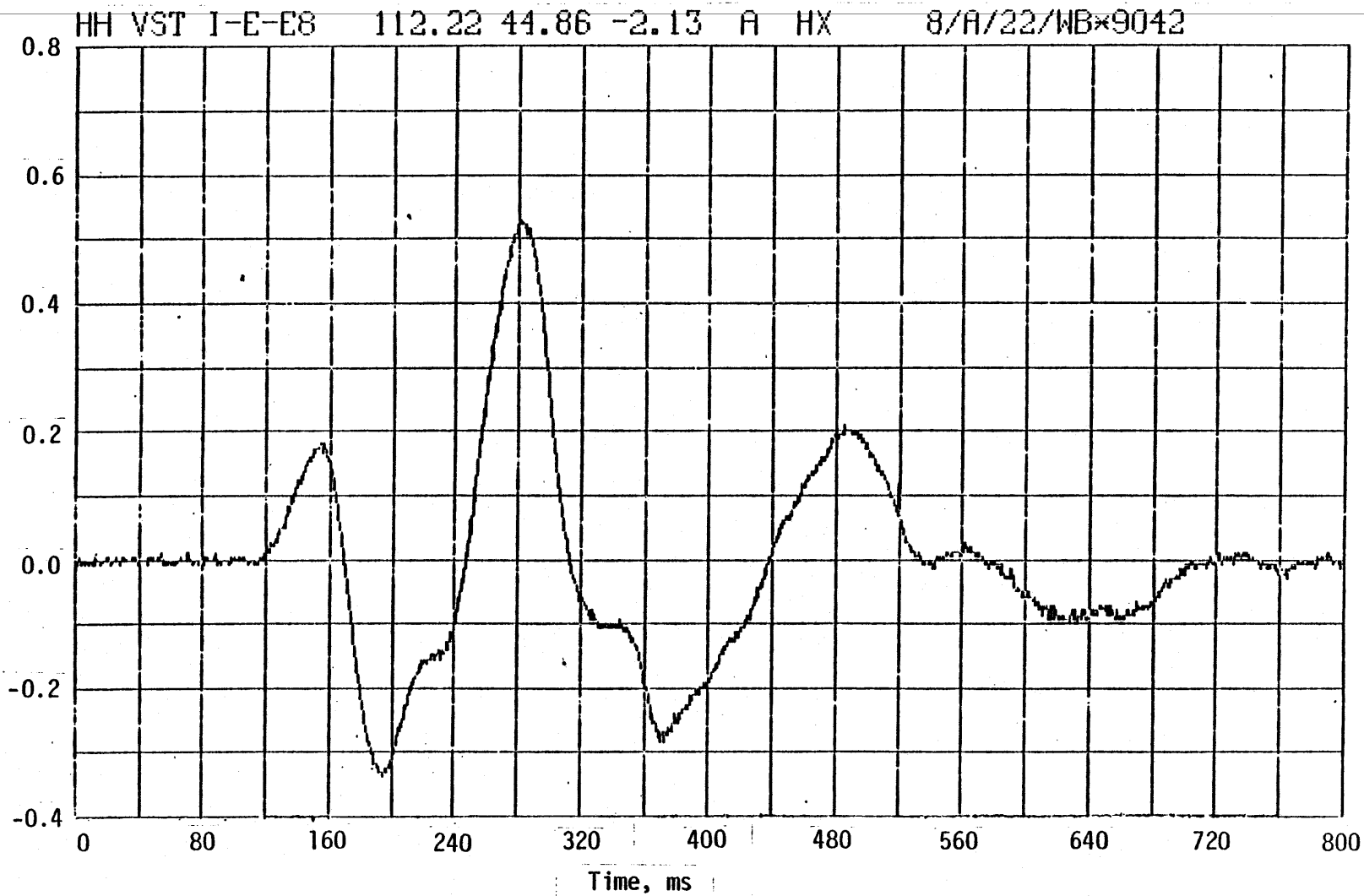
77

Vertical acceleration adjacent to shelter, MN 9040



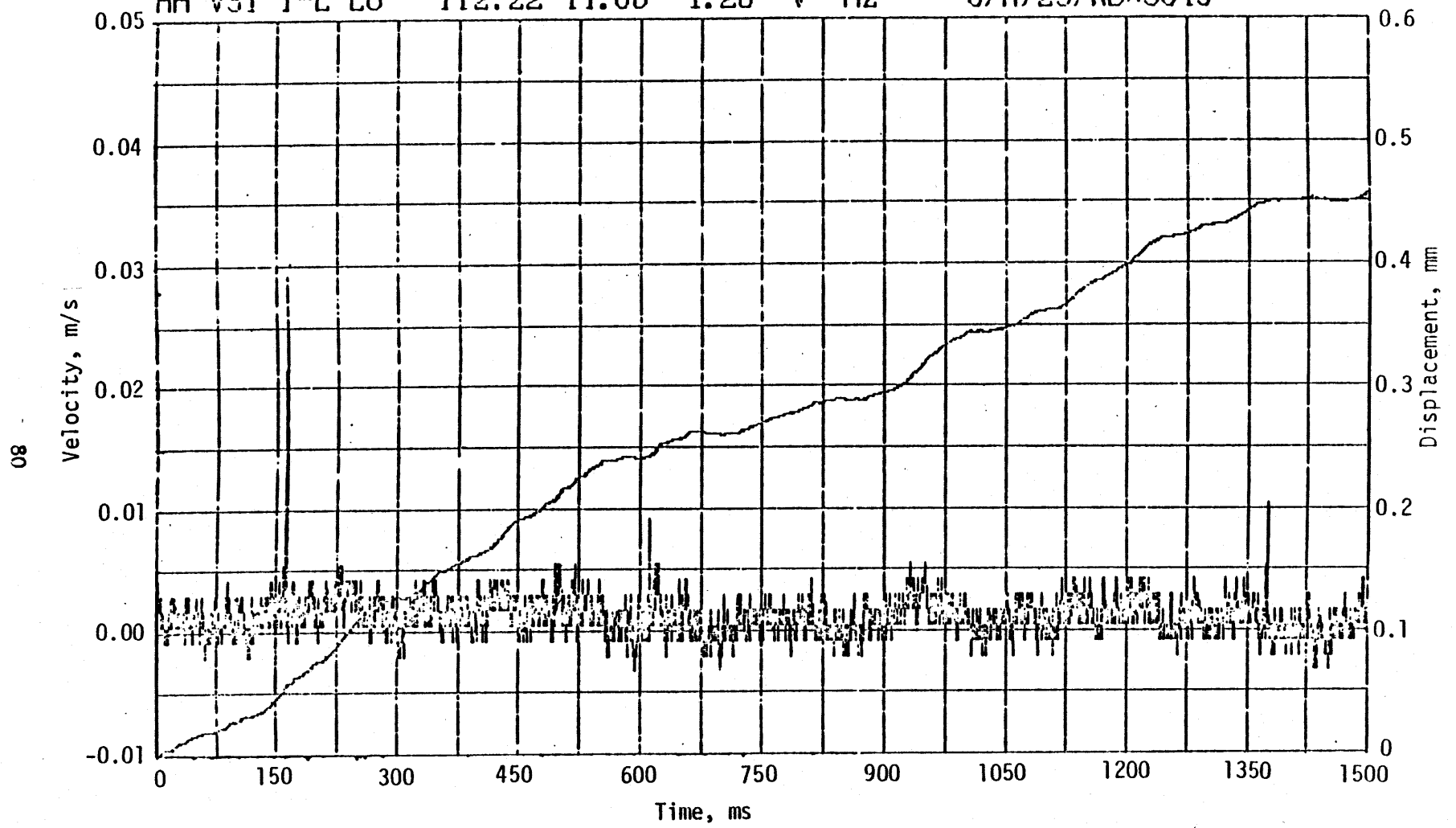
Vertical acceleration adjacent to shelter, MN 9041.

69



Horizontal acceleration of front wall.

HH VST I-E-E8 112.22 44.86 -4.26 V HZ 8/A/23/WB\*9043



Vertical velocity under van.



APPENDIX C  
VST NEAR-FIELD ENVIRONMENT PREDICTIONS AND  
EXPLOSIVES DOCUMENTATION

The predictions reported here were prepared by J. Edwards of AFWL/NTED-A. They are somewhat low in comparison to the actual measurements for any of a number of possible reasons. However, predictions of this type are certainly necessary to the process of choosing a location for a close-in data-acquisition system.

The worst-case debris predictions point to the necessity of protecting close-in vans. In this type of test, debris is the only significant hazard.

VST NEAR-FIELD PRESSURE PREDICTION

For maximum near-field pressure, use maximum predicted pressure in the impulse code. Take the pressure and volume at vent, assume no shock, convert to the pressure and volume in an equivalent hemisphere, and expand the gas adiabatically as a gamma law gas using  $\gamma = 1.4$  (air).

$$P_2 = \frac{P_1}{\left(\frac{R_2^3}{R_1^3}\right)^\gamma}$$

$$\begin{aligned} \text{Volume at vent} &= 104 \times 112 \times (4.78 + 1.575) \\ &= 74,023 \text{ ft}^3 \end{aligned}$$

$$\text{Convert to an equivalent hemisphere: } 2/3\pi R^3 = 74,023$$

$$R_1 = \sqrt[3]{\frac{74,023 \times 3}{2\pi}} = 32.82 \text{ ft} = 10 \text{ m}$$

Pressure at vent ( $P_1 = 170 \text{ lb/in}^2$ ), from the Impulse Code

R,		P,	
m	(ft)	MPa	(lb/in <sup>2</sup> )
30	( 98)	1.164-E2	(1.690)
35	(115)	6.090-E3	(0.880)
40	(131)	3.480-E3	(0.500)
45	(148)	2.110-E3	(0.310)
50	(164)	1.360-E3	(0.200)
55	(180)	9.120-E4	(0.130)
60	(197)	6.330-E4	(0.090)
65	(213)	4.520-E4	(0.070)
70	(230)	3.310-E4	(0.050)
75	(246)	2.480-E4	(0.040)
80	(262)	1.890-E4	(0.030)
85	(279)	1.470-E4	(0.020)
90	(295)	1.150-E4	(0.017)
95	(312)	9.190-E5	(0.013)
100	(328)	7.400-E5	(0.011)

#### VST DEBRIS RANGE

##### A. Worst case:

Maximum initial velocity of overburden = 165 ft/s (from Impulse Code)

Assume a particle launched at 45 deg:

$$V = 165 \text{ ft/s at } 45 \text{ deg}$$

$$V_{\text{horiz}} = 165 \cos 45 \text{ deg} = 117 \text{ ft/s}$$

$$V_{\text{vert}} = V_{\text{horiz}} = 117 \text{ ft/s}$$

Maximum height:

$$V = V_0 + a t$$

$$t \text{ at top} = \frac{117 \text{ ft/s}}{32.2 \text{ ft/s}^2} = 3.63 \text{ s}$$

Neglect air drag:  $T_{\text{total}} = 2 t = 7.26 \text{ s}$

Maximum distance =  $V_{\text{horiz}} XT = 849 \text{ ft} = 258.8 \text{ m}$

B. Main body of overburden:

Test bed is sloped from the center to the edges at 1 ft per 52 ft.

$$\alpha = \arctan 1/52 = 1.1 \text{ deg}$$

$$\sin \alpha = 0.0192$$

$$\cos \alpha = 0.9998$$

Maximum height:

$$V_{\text{vert}} = 165 \cos \alpha = 164.97 \text{ ft/s}$$

$$V_{\text{horiz}} = 165 \sin \alpha = 3.172 \text{ ft/s}$$

Horizontal translation = 3.172 x time of flight

$$T = \frac{2 \times 165}{32.2} = 10.25 \text{ s}$$

$$\text{Horizontal translation} = 3.172 \text{ ft/s} \times 10.25 \text{ s} = 32.5 \text{ ft} = 9.9 \text{ m}$$

$$\begin{aligned} \text{Maximum height: } S &= 1/2 a t^2 \text{ where } t = 5.12 \text{ s} \\ &= 423 \text{ ft} = 128.9 \text{ m} \end{aligned}$$

#### VST EXPLOSIVE QUANTITY

$$\text{Volume} = 104 \text{ ft} \times 112 \text{ ft} \times 1.55 \text{ ft} = 18.054 \text{ ft}^3 = 511.1 \text{ m}^3$$

$$\text{Design charge density} = 1.162 \text{ lb/ft}^3 = 18.61 \text{ kg/m}^3$$

$$\text{Explosive quantity} = 21,000 \text{ lb} = 9525.54 \text{ kg}$$

Kinds of explosive:

Main charge, Iremite 60

Backup firing system, detcord, 400 gr/ft

Plane wave generator, detcord, 54 gr/ft

SYMBOLS

- B magnetic field strength
- $\dot{B}$  time derivative of the magnetic field
- E electric field strength
- H henry
- I current
- R' resistance per unit length
- S Seeman (inverse  $\Omega$ )
- f frequency
- g acceleration due to gravity
- $r_0$  inner radius of cylindrical shield
- z impedence
- $\Delta$  shield thickness
- $\Omega$  ohm
- $\delta$  electrical skin depth
- $\mu$  permeability
- $\mu_0$  permeability of free space  $4\pi \times 10^{-7}$  H/m
- $\sigma$  conductivity